The role of TASK-3 potassium channels in theta oscillations and behaviour

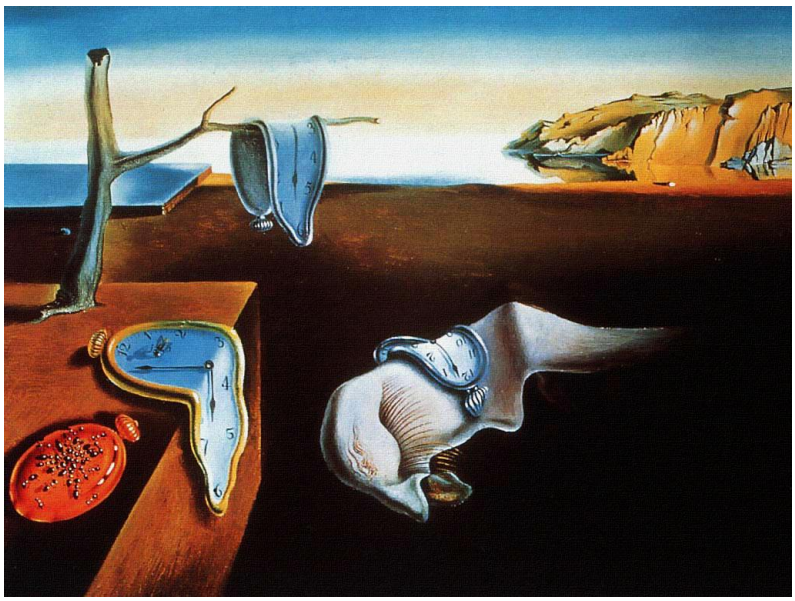

David R. Carr

A thesis submitted in fulfillment of the requirements for the degree of
Doctor of Philosophy of Imperial College London

Biophysics Section

January 2013

ABSTRACT

The two pore-domain potassium channel TASK-3 provides a potassium leak conductance in the mammalian brain and is activated by volatile anaesthetics. Previous studies have shown that TASK-3 knockout (KO) mice have a number of physiological and behavioural abnormalities. In particular, TASK-3 KO mice lack the type-2 theta oscillation (4-8 Hz) usually present in the electroencephalogram (EEG) under halothane anaesthesia, while the higher frequency type-1 theta oscillation (8-12 Hz) recorded during exploratory behaviour is unaffected. That TASK-3 KO mice also have moderate memory impairments, led us to ask whether there might be a link between type-2 theta deficits and impaired mnemonic behaviour.

Our results indicate that TASK-3 KO mice also have impaired type-2 theta oscillations during freezing behaviour in a predator exposure test, suggesting possible sensorimotor integration problems. TASK-3 KO mice were found to have a mild impairment in working memory in the T-maze, but object recognition and emotional memory were intact, excluding a role for the TASK-3-dependent theta oscillation in these processes.

Further studies then sought to understand the mechanistic role of TASK-3 in the theta oscillation using recombinant Adeno-associated viruses (rAAVs). We first investigated a possible functional role for the type-2 theta oscillation in mediating anaesthesia, and then confirmed that the halothane-associated theta oscillation was dependent upon cholinergic input from the medial septum to the hippocampus. TASK-3 was then re-expressed via rAAV in the medial septum in KO mice, resulting in partial rescue of the type-2 theta oscillation.

Our results show that (1) the type-2 theta oscillation plays a redundant role in halothane anaesthesia, (2) type-2 theta deficits in TASK-3 KO mice have minimal effect on memory processing, and (3) that TASK-3 channels in the medial septum play a facilitatory role in type-2 theta oscillations.

TABLE OF CONTENTS

TABLE OF FIGURES

MISCELLANEA

0.1 Contact details

Biophysics Section
Division of Cell & Molecular Biology
Imperial College
SW7 2AZ
david.carr07@imperial.ac.uk

0.2 Cover illustration

The Persistence of Memory (MoMA, New York City) by the Spanish surrealist Salvador Dali, painted in 1931, depicts a dreamscape with numerous melting pocket watches. To me, this has connotations of an anaesthetised state where time fades away to nothing. Dali is said to have gained inspiration for his paintings from various states of consciousness including dreams and so his works often contain Freudian symbols. Furthermore, the passage of time is nuanced by our memories of our experiences and the processes involved require the hippocampus and the theta rhythm. In a way, the hippocampus is a spatio-temporal clock that is important in many aspects of integrated behaviour, and so provides a possible target for inducing anaesthesia. It is therefore appropriate then to use this painting as a cover illustration for this report.

0.3 Acknowledgements

Thanks firstly to my supervisor Professor Nicholas Franks for his time, support and words of wisdom throughout my PhD project. Thanks to Professor William Wisden for his encouragement and for introducing me to molecular biology. Thank you also to the various PIs in the department who have provided help and advice: Dr Alistair Hosie, Dr Stefan Trapp, Dr Stephen Brickley, Dr Robert Dickinson, and Dr Giorgio Gilestro.

Thank you to the post-docs in the lab – Dr Anna Zecharia (also for the γ2 plasmid), Dr Valentina Ferretti, Dr Cigdem Gelegen, and Dr Catriona Houston – for all their experience, to Raquel Yustos for her patient knowledge, and to Dr Daniel Pang for aiding me with everything at the beginning of this project.

Thank you to the students with whom I have had the great pleasure of working over the years: Giorgia Albieri and Elisa Forteza Behrendt (rat exposure test), Thomas Roberts and Taha Shahid (video tracking), James Ip (medial septum cannulations), Silvia Coassin (rAAV construction), and Polona Jager (*in situ* hybridisation).

Thanks to the other students in the lab for being there too: Rowan Baker, Scott Armstrong, Eleonora Steinberg, Katie Harris (also for the organotypic slices), Grace Yip, Xiao Yu (also for the Cre-Venus rAAV), Zhiwen Ye, Zhe Zhang, David Uygun, Dr Thomas McGee (also for the electrophysiology) and Damian Droste (also for the iTurn). Very special thanks also to Dorothy Overington.

0.4 Declaration of originality

I, David Carr, declare that all the work in this report is my own, and that the work of others has been appropriately referenced and acknowledged.

0.5 Abbreviations

2PK	Two pore-domain potassium
aCSF	Artificial cerebrospinal fluid
bp	Base pair
Cre	Cyclization recombinase
DMEM	Dulbecco's modified Eagles medium
ECoG	Electrocorticography
ED	Effective dose
EDTA	Ethylenediaminetetraacetic acid
EEG	Electroencephalography / Electroencephalographic / Electroencephalogram (as context appropriate)
(e)GFP	(Enhanced) green fluorescent protein
EMG	Electromyography
FFT	Fast Fourier transform
Flp	Flippase
GABA	γ-aminobutyric acid
GPCR	G protein-coupled receptor
HEK	Human embryonic kidney
ICV	Intracerebroventricular
$I_{K(An)}$	Anaesthetic-activated potassium current
i.p.	Intra-peritoneal
ITR	Inverted terminal repeat
KO	Knockout
LB	Luria broth
LC	Locus coeruleus
LED	Light emitting diode
LFP	Local field potential
LIA	Large irregular amplitude
LOC	Loss of consciousness
LOM	Loss of movement
LOTW	Loss of tail withdrawal
LORR	Loss of righting reflex

MAC	Minimum alveolar concentration
mAChR	Muscarinic acetylcholine receptor
MnPO	Median pre-optic area
MS	Medial septum
NAc	Nucleus accumbens
nAChR	nicotinic acetylcholine receptor
NBM	Nucleus basalis magnocellularis
NCC	Neural correlates of consciousness
NGS	Normal goat serum
NEO	Neomycin
NMDA	N-methyl-D-aspartate
PET	Positron emission tomography
PCR	Polymerase chain reaction
PLC	Phospholipase C
(r)AAV	(Recombinant) Adeno-associated virus
RE	Restriction endonuclease
REM	Rapid eye movment
RT	Room temperature
SUM	Supramammillary nucleus
TASK	TWIK-related acid sensitive potassium (hcannel)
TAE	Tris base, Acetic acid, EDTA
TEA	Tetraethylammonium
TM	Transmembrane
TMN	Tuberomammillary nucleus
TSA	Tryticase soy agar
VLPO	Ventrolateral pre-optic area
VP	Virion protein
VTA	Ventral tegmental area

.

INTRODUCTION

1.1 Anaesthesia

1.1.1 Anaesthesia and unconsciousness

The ability to induce reversible loss of consciousness – general anaesthesia – through pharmacological means is a cornerstone of modern clinical and veterinary practice, such that every year tens of millions of patients are safely anaesthetised for a variety of medical reasons.

Used in crude herbal formulations for thousands of years, anaesthesia became an important discipline in its own right in the nineteenth century, with the first public demonstration of general anaesthesia in 1846 when William T.G. Morton successfully administered diethyl ether to Ebenezer Frost. Practically all surgical innovations of the last 150 years have depended upon this arresting phenomenon. And yet, to this day, the mechanisms of how diethyl ether, or the diverse multitude of other anaesthetic agents, cause loss of consciousness (LOC) remains unknown and ripe for investigation.

LOC in humans can be defined as the inability to respond meaningfully to a verbal command, an empirical endpoint that attempts to avoid the philosophical ambiguity raised by questions of consciousness. Typically, anaesthetic-induced LOC is a dose dependent phenomenon which proceeds through qualitatively distinct states such as delirium (hyperactivity and confusion) and sedation (sleepiness) to hypnosis (unconsciousness). Anaesthetic agents also provide various degrees of analgesia, amnesia and immobility and are often titrated in combination in the clinic to satisfy surgical or intensive care requirements.

Aside from being a fascinating scientific venture, understanding the mechanisms behind these phenomena may improve the practice and safety of clinical anaesthesia and potentially lead to the discovery of novel or more effective anaesthetic drugs.

1.1.2 Mechanisms of anaesthetic action

One of the most interesting and baffling aspects of anaesthesia is how such a diverse array of drugs can induce the same qualitative endpoint. It was partly for this reason that anaesthetic drugs were proposed to act non-specifically, and various physiochemical theories were sought to explain how compounds as different as the opiate morphine and the inert atomic gas xenon could produce unconsciousness.

Evidence for the first major unitary theory of anaesthesia was independently provided by Hans Meyer and Charles Overton at the turn of the twentieth century (Meyer, 1899; Overton, 1901). The famed Meyer-Overton correlation shows an approximately linear relationship between the potency of an anaesthetic and its oil:gas partition coefficient, with the implication that anaesthetics affect the lipid bilayer of neurons in some way to impair brain function.

Versions of this theory, including membrane expansion theories, predominated until the 1980s, when Nicholas Franks and William Lieb first showed that anaesthetic drugs bind to protein targets (Franks *et al.*, 1984). A series of seminal studies first showed evidence that contradicted lipid theories of anaesthesia (Franks *et al.*, 1978; Franks *et al.*, 1981; Franks *et al.*, 1982); and then came a paradigm shifting moment. Franks and Lieb (1984) purified a lipid-free extract of the bacterial enzyme luciferase and demonstrated a strong correlation between the ability of anaesthetic drugs to inhibit the light-producing enzymatic reaction and their anaesthetic potency (Figure 1.1A)

An especially important finding at that stage was that the inhibition of luciferase was competitive, demonstrating a generalizable mechanism for how anaesthetics might target other more clinically relevant protein targets.

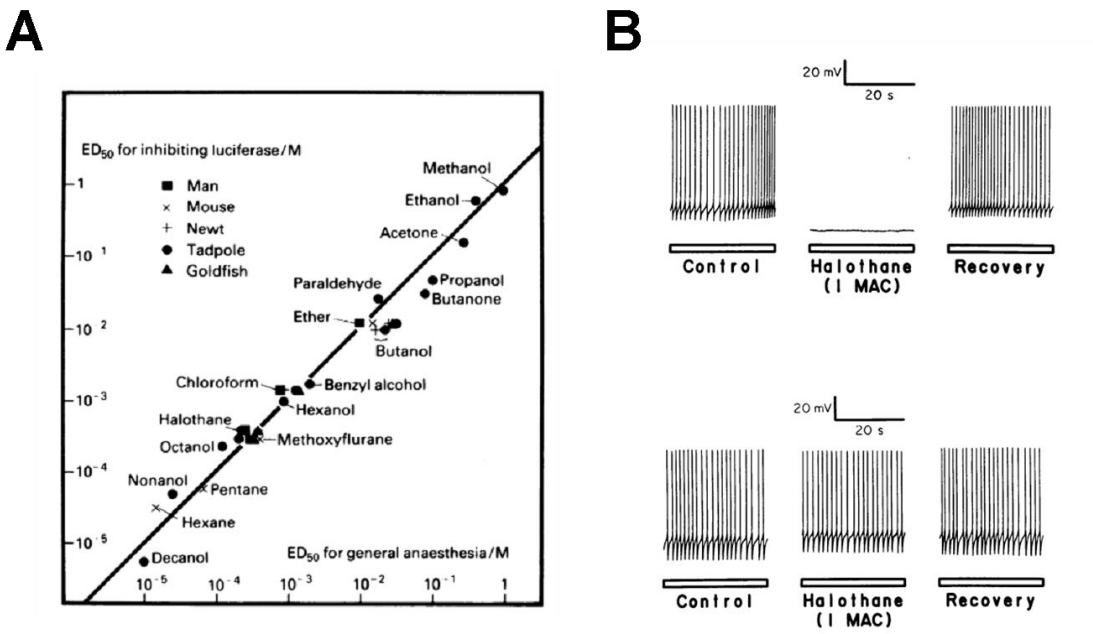

Figure 1.1 Evidence for a protein theory of anaesthesia, against a lipid one.
A – There is a good correlation between the potency of anaesthetics and the extent to which they inhibit the protein luciferase. B – One neuron from Lymnaea stagnalis is sensitive to 1MAC halothane (top), while another is not (bottom). [Adapted from Franks et al. (1990)]

1.1.3 Molecular targets of anaesthesia

Following these early results, much activity was spent attempting to discover plausible molecular targets for anaesthetics. Franks and Lieb were again influential here. Out of forty patched neurons in the pond snail *Lymnaea stagnalis* they found just one that was sensitive to the volatile anaesthetic halothane (Franks *et al.*, 1988). This result uncovered a novel anaesthetic-activated K^+ current, dubbed $I_{K(An)}$, and the cellular specificity (i.e., one out of forty) provided further evidence against the lipid theory of anaesthesia (Figure 1.1B).

The finding that the enantiomers of chiral anaesthetic compounds had different anaesthetic potencies both *in vitro* (Huang *et al.*, 1980) and *in vivo* (Dickinson *et al.*, 2000) also indicated that the targeting of specific molecular pockets (on proteins) was responsible for anaesthetic action.

Since then, research has continued to focus on specific molecular targets – neuronal receptors and ion channels – in the nervous system (Rudolph *et al.*, 2004). Three neuronal receptor families provide the main focus of this endeavour: (i) γ-

aminobutyric acid $(GABA)_A$ receptors, (ii) N-methyl-D-aspartate (NMDA) receptors and (iii) two pore-domain potassium (2PK) channels.

$GABA_A$ receptors

As the main inhibitory neurotransmitter in the central nervous system, GABA acts to modulate brain excitation through a number of receptors. The $GABA_A$ receptors in particular provide a *prima facie* target because their potentiation inhibits neuronal activity through an inward Cl^- current (Franks *et al.*, 1994).

NMDA receptors

Whereas GABA acts to inhibit neurons, the endogenous neurotransmitter glutamate acts on a variety of receptors to excite neuronal activity. The NMDA receptor mediates the slow component of synaptic neurotransmission and therefore provides a potential anaesthetic target through its inhibition (Flohr *et al.*, 1998).

Two pore-domain potassium channels

The two-pore-domain-potassium (2PK) channels are a family of related K^+ "leak" channels that function independent of voltage and time to modulate the membrane resting potential and also affect the excitatory capacity of the cell. Their activation leads to inhibition (Ketchum *et al.*, 1995). The 2PK channel member TASK-3 is the focus of this investigation.

1.1.4 Anaesthetic systems

As well as identifying primary molecular targets, research has also extended towards discovering how these receptors and channels are linked in cellular networks in the central nervous system, predominantly in the brain.

In general, anaesthetic drugs inhibit neuronal firing to interfere with waking brain activity and ultimately induce LOC at a point where functionality ceases (Alkire *et al.*, 2008). The human brain exists as a complex and dynamic system containing an estimated 100 billion neurons connected by potentially 100 trillion synapses. At any one time, a concert of neurotransmitter systems modulate brain activity and function, depending upon arousal state and ongoing external (sensual) and internal (perceptual) stimulation.

In William James' terms, these systems ensure four characteristics: (i) that every "state" tends to be part of a personal consciousness, (ii) that within each personal consciousness, states are always changing, (iii) that each personal consciousness is sensibly continuous and (iv) that it is interested in some parts of its object to the exclusion of others (James, 1890).

Various mechanisms for how exactly the awake brain achieves these characteristics, and how anaesthetics interrupt them, have been proposed; some arguing for common molecular targets (Eger *et al.*, 2008), others for neurological models (John *et al.*, 2005). Among the more gestalt network theories, there is argument to whether "bottom-up" or "top-down" inhibition is more relevant.

One of the "bottom-up" theories proposes that anaesthetics act on brain processes involved in regulating the sleep-wake cycle; by either impairing arousal pathways or potentiating sleep-promoting pathways (Franks, 2008). Evidence for this theory is not purely intuitive. Electroencephalographic (EEG) recordings in humans and animals show that the low amplitude desynchronised activity present during wakefulness changes to spindling activity and higher amplitude lower frequency oscillations during both deep sleep and anaesthesia (Sloan, 1998), a process that also correlates with decreased blood flow to the thalamus (Hofle *et al.*, 1997).

The brain regions responsible for the sleep-wake transitions, residing primarily in the hypothalamus and brain stem, integrate and synchronise in complex feedback loops during the circadian cycle.

Evidence for nuclei-specific anaesthetic targeting comes from the sedative drug dexmedetomidine, which is proposed to act selectively on α_{2A}-adrenoceptors to inhibit firing of locus ceruleus (LC) neurons and their noradrenergic innervation of the forebrain. This disinhibits the sleep-active ventrolateral pre-optic nucleus (VLPO), which once released can inhibit the wake-active histaminergic cells of the tuberomammillary nucleus (TMN), which project widely throughout the cerebral cortex. Its mode of action is therefore more pharmacologically and regionally specific than other anaesthetics, such as propofol, which potentiates $GABA_A$ receptors expressed more widely throughout the brain.

However there is the opposing viewpoint, that of "top-down" cortical suppression. This view is backed up by an experiment that shows similarly marked suppression of cortical neurons at sedative doses of volatile anaesthetics both in the whole animal and in isolated cortical neurons (Hentschke *et al.*, 2005). Other work, in

Parkinson's patients showed that electrical signals in the cortex but not in the thalamus decreased at LOC, suggesting "top-down" effects. This could be due to the increased density of $GABA_A$ receptors in the cortex, and thus of inhibitory anaesthetic currents in this region, being more fundamental to anaesthesia (Velly *et al.*, 2007). Positron Emission Tomography (PET) scanning shows that in addition to a global depression of neuronal activation with anaesthesia, there is a further relative decrease in activity in higher cortical centres such as the precuneus and posterior cingulate, while primary sensory areas remain labile to stimulation (Fiset *et al.*, 1999; Laitio *et al.*, 2007). This points toward LOC being mediated through the disintegration of higher functioning processing modules, as opposed to simply shutting off all sensory inputs.

Other theories argue that interactions between the thalamus and the cortex mediate the most important facets of consciousness and that disruption of normal connectivity between these two areas is responsible for anaesthetic action. Indeed the thalamus is thought to be responsible for the sleep-related delta oscillation (Steriade, 2003).

The Jamesian definition of consciousness given above clearly has its limits when applied to the empirical study of anaesthesia and especially when applied to the study of animals other than adult humans. Attempts have been made to describe the effects of anaesthetics in more objective terms, and Paul Flecknell's important reference manual *Laboratory Animal Anaesthesia* (Flecknell, 2009) gives the following anaesthesia-related definitions:

- Sedation (light, medium or heavy): The animal will have reduced activity and may become completely immobile, but easily aroused, particularly by painful stimuli.
- Analgesia: Some pain-alleviating effect is present.
- Immobilization: The animal is immobilized but still responds to painful stimuli.
- Light anaesthesia: The animal is immobile and unconscious, but still responsive to even minor surgical procedures.
- Medium anaesthesia: Most surgical procedures (e.g., laparotomy) may be carried out without causing any response, but the animal may still respond to major surgical stimuli (e.g., orthopaedic surgery).
- Deep anaesthesia: The animal is unresponsive to all surgical stimuli.

These classifications can be used to give an anaesthetic score, but in that instance a linear scale is not representative of the complex systems at work in the live animal. Effective doses (ED) of anaesthetic drugs to a certain endpoint – immobility, defined pain threshold, unconsciousness, etc. – are often used to more accurately define anaesthetic sensitivity. Potencies of anaesthetic vapours are often compared using minimum alveolar concentration (MAC), a term devised by Edmond Eger and colleagues (1965), which defines the concentration of vapour in the lungs required to prevent movement in 50% of subjects in response to surgical stimulus.

But the question of how to suitably compare the point of LOC between animals and humans still remains. First though, a measure of LOC in humans is needed. To this end, human LOC has been defined as the inability to respond meaningfully to a verbal stimulus (Franks, 2008), something that cannot be applied to animals. The most common comparative measure in animals is the loss of righting reflex (LORR). When an animal (including mice and rats) is turned on its back its natural reaction is to get back on its feet. This righting reflex is sensitive to anaesthesia and at a certain anaesthetic concentration the animal will lose its righting reflex. Thus LORR can be used as binary measure to score anaesthetic sensitivity which can be repeated in any laboratory by a trained technician or scientist. One of the most significant reasons for adopting LORR as an anaesthetic measure is the pharmacological correspondence between LOC in humans and LORR in other animals (Figure 1.2).

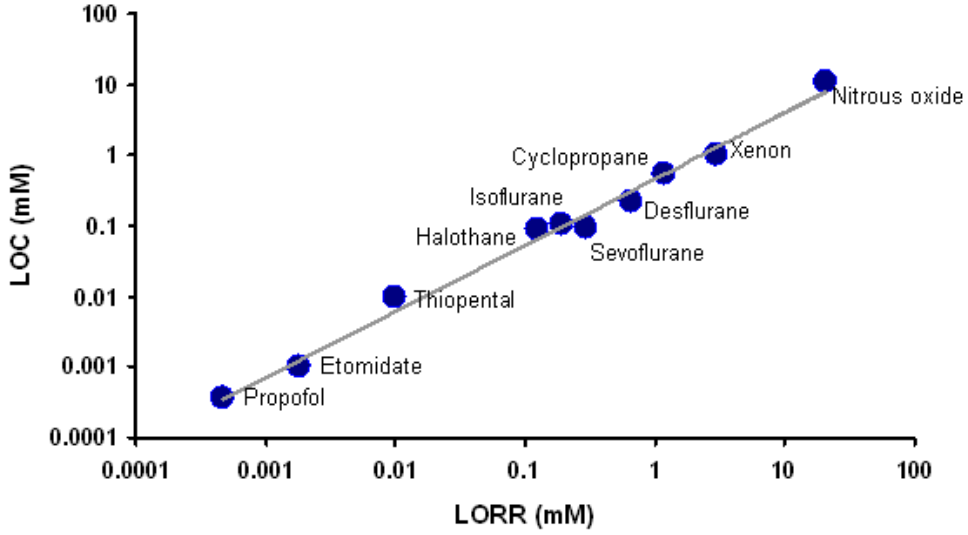

Figure 1.2 The pharmacological correlation between LOC in humans and LORR in rodents.

This indicates that they measure similar physiological processes. [Re-drawn with data from Franks (2008)]

1.2 Two pore-domain potassium channels

1.2.1 History

The existence of a hypothetical group of potassium channels that provide a membrane leak conductance was predicted by Alan Hodgkin and Andrew Huxley through their work on the squid giant axon (Hodgkin *et al.*, 1952). Functioning independent of voltage and time, these channels were proposed to regulate the excitatory capacity of the cell through a "leak" conductance, and were later confirmed to modulate the membrane resting potential (Hille, 1973).

While still not identified molecularly, a role for this potassium current in anaesthetic action was indicated in rat hippocampal pyramidal cells (Nicoll *et al.*, 1982) and a ganglion of the pond snail (Franks *et al.*, 1988). The currents were insensitive to the traditional K^+ channel blockers and activated at clinically relevant concentrations of anaesthetic drugs, suggesting a new molecular mechanism of anaesthesia.

By searching genomic databases for the pore domain of potassium channels, Ketchum *et al.* (1995) identified a novel class of channels in *Saccharomyces cerevisiae* that, once subsequently cloned and expressed in *Xenopus* oocytes, displayed the physiological characteristics of the hypothesised channel. Interestingly, the functional channel appeared to consist of two subunits, rather than the four associated with voltage-gated potassium channels, with each having two pore domains; hence the channels being classified as two pore-domain potassium channels (or 2PK channels). Soon afterwards, homologous channels were identified in *Drosophila melanogaster*, providing more evidence for the "leak" model of membrane regulation (Goldstein *et al.*, 1996), before being identified in mammals (Fink *et al.*, 1996; Lesage *et al.*, 1996). Several studies soon confirmed that these channels were indeed sensitive to volatile anaesthetics such as halothane (Patel *et al.*, 1999; Sirois *et al.*, 2000).

More recently, the crystal structures of two human 2PK channels have been reported, revealing fenestrations that provide a structural basis for how anaesthetics might interact with the channels (Brohawn *et al.*, 2012; Miller *et al.*, 2012).

1.2.2 Physiology and pharmacology

There exist over 70 genes for K^+ channels divided into four major subfamilies: (i) the voltage-gated K^+ channels, (ii) the inwardly-rectifying K^+ channels, (iii) Ca^{2+}-activated and K^+-activated channels and (iv) the 2PK channels.

The voltage-gated K^+ channels comprise four subunits, each of which has six transmembrane (TM) spanning domains. A re-entrant helix between the fifth and sixth TM domains forms the basis for the selectivity filter and charged amino acids on the fourth TM domain confer voltage sensitivity.

Inwardly rectifying K^+ channels are also formed from four subunits, with the *P* domain situated between the two TM domains on each one. Some members of this family are open at rest, while others are regulated by G-protein coupled receptors (GPCRs) and other modulators.

2PK channels, on the other hand, form from the dimerisation of two subunits; each having four TM domains and two pore domains (Figure 1.3A). The 2PK family, given the genetic identification KCNK and named according to their physiochemical attributes (see footnotes), can be further divided into groups based on sequence homology and functional similarity: TWIK[1] channels (TWIK-1, TWIK-2, and the non-functional KCNK7) are weakly inwardly rectifying; THIK-1[2] channels are inhibited by halothane and are related to non-functional THIK-2; TREK[3] channels (TREK-1, TREK-2, and TRAAK[4]) are sensitive to arachidonic acid and stretch; TALK[5] channels (TASK-2, TALK-1, and TALK-2/TASK-4) are alkaline-activated; TRESK[6] channels are specifically located in the spinal cord; and TASK[7] channels (TASK-1, TASK-3, and the non-functional TASK-5) are acid-sensitive.

Usually open at membrane resting potential, 2PK channels are responsible for the K^+ leak current and act to hyperpolarise the cell. This takes the resting potential

[1] TWIK channel: tandem of P domains in a weak inwardly rectifying K+ channel
[2] THIK channel: tandem pore domain halothane-inhibited K+ channel
[3] TREK channel: TWIK-related K+ channel
[4] TRAAK channel: TWIK-related arachidonic acid-stimulated K+ channel
[5] TALK channel: TWIK-related alkaline pH activated K+ channel
[6] TRESK channel: TWIK-related spinal cord K+ channel
[7] TASK channel: TWIK-related acid-sensitive K+ channel

away from the action potential threshold thereby limiting neuronal excitability. However, the full story is not so simple: expressed pre-synaptically on inhibitory neurons, TREK-1 channel activation reduces GABA release, potentially causing excitation of downstream neurons (Westphalen *et al.*, 2007); and additionally, TASK-3 channels play an important role in mediating increased firing rates of cerebellar granule cells due to their rapid repolarisation of the cell (Brickley *et al.*, 2007).

2PK channels are insensitive to the conventional K^+ channel blockers tetraethylammonium (TEA), 4-aminopyridine, Cs^+ and Ba^{2+} (Bayliss *et al.*, 2003) and are regulated by GPCRs in a subtype specific manner (Mathie, 2007). Widely and differentially expressed throughout the body, 2PK channels are thought to be important in immune, heart and kidney function, and may play other as yet unknown physiological roles. Several members of the 2PK family – TREK-1, TREK-2, TASK-1, TASK-3 and TRESK – are sensitive to volatile anaesthetics, and as such have become a focus for research into anaesthetic mechanisms (Figure 1.3B).

Recently acquired crystallographic structures of the human TWIK-1 channel (Miller *et al.*, 2012) and TRAAK channel (Brohawn *et al.*, 2012) show that 2PK channel dimers afford four-fold symmetry in the pore-forming region. Marked fenestrations between the TM domains also suggest target sites for hydrophobic modulators such as arachidonic acid and anaesthetics, which may achieve access via the lipid membrane.

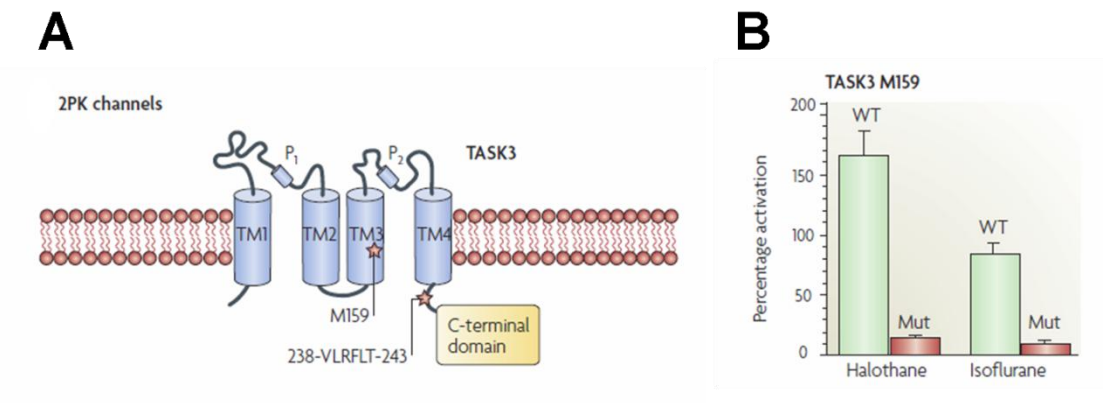

Figure 1.3 Two-pore domain potassium (2PK) channels are sensitive to anaesthetics.

A – One TASK-3 subunit of the 2PK channel dimer has four transmembrane domains and 2 pore-forming regions. B – The M159A mutation in TASK-3 ablates the activation of the channel by halothane and isoflurane. [Adapted from Franks (2008)]

1.2.3 TASK channels

The TASK-1 and TASK-3 subtypes generate pH-sensitive whole-cell K^+ currents with extremely fast kinetics and weak rectification. Much interest has focused on these channels due to their widespread expression in the brain and the key role they play in maintaining neuronal function. Furthermore, TASK channels are sensitive to a number of anaesthetics, as demonstrated firstly in heterologous expression systems (Patel *et al.*, 1999) and then in rodent neurons (Sirois *et al.*, 2000).

Recent research has proceeded on several related fronts: (i) identifying endogenous TASK-like conductances in the murine brain slice preparation before (ii) knocking out the TASK genes to observe electrophysiological changes that may explain (iii) any pharmacological and behavioural phenotypes.

In mice, TASK-1 channels are strongly expressed in the cerebellar granule cells, motor neurons, pontine nuclei, interpeduncular nucleus, locus coeruleus and medial mammillary nucleus and also the olfactory bulb granule cells (Bayliss *et al.*, 2003; Kang *et al.*, 2004). There is a smaller proportion of TASK-1 gene expression in the neocortex, raphe nuclei, reticular thalamus, certain central thalamic nuclei, parafascicular thalamic nucleus and medial geniculate nucleus (Bayliss *et al.*, 2003).

The expression of TASK-3 differs in some thalamic, hypothalamic and pontine nuclei although there is coexpression in the cerebellar granule cells, locus coeruleus, motor neurons, pontine nuclei, some cells in the neocortex, habenula, olfactory bulb granule cells, and cells in the external plexiform layer of the olfactory bulb (Bayliss *et al.*, 2003). TASK-3 channels are also expressed in the hippocampus; both on pyramidal cells and interneurons (Torborg *et al.*, 2006). The channels form homodimers and may form heterodimers where their expressions co-localise (Berg *et al.*, 2004; Kang *et al.*, 2004).

TASK-1 KO mice display a relatively normal behavioural phenotype as judged by standardised behavioural testing (Linden *et al.*, 2006). However, TASK-1 KO mice have a reduced sensitivity to inhalation anaesthetics: they are less sensitive to halothane as judged by the loss of tail withdrawal (LOTW), less sensitive to isoflurane as judged by loss of righting reflex (LORR), and less sensitive to the sedative action of dexmedetomidine.

While knock-out of the TASK-1 gene in mice does not have a significant effect on the expression of other 2PK channels or $GABA_A$ receptors, TASK-1 KO mice show increased sensitivity to the ataxic and hypnotic effects of $GABA_A$ receptor ligands, indicative of a functional $GABA_A$ receptor upregulation (Linden *et al.*, 2008).

TASK-3 KO mice have reduced sensitivity to inhalation anaesthetics (Figure 1.4A), exaggerated nocturnal activity, and cognitive deficits (Linden *et al.*, 2007; Pang *et al.*, 2009), as well as significantly increased appetite and weight gain (Robledo-Zapico, 2008). A role for TASK-3 channels in neuronal network oscillations has also been described: TASK-3 KO mice lack the atropine-sensitive halothane-induced theta oscillation (4-7 Hz) from the hippocampus (Figure 1.4C&D) and are unable to maintain theta oscillations during rapid eye movement (REM) sleep (Pang *et al.*, 2009).

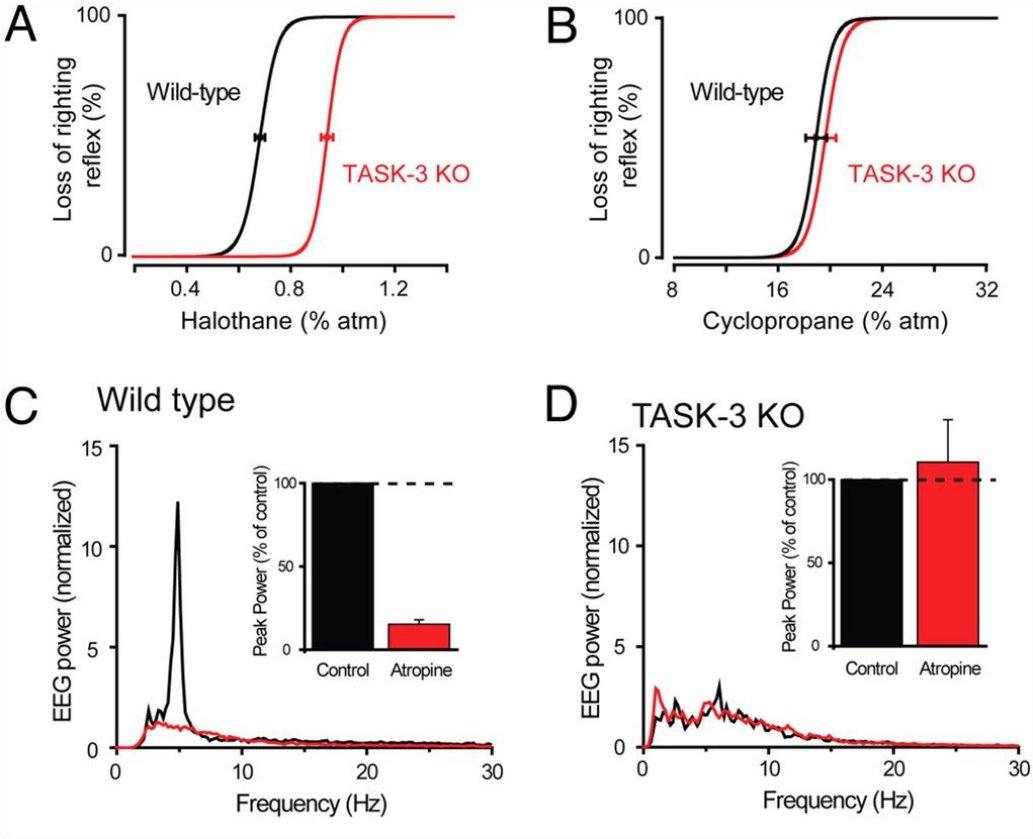

Figure 1.4 TASK-3 channel deletion reduces halothane sensitivity and ablates an anaesthetic type-2 theta oscillation.

A – TASK-3 KO mice are less sensitive to halothane. B – Cyclopropane sensitivity remains intact in TASK-3 KO mice. C – In wild-type mice halothane causes an atropine sensitive theta oscillation. D – The atropine sensitive theta oscillation is absent in TASK-3 KO mice. [Adapted from Pang et al. (2009)]

The sequelae of physiological phenotypes in the TASK-3 KO mouse suggest specific deficits in hypothalamic and limbic brain regions. One cellular mechanism that could explain some of the circadian and metabolic differences is the orexinergic system of the lateral hypothalamus. Here, TASK-3 channels are important in mediating inhibition of orexinergic neurons in response to glucose (Burdakov *et al.*, 2006) so, in their absence, animals might over-eat and hence gain more weight. Orexinergic neurons are also hypothesised to play a role as a "flip-flop" switch in the sleep-wake circuitry to "lock-down" sleep state and prevent aberrant state-switching (Lu *et al.*, 2006). Indeed, TASK-3 KO mice also show subtle changes in their sleep-wake architecture but they do not show signs of a narcoleptic phenotype (Robledo-Zapico, 2008) as might be expected from orexinergic mutants (Lin *et al.*, 1999).

That TASK-3 KO mice show changes in sleep and anaesthetic sensitivity points towards overlapping mechanisms between these processes, possibly also in the hypothalamus. However, there is evidence that halothane exerts its immobility effects through TASK-3 channels in motoneurons. In a comprehensive study, the effects of isoflurane and halothane were tested on TASK-1 KO mice, TASK-3 KO mice and the double mutant (Lazarenko *et al.*, 2010). Each genotype showed reduced sensitivity to halothane in measures of immobility (as tested by LOTW), hypnosis (LORR) and sedation. However, only sensitivity to LOTW was reduced for isoflurane.

When TASK channels were knocked out of cholinergic neurons only, the sensitivity to halothane and isoflurane was the same as the global double mutant apart from LORR by halothane (Lazarenko *et al.*, 2010). Thus, other systems, such as the aminergic system (Washburn *et al.*, 2002) or the thalamocortical system (Meuth *et al.*, 2006; Meuth *et al.*, 2003), are important in TASK-mediated hypnosis.

1.3 The hippocampal theta oscillation

1.3.1 Electroencephalography

The electrical activity of the human brain was first recorded in 1924 by Hans Berger, who, after an apparent telepathic experience as a child, was attempting to discover evidence for the psychic possibilities of the mind. The voltages he recorded in the electroencephalogram (EEG; also used for elecroencephalography, elecroencephalographic) were far too low to be transmitted from one person to another, but the observation that the activity changes even with simple behaviour such as opening and closing the eyes demonstrated the possibilities of this technique for observing the brain in action.

The scalp electrodes used in EEG are unable to detect the activity of single neurons; rather, they measure the synchronous activity of thousands or millions of neurons oscillating at the same frequency, as in figure 1.5 (Buzsaki *et al.*, 2012). In a laminar structure such as the cortical mantle or the hippocampus, the electrical dipoles of functionally related neurons can oscillate at the same frequency, causing detectable changes in a nearby electrode. EEG is therefore particularly suited to measuring gross changes in the network state of the brain over millisecond time scales, such as between waking and the different stages of sleep, where large parts of the brain are coordinated to produce a specific functional state.

The first state measured, with the subject closing their eyes, showed oscillatory activity between 8 and 12 cycles per second (Hertz: Hz) and was dubbed the alpha range, whereas opening the eyes typically shifts the activity to the beta range, between 12 and 30 Hz. In keeping with the Greek alphabet, the gamma range was identified between 30 and 100 Hz, the delta range between 0 and 4 Hz and the theta range between 4 and 8 Hz.

Over time, EEG has been a useful technique in the clinic and the laboratory to measure both normal and abnormal brain activity. More invasive methods have also been developed in humans and animals to record activity on the surface of the cortex, known as electrocorticography (ECoG), and can be used chronically to measure brain

activity over long durations. This makes EEG a useful tool for investigating anaesthetic mechanisms in the mammalian brain, where large scale network changes, detectable as changes in EEG characteristics, are likely to have some role in mediating different anaesthetic states.

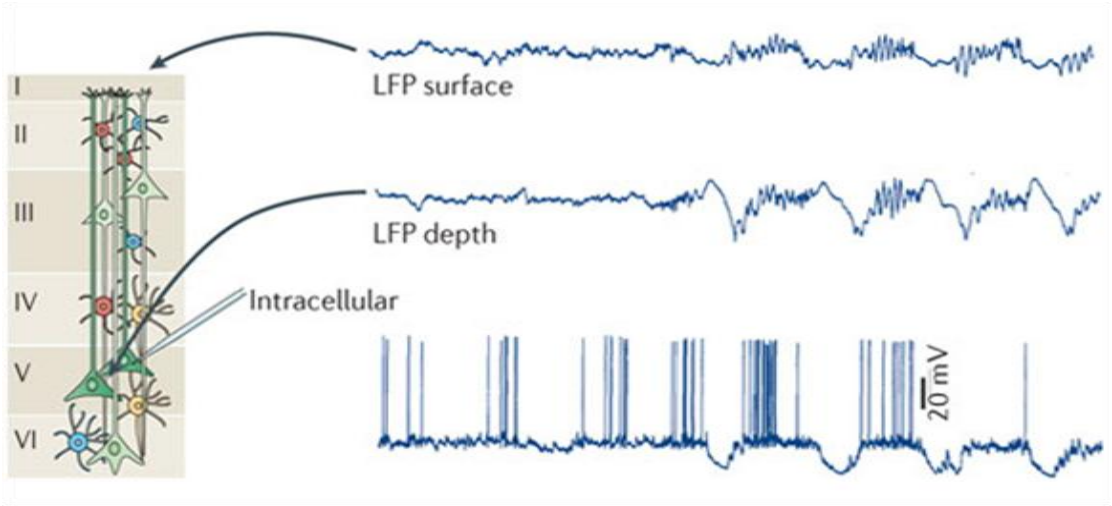

Figure 1.5 Electrical recording from the surface of the brain reflects deeper activity.

Note the correspondence between the activity of a single cell and local field potentials (LFPs) during the slow waves in the depth recording. [Adapted from Buzsaki et al. (2012)]

1.3.2 The theta oscillation

The theta oscillation is one of the most robust patterns observable in the EEG of the rodent, as well as other mammals, including humans. Expanded to cover a range of frequencies from 4 to 12 Hz, the theta rhythm is a nearly sinusoidal oscillation observable during rapid eye movement (REM) sleep and in a number of voluntary behaviours.

While many brain regions can oscillate at theta frequencies, the major source of the theta oscillation is the hippocampus; a cortical convolution in the shape of a ram's horn that makes up part of the limbic system (Figure 1.6A). The hippocampus plays an important role in memory processes (Lisman, 2005) and thus the hippocampal theta oscillation has come under intense research as a functional correlate of memory.

The dynamics of the theta oscillation are mediated by a number of different neurotransmitters and neuronal subtypes that set the frequency and amplitude differentially across the hippocampal formation. The largest amplitude theta oscillations are recorded in the stratum locunosum-moleculare of the CA1 region and there is a relative phase shift across the dorso-ventral axis of the hippocampus, such that the peak of theta in the stratum pyramidale is synchronous with the trough of theta in the hippocampal fissure, as in figure 1.6B (Bland *et al.*, 1976).

Much of the first research into theta oscillations was originally done in the rabbit, where the theta oscillation was divided into two distinct types (Kramis *et al.*, 1975). Type-1 theta typically occupies the higher end of the frequency spectrum (~7-12 Hz) and is present during volitional movements: there is also a good positive correlation between the frequency of the type-1 theta oscillation and running speed of the animal. Pharmacologically, type-1 theta is sensitive to anaesthetics but resistant to cholinergic antagonism by atropine. Type-2 theta, on the other hand, is found at the lower end of the frequency spectrum (~4-7 Hz) and, present during alert immobility, is resistant to anaesthetics but sensitive to atropine.

The prevailing view is that the type-1 theta oscillation is mediated through glutamatergic inputs from the entorhinal cortex (Buzsaki, 2002), whereas the key region in the generation of the type-2 theta oscillation is the medial septum-diagonal band of Broca (henceforth: medial septum, MS). Classically thought of as the major pacemaker, lesions of the medial septum in rabbits eliminate the theta rhythm in the hippocampal formation and associated cortical structures (Petsche *et al.*, 1962). The MS contains a number of different cell types, including cholinergic, GABAergic and glutamatergic cells, all of which have been shown to be important in regulating the theta oscillation (Bland *et al.*, 2007a; Yoder *et al.*, 2005).

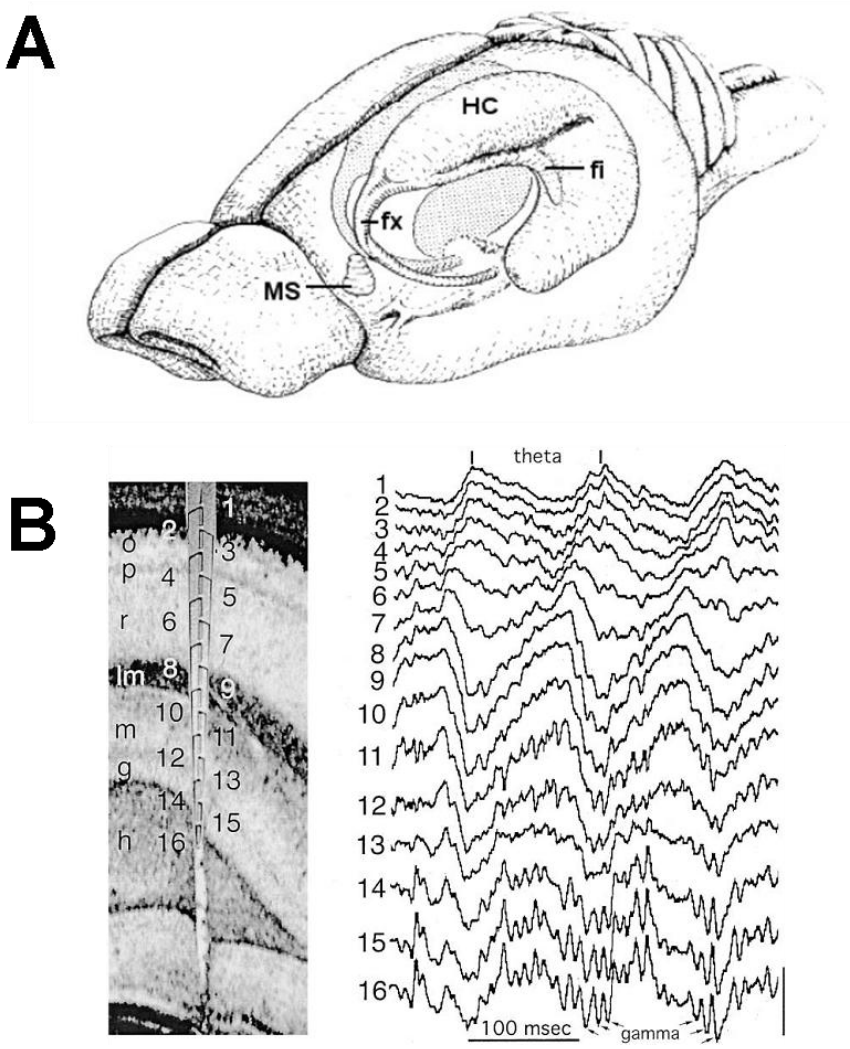

Figure 1.6 The hippocampus and theta oscillations.

A – A rodent brain showing the hippocampus (HC) and medial septum (MS), and associated fornix (fx) and fimbria (fi). B – The theta oscillation and superimposed gamma rhythm changes through the layers of the hippocampus. [Adapted from Buzsaki (2002)]

In the rat, pharmacological modulation of the cholinergic and GABAergic systems in the medial septum had significant effects on the theta oscillation observed during urethane anaesthesia (Smythe *et al.*, 1991) and during alert immobility (Lawson *et al.*, 1993). An important contribution to understanding theta regulation was made by Yoder and Pang (2005), who used neurotransmitter-specific lesions to reveal a dynamic concert of cholinergic and GABAergic neurotransmission in the medial septum. 192 IgG-Saporin destruction of cholinergic neurons and kainic acid destruction of GABAergic neurons, individually and in combination, vastly reduced

the power of the type-2 theta oscillation during urethane anaesthesia (Yoder *et al.*, 2005). These results support the view that theta activity requires a fine balance of excitation and inhibition.

A third, glutamatergic pathway also exists in the septohippocampal system, and may act as a bridge between type-1 and type-2 theta systems. Injections of NMDA into the hippocampus increased theta amplitude without affecting frequency, whereas NMDA infusions in the MS increased frequency and not amplitude (Bland *et al.*, 2007a). Correspondingly, MS infusions of the NMDA antagonist AP5 into the MS attenuated theta activity.

The exact mechanism for how systemic atropine blocks type-2 theta is unclear, since the temporal dynamics of muscarinic receptor activation in pyramidal cells is too slow to be a direct target (Hasselmo *et al.*, 2001). A more plausible target for muscarinic blockade are inhibitory interneurons in the MS (Freund *et al.*, 1988). In fact, the essential factor in type-2 theta might be cholinergically-mediated excitation of medial septum GABAergic cell bodies (via PLC and TASK-3 dependent intracellular mechanisms), which have been shown to lead hippocampal activity during the theta oscillation (Hangya *et al.*, 2009). This inhibition of hippocampal interneurons (Wu *et al.*, 2000) releases their inhibition on pyramidal cells so they can oscillate at theta frequencies.

1.3.3 The hippocampus and anaesthesia

Since the type-2 theta oscillation was first described in rodents anaesthetised with urethane, many studies have used the anaesthetised animal as a model system for an oscillating network, attempting to piece out the major molecular and cellular regulatory components.

However, the type-2 theta oscillation also appears during exposure to the volatile anaesthetic halothane, leading to the interesting hypothesis that the oscillation might have a functional relevance to inducing the anaesthetic state.

The Bland group has extensively studied the type-2 theta oscillation in response to halothane, showing that incremental increases in halothane concentration resulted in decreasing frequencies and increasing amplitudes of theta (Bland *et al.*, 2003). Importantly, this theta rhythm could be abolished by the muscarinic antagonist atropine indicating the involvement of cholinergic neurotransmission; however,

GABA-mediated inhibition by interneurons is also predicted to have a facilitatory role.

To maintain the type-2 theta oscillation over long periods or cycle between theta and non-theta states, a balance between excitatory cholinergic activity and inhibitory GABAergic activity must be reached during halothane anaesthesia. Since halothane uncouples gap junctions, direct electrical coupling between interneurons can be ruled out as a facilitatory mechanism for hippocampal synchrony.

A role for the hippocampus and the septohippocampal system in directly mediating anaesthetic states has not been extensively studied; however, there are several studies that suggest that might be the case. Potentiating GABAergic neurotransmission with muscimol injections in the MS or the hippocampus increased the potency of propofol, isoflurane and halothane (Ma *et al.*, 2002). That study also showed that the behavioural excitation induced on initial exposure to an anaesthetic (stage II or the delirium phase) and accompanying neurophysiological activation are attenuated by septohippocampal inactivation.

Further work in that lab showed that muscimol injections into the nucleus accumbens (NAc), ventral pallidum, supramammillary nucleus (SUM) and the ventral tegmental area (VTA) all potentiated the effects of anaesthesia. Interestingly though, inactivation of the median raphe had no effect (Ma *et al.*, 2006). Taken together, these results indicate a role for the entire limbic system in supporting the anaesthetic state; however, these studies measured anaesthetic potency on the basis of duration of loss of righting reflex, which has a significant pharmokokinetic component meaning that drug effects on respiration and metabolism cannot be ruled out. Indeed, there is evidence that anaesthetic induction and emergence comprise two asymmetric processes.

The major component of this theory is the orexinergic wake switch. Orexinergic neurons in the lateral hypothalamus are inhibited under isoflurane and sevoflurane anaesthesia to the same degree as in sleep, but selective ablation of orexinergic neurons does not affect anaesthetic induction. However, ablated orexinergic output delays emergence time, suggesting that orexinergic neurotransmission is an asymmetric wake switch (Kelz *et al.*, 2008).

The issue is slightly more complicated with the finding that halothane anaesthesia is neither accompanied by a reduction in orexinergic cell activity nor a

delayed emergence when these neurons are ablated (Gompf *et al.*, 2009). Additionally, there was no decrease in locus coeruleus firing rate during halothane anaesthesia, an effect considered fundamental to non-orexinergic dexmedetomidine anaesthesia, suggesting a different mechanism of action for halothane.

One potential target for halothane, as well as other anaesthetics, is the cholinergic system of the basal forebrain. One study showed that cholinergic lesions in the medial septum but not in the nucleus basalis magnocellularis (NBM) caused reduced acetylcholinesterase staining in the hippocampus and in the cortex and increased sensitivity to propofol (Laalou *et al.*, 2008). In contrast, another study, using a different measure of anaesthetic sensitivity, indicated that NBM lesions did enhance the effect of propofol on righting reflex (Leung *et al.*, 2011), whereas these lesions did not affect the duration of halothane LORR.

Muscimol injection into the same area increased the potency of propofol and halothane, as well as pentobarbital (Leung *et al.*, 2011). In addition, the delirium phase of both propofol and halothane anaesthesia was blunted by physical and pharmacological blockade of the system.

The authors of this study also make the interesting observation that although muscimol injection into the NBM caused neocortical slow wave activity, there was no behavioural sign of anaesthesia. This phenomenon has also been observed with atropine injection into the pontine reticular formation (Vanderwolf, 1988), suggesting dissociation between these two phenomena.

As well as inducing LOC, anaesthetics cause a range of other effects, including analgesia, immobility and amnesia. And here, there is evidence for the hippocampus and related theta oscillation as a functional target. Sub-anaesthetic doses of halothane impair contextual memory in fear conditioning with an EC50 of 0.14%, much lower than the concentration needed to induce LORR (Perouansky *et al.*, 2010). Accompanying this impairment was a reduction in hippocampal network frequency from 7.4 Hz to 6.9 Hz, which is just in the type-1 theta range. However, since there is evidence that type-2 and type-1 theta can exist simultaneously and the authors of this study do not ablate type-2 theta with atropine, a role for the lower frequency oscillation cannot be ruled out.

Given that isoflurane and nitrous oxide had similar effects on contextual memory and the theta oscillation, but are proposed to act at different molecular

targets, it appears that anaesthetic compounds might converge at the network level to exert their similar functional effects.

At least one of these many anaesthetic target sites is likely to be inactivation of cholinergic forebrain-hippocampal-cortical projections, since potentiation of this system reverses the decrease in cross-approximate entropy in the EEG (a marker for the number of active brain modules) caused by isoflurane (Hudetz, 2002; Hudetz *et al.*, 2003). How important this is in the direct switching between conscious states remains an open question.

1.4 Aims and hypotheses

This study first sought to gain a clearer understanding of the role of the type-2 theta oscillation in halothane anaesthesia. So far, previous research has focused on the cellular mechanisms responsible for producing type-2 theta, but no studies have investigated whether the oscillation itself is involved in mediating an anaesthetic state *per se*.

Contained within chapter 3 of this report is an analysis of the mouse EEG in response to halothane with relation to LORR. The possibility that the type-2 theta oscillation represented a state of sensory awareness was investigated by blocking it with systemic or central cholinergic antagonism. Would halothane sensitivity change as a result?

Chapter 4 set out to investigate the type-2 theta oscillation in TASK-3 KO mice. It is already known that TASK-3 KO mice have impairments in type-2 theta oscillations in response to halothane anaesthesia, but what about during normal behaviours?

The ability of TASK-3 KO mice to produce type-2 theta oscillations during the stereotyped behaviour of "alert immobility" was tested with predator-induced freezing. Working memory, object recognition and conditioning responses were also tested in TASK-3 KO mice.

The next part of this report aimed to investigate the role of septohippocampal TASK-3 channel expression in type-2 theta oscillations. Chapter 5 details the construction and validation of two Adeno-associated viruses (AAVs) that would express the TASK-3 gene in selective regions of the KO mouse brain. Would putting TASK-3 channels back into either the medial septum or the hippocampus (key regions in the type-2 theta mechanism) be enough to rescue the oscillation?

METHODS & MATERIALS

2.1 Animals

2.1.1 Basics

All experiments were carried out in accordance with the United Kingdom Animals (Scientific Procedures) Act of 1986 and have been approved by the Ethical Review Committee of Imperial College London. All mice were of at least 8 weeks of age and 20 grams in weight before surgery. C57Bl6 ordered from off-site distributors served as wild-type. TASK-3 KO mice were bred in-house from a line originally provided by Professor William Wisden (Imperial College, UK). Animals were housed in standard Plexiglas cages in humidity and temperature controlled conditions under 12:12 hour light:dark cycle. Male mice only were used for experiments and food and water were available *ad libitum*.

In addition, every effort was made to implement the 3Rs of best *in vivo* practice; namely, reduction, replacement, and refinement. With that said, the only way to model anaesthetic mechanisms accurately is by using the live animal.

2.1.2 Generation of TASK-3 knockout mice

TASK-3 KO mice were created by the Wisden Laboratory at the Ruperto-Carola University of Heidelberg, Germany, prior to the studies in this report. As described in Brickley *et al.* (2007), the TASK-3 gene was inactivated by combined homologous and insertional recombination. While the intended strategy was to flank exon 1 of the TASK-3 gene with loxP sites in the same orientation by homologous recombination and insert an frt site-flanked neomycin resistance gene cassette to serve as a positive selection marker for embryonic stem (ES) cell culture, the actual targeting event produced an insertion of 4 copies of the neomycin cassette and inverted repeats of the TASK-3 exon 1 into the TASK-3 locus. Although unconventional, this served to knockout the TASK-3 gene, as confirmed by *in situ* hybridisation.

2.1.3 Genotyping

DNA was extracted from ear punch samples by heating for 1 hour at 95°C in 50 µl 25 mM NaOH, 0.2 mM ethylenediaminetetraacetic acid (EDTA) (pH 12) and, once cooled to room temperature (RT), 50µl 40mM Tris (pH 5) was added. Samples were used immediately or stored at -20°C.

1 µl of DNA extract was added to 12.5 µl "Go Taq Green Master Mix" (Promega, UK), 1 µl DMSO and 10 µM primer mix* in a total volume of 25 µl. DNA was amplified in standard PCR conditions as follows: 5 minutes at 95°C, followed by 35 cycles of 1 minute at 95°C, 1 minute at 60°C and 1 minute at 72°C, then 5 minutes at 72°C and held at 4°C.

Each sample was then run on a 1.3% agarose gel containing SYBR-Safe (Invitrogen, USA) using TAE running buffer (from a 50x stock of 500 ml containing 121 g Tris base, 28.55 ml glacial acetic acid, 50 ml 0.5 M EDTA) and compared against a 1500 bp DNA ladder (Promega, UK). Gels were run for 1 hour at 90 V and visualised using a Kodak DC290 camera (USA), as in figure 2.1.

* TASK-3 genotyping primers:

The following primers were designed to flank the 5' loxP site of the TASK-3 KO, producing a 350 base pair (bp) amplification product for littermate (LM) and a 400 bp amplification product for TASK-3 KO.

Forward:

5'- CTC TGT CCC GGC TAC CGA TCC TGC-3'

Reverse:

5'-TTC CGT GGG CGC AGC GGG TTC CGC-3'

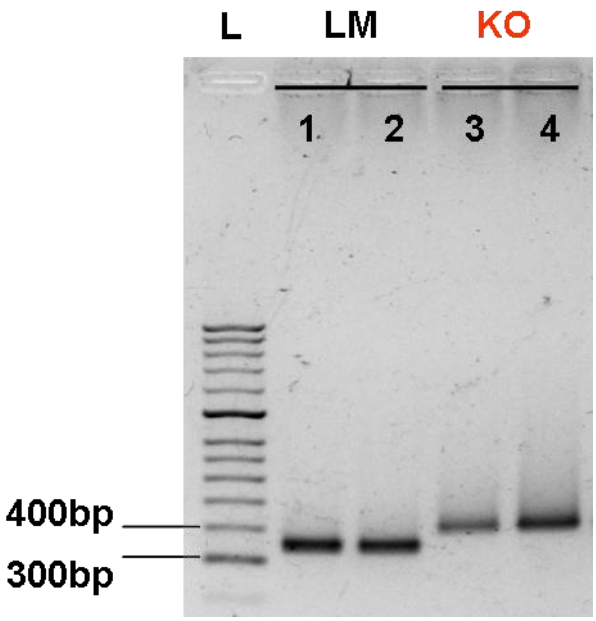

Figure 2.1 Genotyping results.

Genotyping separates homozygous TASK-3 KOs (KO: -/-) from homozygous littermates (LM: +/+) by a 50bp difference in the PCR amplification product. Heterozygotes (+/-) display as a double band at both levels (data not shown). [L = DNA ladder]

2.2 Surgery

2.2.1 Preparation

All surgical tools were sterilized in an autoclave or disposable sterile items were used where appropriate and aseptic technique was used throughout. After weighing the animal, anaesthesia was induced via intra peritoneal (i.p.) injection of a ketamine (80 mg/kg)/xylazine (15 mg/kg) mix or 2% halothane (Merial, UK). All drugs were made up in sterile physiological saline (0.9% w/v NaCl).

After loss of pedal withdrawal reflex the hair over the skull was clipped and lubricant was applied to the eyes (Lacri-lube, Allergan, UK). The animal was placed in a stereotaxic frame (Harvard Instruments, USA) and 0.5 ml saline (0.9% w/v NaCl) was administered subcutaneously to compensate for fluid loss during surgery. An incision was made along the midline over the skull and the retracted skin was held in place by suture material. The periosteum was removed and the skull area was cleaned and dried. The stereotaxic frame and arm enabled the precise localisation of electrode/cannula/needle positions relative to bregma and lambda.

2.2.2 ECoG instrumentation

Mice were instrumented with ECoG and EMG (electromyography) recording electrodes. Using a stereotaxically-mounted drill (Fordham, USA) three holes were drilled for the EEG electrode 1 (-1.5 mm Lambda, 0 midline), EEG electrode 2 (+1.5 mm Bregma, -1.5 mm midline) and reference electrode (-1.5 mm Bregma, +1.5 mm midline). Gold-plated screws were inserted into the holes and connected to an electrode rig via insulated wires, as in figure 2.2A. Three flexible insulated wires with the tip exposed were sutured into the nuchal muscles of the neck and served as EMG electrodes. The exposed area was sealed and protected with Orthoresin dental cement (Dentsply, Australia).

2.2.3 Medial septum cannulation

For acute administration of drugs to the septohippocampal system, mice were instrumented with cannulas into the area above the medial septum. 27-gauge stainless steel tubing (Small Parts Inc., USA) was cut to 13 mm and stereotaxically implanted so that the tip was located 3 mm above the medial septum itself (+0.80 mm Bregma, midline, -2.0 mm DV). The exposed tip of the cannula was protected by a plastic guard and a 32-gauge stainless steel stylet was placed into the cannula. Correct cannula placement was confirmed in fixed and sliced tissue after the experiments.

2.2.4 Adeno-associated virus (AAV) delivery

AAVs were prepared for injection by mixing the purified sample (See ***2.6.4***) with an equal volume of 20% D-mannitol (to aid virus dispersion) and a small amount of blue dye (to aid visualisation) and drawn into a glass tip. After securing the animal in a stereotaxic frame attached to a PC, Leica Angle Two software (Germany) enabled the calibration of the whole brain with a built-in mouse brain atlas. Using bregma and lambda as reference points, holes were drilled over the injection sites and the glass tip was lowered into the correct position according to the coordinates below (mm relative to bregma).

	Mediolateral	Anterioposteriar	Dorsoventral
Medial septum:	0.00	+0.86	-4.70
Left hippocampus:	-1.35	-1.94	-1.49
Right hippocampus:	+1.35	-1.94	-1.49

2.2.5 Post-operative care

Prior to anaesthetic recovery 30 µg/kg buprenorphine (Alstoe Animal Health, UK) was administered subcutaneously for post-surgical analgesia. In addition, for 7 days following surgery, carprofen (Rimadyl, Pfizer Animal Health, USA) for analgesia and enrofloxacin (Baytril 2.5%, Bayer, Germany) for prophylaxis were diluted in the drinking water (100 ppm). At least 7 days was allowed for recovery before further experiments.

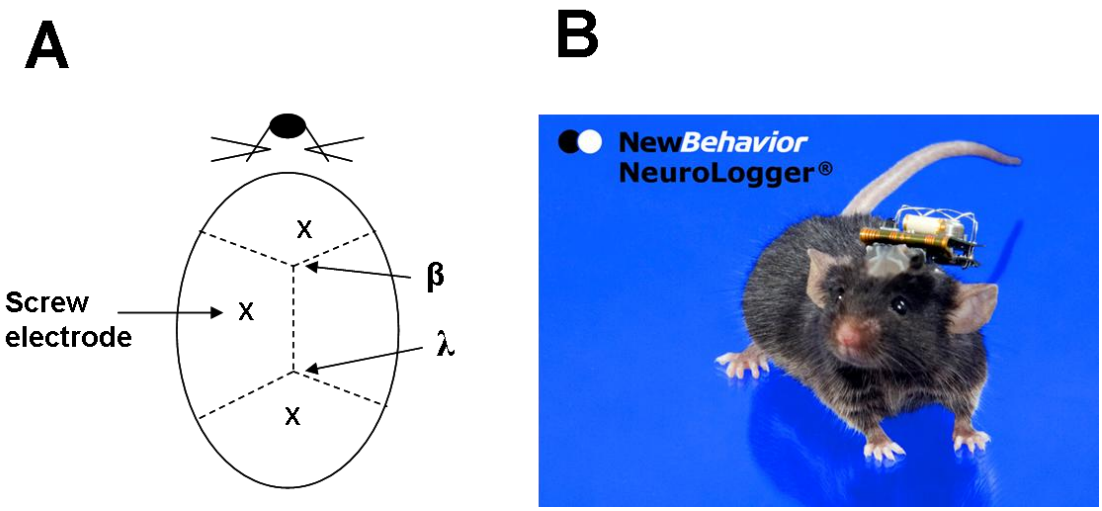

Figure 2.2 Electrocorticography using the Neurologger.

A – Stereotaxically implanted screw electrodes, marked with an "x", detect activity from the surface of the cortex. B – The Neurologger is a tether-free recording device that can monitor brain and muscle activity in any environment.

2.3 Electrocorticographic (ECoG) recording

2.3.1 Recording technique

Electrocortigography (ECoG) is a subtype of electroencephalography (EGG) that involves recording global field potentials from the surface of the brain. ECoG provides a measure of the summated electrical activity of many thousands of neurons, depending upon the electrode configuration, giving a gross representation of the brain state over millisecond timescales.

In this study, screws overlying the cortical dura (See 2.2.2) detected potentials representative of distributed cortical and subcortical activity, which were recorded on a lightweight and tetherless device, the Neurologger (NewBehaviour, Switzerland).

The Neurologger (Figure 2.2B), designed and built by Dr Alexei Vyssotski (University of Zurich, Switzerland), is an autonomous wireless device capable of recording up to four electrical signals in an internal 256 Mb memory chip. Weighing only 2 grams, the Neurologger can be docked onto the electrode rig of the animal to provide in excess of 24 hours of recordings. The Neurologger has a sampling frequency of 200 Hz and has an internal bandpass filter between 1 and 70 Hz. After collection, data was transferred to a PC for analysis using Spike2 Version 5.14 (Cambridge Electronic Design, UK).

Typically, two ECoG signals were recorded from screw electrodes over the frontal and parietal cortices, relative to a common reference electrode over the occipital lobe. Two EMG signals were recorded from solder-tipped wire electrodes fixed into the nuchal muscles of the neck, relative to an adjacently positioned reference electrode wire.

2.3.2 ECoG data analysis using fast Fourier transforms

When plotted as a time series of potential differences, the recorded ECoG signal shows characteristic oscillatory patterns depending on behavioural and arousal state that can be defined by frequency (in Hertz), relative and absolute amplitude (in Volts) and shape (Figure 2.3A). The frequency component (as well as the attendant amplitude) can be analysed by the fast Fourier transform (FFT).

The FFT is a computationally faster version of the discrete Fourier transform (DFT), both of which are algorithms that decompose a sequence of values, which in the case of ECoG is a time series of potential differences, into its component frequencies. Depending upon the parameters of the algorithm, the power (square of the amplitude) of the signal in defined frequency bins can be plotted as a power spectrum. The power spectrum provides a visual representation of the proportions of recorded brain frequencies present within the defined time epoch (Figure 2.3B).

The ECoG recordings in this study were analysed using the Hanning window FFT in Spike2 Version 5.14 (Cambridge Electronic Design, UK). Frequency binning depended upon the length of the time epoch. Stable, long term oscillations, in the minutes range, were analysed using 512 bins over 100 Hz giving a frequency resolution of 0.1953 seconds. Very short epochs, on the order of a few seconds, sacrificed frequency resolution for time resolution, as appropriate. Lorentzian curves were fitted to the power spectra using Origin 5.0 (Microcal, USA).

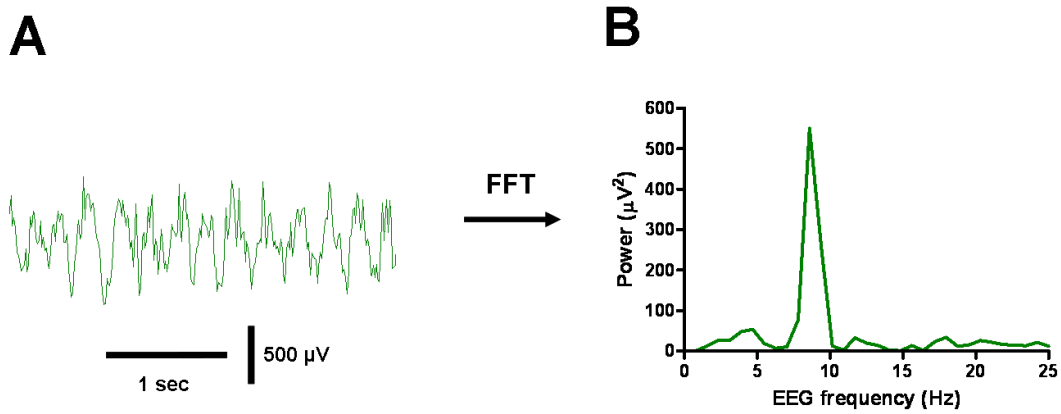

Figure 2.3 Fast Fourier transforms of the electrocorticogram provide a visual way to inspect the prominent resonant oscillatory frequencies.

A – The electrocortical waveform of a running mouse shows activity of varying frequency and amplitude. B – Deconvoluting the electrocortical time-series using FFTs shows a prominent oscillation at 9 Hz indicative of a moving animal.

2.4 Anaesthetic experiments

2.4.1 Halothane LORR

Six wild-type mice were used to test the effect of increasing halothane ($C_2HBrClF_3$) concentration on the ECoG. After docking the Neurologger onto the animal, and i.p. injection of saline or 50 mg/kg atropine sulphate (a muscarinic antagonist), the animal was placed in a cylindrical glass jar (volume ~1000 ml). Medical oxygen (BOC, UK) was fed through a vaporiser at a flow rate of 2 L/min, controlled by a regulator. After 10 minutes, the halothane concentration was increased to 0.4% and then further increased by 0.1% every 10 minutes until 1.5%. At the end of each concentration step the ability of the animal to right itself after being placed in the supine position was tested by gently turning the glass jar until the animal was on its back (Figure 2.4). The score was judged as a negative righting response if the animal remained on its back for 30 seconds or longer. Experiments on the same animal were separated by at least one week. Anaesthetic concentrations were measured throughout by a Capnomac II (Datex, Finland).

2.4.2 Medial septum injections

The ECoG was recorded in six wild-type mice that received medial septum microinjections of various pharmacological agents while anaesthetised with halothane. After 10 minutes of baseline recording in the glass jar, halothane was introduced at a sub-anaesthetic concentration; e.g., 0.6%. After 10 minutes the halothane concentration was increased to anaesthetic levels, that is, for LORR to occur; e.g., 0.8-1.0%. After ~20 minutes at this level, either 40 µg lidocaine or 50 µg atropine sulfate or artificial cerebrospinal fluid (aCSF) vehicle was injected into the medial septum. The animal was swiftly returned to the anaesthetic vapour and left for up to 1 hour. One week was allowed between drug exposures.

The halothane LORR in response to pre-administration of medial septum aCSF or 50 µg atropine sulfate was measured as described above (See 2.4.1), with simultaneous ECoG recording.

2.4.3 Halothane delirium

The effect of modulating systemic cholinergic neurotransmission on halothane-induced behavioural excitability was investigated as follows. Wild-type mice were injected i.p. with either saline vehicle (control), 50 mg/kg atropine sulfate or 0.2 mg/kg eserine/physostigmine (a cholinergic enhancer) and placed into a sealed Med Associates Activity Monitor System (USA) for 30 minutes before 2% halothane in medical oxygen was introduced at a rate of 4 L/min for a further 10 minutes.

The activity monitor consists of a 28 cm x 28 cm x 20 cm box with perpendicular infrared beams running along the base, which are broken as the animal moves around the box and are recorded as a series of coordinates. The distance travelled was binned into 30 second epochs and correlated with ECoG activity.

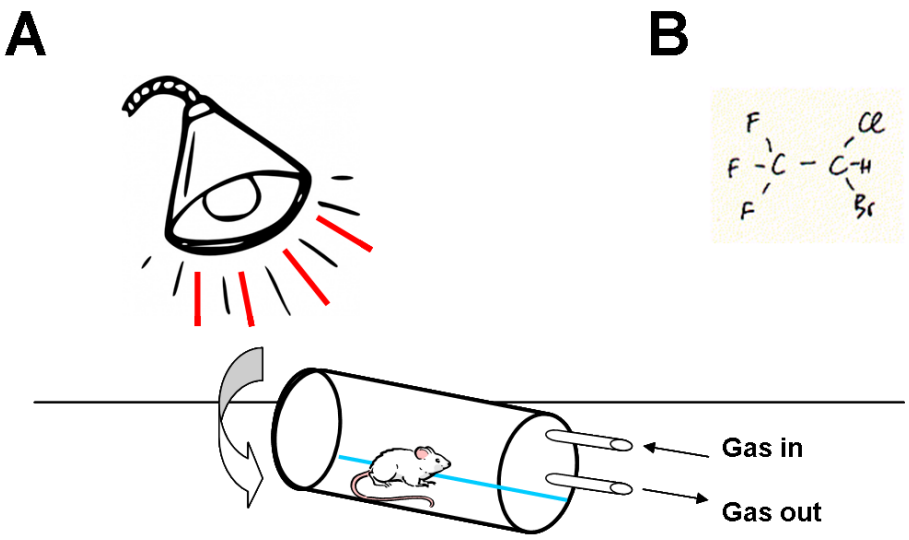

Figure 2.4 The loss of righting reflex is tested in response to increasing concentrations of halothane.

A – The thermoregulated cylindrical chamber is turned gently to measure loss of righting reflex in response to the application of halothane (B).

2.5 Behavioural experiments

2.5.1 Video tracking and Neurologger synchronizing

In addition to locomotor tracking using the Activity Monitor (Med Associates, USA), video tracking methods were also developed. The advantages of video tracking are numerous: firstly, video tracking is more accurate; and secondly, the locomotion arena can be changed to any shape required.

Videos were recorded using a Logitech webcam (Switzerland) on Debut Video Capture (NCH Software, USA). Video files were analysed using SwisTrack tracking software (Switzerland) which uses contrast separation to find the centre of mass of a moving object over time. The "real world" dimensions and speed of the mouse can be calculated from these co-ordinates.

This tracking data can be synchronised with the neurophysiological data collected on the Neurologger by exposing the grounded Neurologger to an electromagnetic pulse from a signal generator that simultaneously turns on a light emitting diode (LED). The "spike" created in the Neurologger signal can then be aligned with the light that appears on the video. In this way, the ECoG trace can be analysed according to periods of different behaviour selected from the video, tracking output and EMG information.

2.5.2 Rat exposure test

The rat exposure test is a validated paradigm for measuring natural defensive behaviours in mice (Yang *et al.*, 2004). The test involves exposing a mouse to the sight and smell of a natural predator, i.e. a rat, to illicit stereotyped behaviour. Different strains of mice have different responses to the test indicating a strong genetic predisposition. The test apparatus, modified from Yang *et al.* (2004), consists of a transparent glass tank measuring 60 cm x 30 cm x 30 cm, housed in a sound attenuating chamber under low background light levels, separated into two compartments by a wire mesh grill and removable black screen (Figure 2.5).

Each test session was video-recorded as described previously and saved on a PC. Neurologgers were attached to five TASK-3 KO mice and seven littermate mice before being individually habituated to one of the compartments for 10 minutes for four consecutive days. On the next day, each mouse was again placed in the same compartment. A Sprague Dawley rat was introduced to the other compartment behind a screen and after 2 minutes the screen was removed. The test continued for another 10 minutes. The amount of behavioural freezing of the mice was compared in the pre- and post-stimulus sessions and between genotypes. The cage was cleaned with a 10% ethanol solution between animals. All tests were conducted during the dark phase of the light/dark cycle under low level ceiling lights.

Freezing was scored blinded using a threefold method after the experiment. Once the data file for the video tracking had been aligned with the Neurologger data, episodes of movement and freezing could be isolated. Movement was scored when the (filtered and smoothed) EMG was high and the speed of the animal was above 2 cm/s, whereas freezing was scored when the EMG was flat and the speed was 0 cm/s. The video was double-checked to ensure that correct behaviours had been identified. Three 2-second epochs of ECoG for each behaviour and animal were analysed using FFT, giving an average power spectrum for each genotype and behaviour.

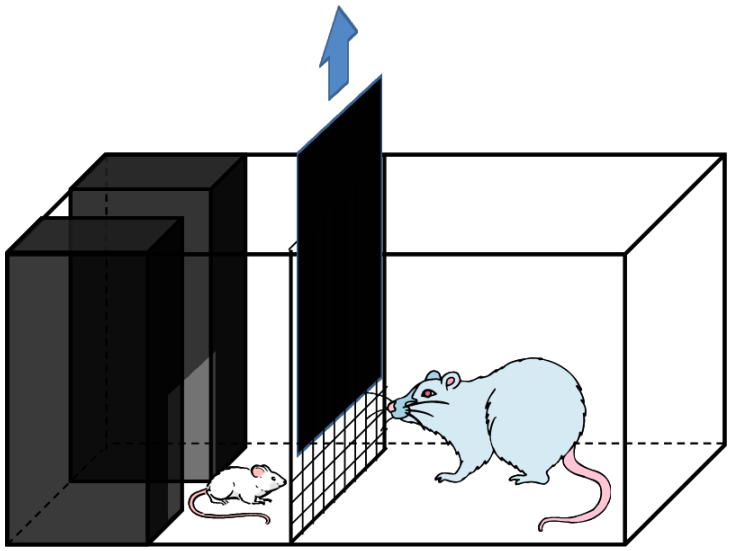

Figure 2.5 The rat exposure test elicits freezing behaviour in mice.

On exposure to a rat in a previously neutral environment a mouse will perform a variety of defensive behaviours including freezing (alert immobility). [Adapted from Albieri (2009)]

2.5.3 Spontaneous alternation in the T-maze

The spontaneous alternation test utilises the mouse's innate disposition to explore novelty. Using a T-shaped maze, a normal animal, when released from a holding chamber at the base of the T, will spontaneously alternate between two choice-arms at the top of the T and deficits in working memory manifest as a reduction in alternation rate (Gerlai, 1998).

The T-maze was made bespoke in grey plastic and consists of three horizontal arms in the shape of a T surrounded by a wall 15 cm high. The start arm (the base of a T-shape) measures 50 cm before splitting into two perpendicular arms, each measuring 50 cm. Slotted panels allow guillotine doors to be placed as desired throughout the maze.

Animals were acclimatised to a featureless test room for two consecutive days prior to the test. On the test day, animals were run individually and the maze was cleaned with 10% ethanol and thoroughly dried before the next subject. The mouse was placed in the base of the start arm in a compartment made by a guillotine door 15 cm along the arm. After 30 seconds, the door was opened and the mouse was free to explore one arm of the T-Maze in a "training" trial (the other being blocked off by a door). Once the animal returned to the start position, the door was closed behind it. After 15 seconds, the door was re-opened allowing the animal to explore either arm in the "test" trial (the blocking door having being opened). Once the animal entered one arm it was briefly confined to allow the other door to be blocked off, preventing entry to this arm. The animal was released and the process was repeated for 10 similar "test" trials (Figure 2.6).

A correct score consisted of the animal choosing the arm that it did not enter on the last trial and, after validation in C57Bl6 mice, the percentage correct alternation was compared between 9 TASK-3 KOs and 11 littermate controls, with the genotypes blinded to the experimenter.

It was especially important in this test to avoid giving any unconscious cues that might bias the decision of the mouse. To ensure that this was the case, the maze was set up in a featureless alcove, with symmetrical surroundings and uniform lighting conditions. The experimenter also made symmetrical movements when removing the doors from each arm (one being a "fake" door removal).

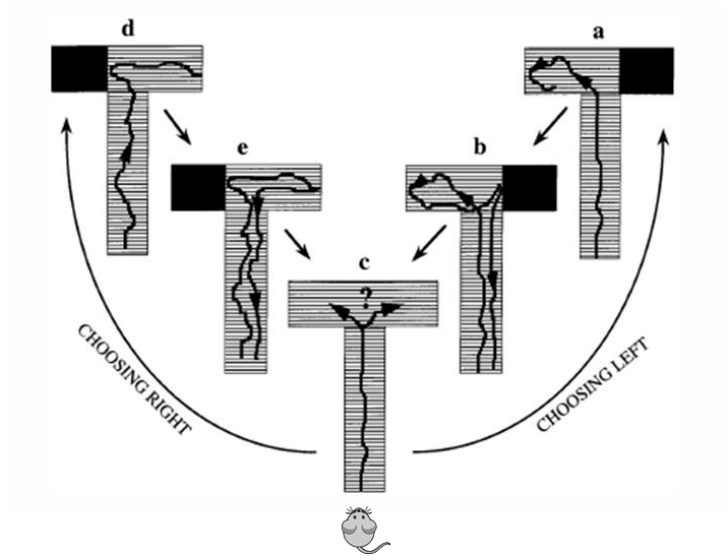

Figure 2.6 The spontaneous alternation T-maze measures working memory. *If the mouse chooses left (a), the opposite arm is blocked (b) and it returns to the start with a free choice (c). With an intact working memory the mouse will seek to explore the novel right arm (d) before repeating the process. [Adapted from Gerlai (1998)]*

2.5.4 Object recognition test

The object recognition test is designed to evaluate object memory, a hippocampus-dependent task. The test consists of three phases, all recorded on video: in the first session mice were habituated to an open field (i.e., the Activity Monitor) for 10 minutes and then placed in a holding cage for an inter-trial period; in the second session two identical novel objects were placed in the open field and the mouse was returned for 10 minutes exploration before being placed in the holding cage; in the third session – either on the same day, to measure short term memory, or on the next day, to measure long term memory – one of the objects was changed and the mouse returned for a further 10 minutes exploration (Figure 2.7).

Object interaction – classified as nose touching the object – was scored using Ethom behavioural analysis software (Taiwan) and the total time of interaction was compared between objects, sessions and genotype. The resulting interaction ratio between the novel and familiar object ($T_{\text{novel object}} / (T_{\text{novel object}} + T_{\text{familiar object}})$) provides a measure of learning, with increased interaction with the novel object deemed to be the best performance. The cage was cleaned with a 10% ethanol solution between animals. All tests were conducted during the dark phase of the light/dark cycle under low level ceiling lights.

The test was first validated using four C57Bl6 mice, a process that took several cohort iterations to produce the strongest results. It was found to be important to handle the mice for several days before the test. This acclimatised the animals to being transferred from cage to arena, desensitising them to smells and surroundings that might provoke anxiety, a confounding factor to any experiment that relies on investigation of novelty.

The choice of objects also required optimisation for maximising interaction. This was achieved by choosing objects with angles and drilling holes into the sides of the objects, to create interesting areas that would elicit exploration. Another major consideration was to make sure that one object was not more interesting than the other. A separate cohort of mice was tested for object preference, ensuring that each object was of equal interest

Only then was it possible to investigate TASK-3 KO (n = 14) and littermate mice (n = 10) in a double-blind protocol.

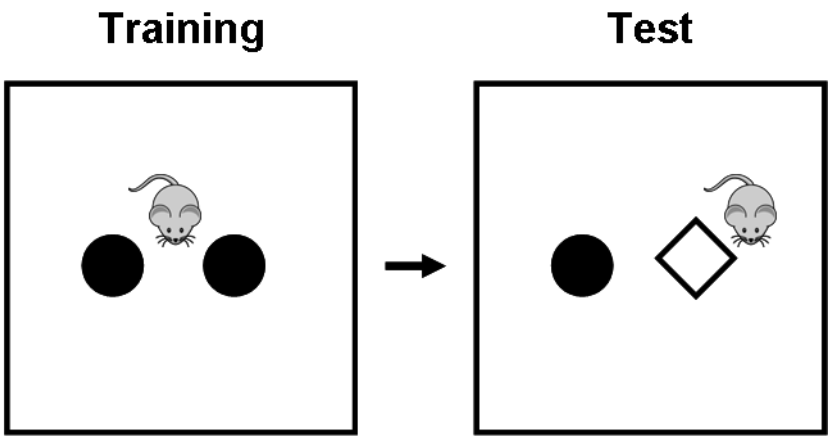

Figure 2.7 The object recognition test measures short-term and long-term memory function.

In the training phase, the mouse is exposed to two identical objects. When one of the objects is swapped for a novel one in the test phase, a mouse that recognises the change will interact with the new object for longer.

2.5.5 Spatial recognition test

The spatial recognition test is a variant of the object recognition test that exposes the animal to five different objects instead of two identical ones and then displaces one or more of the objects. Objects in a novel location are expected to attract greater attention and interaction (Figure 2.8).

After several days of handling to reduce the mice's anxiety levels, the test was validated in four C57Bl6 mice and then performed in TASK-3 KOs and littermates (n = 7), in a double-blind protocol. Each mouse was exposed to the circular test arena (60 cm diameter) five times for 10 minutes each, separated by 3 minutes inter-trial time in the home cage. The first exposure consisted of the empty arena; in the second, third and fourth exposures the animals were free to explore five novel objects in fixed positions in the arena. On the fifth and final exposure, two of the objects were moved into new locations.

Interaction with the objects was scored as for the object recognition test, in all phases of the experiment. In the test phase, increased interaction with the objects in new spatial locations was judged as intact memory processing. However, there is also information in the training phase of the experiment, since any impairment in memory acquisition may manifest as a failure to habituate to the objects.

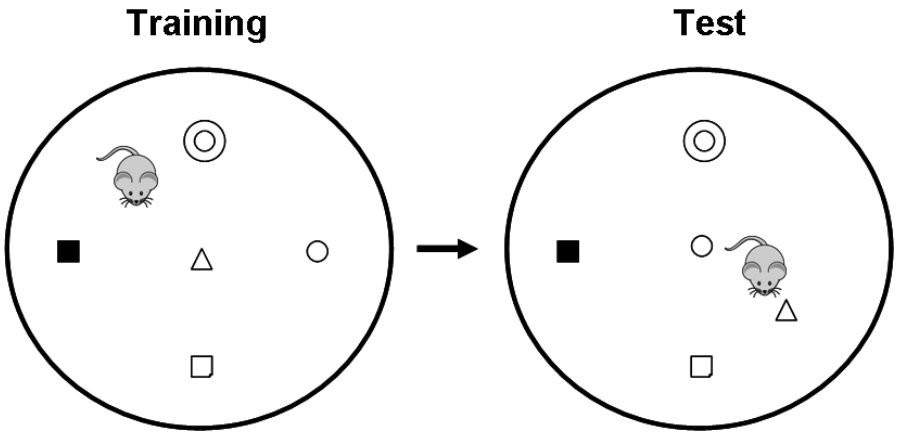

Figure 2.8 The spatial recognition test measures the response of a mouse to a changed topographic environment.

After exposure to the test arena, a mouse with intact hippocampal function should explore the displaced objects for longer than the non-displaced objects.

2.5.6 Dropbox

The dropbox is a novel Pavlovian conditioning paradigm that involves training the animal over two days to associate a 10 kHz tone and the contextual environment with the release of a trapdoor and a plunge into a water pool. This aversive unconditioned stimulus is similar to the electric shock of traditional fear conditioning tests but is preferable because it is a more naturalistic stimulation and avoids painful and stressful manipulations. A probe test is performed on the third day to measure long-term contextual and cued learning. The proportion of alert immobility correlates with environmental awareness and memory recall (Figure 2.9).

The test apparatus consists of a bespoke dropbox (10 cm x 10 cm x 30 cm) made from red transparent plastic, and housed in a sound attenuating chamber under red light. On training days 1 and 2, individual mice were placed inside the dropbox and after 180 seconds of acclimatisation a 10 kHz tone was presented for 10 seconds. With the cessation of the tone, a "trapdoor" was released, dropping the animal into a 6 cm deep pool of water. White tempura paint masked the bottom of the box. After 5 seconds of swimming the trapdoor was replaced and the mouse was "rescued". After an inter-trial period of 30 seconds, there was another tone and drop, and this was repeated for 6 tones in total. A probe test was performed on day 3 with a similar acclimatisation phase of 180 seconds in the drop-box. Freezing behaviour in this phase correlates with contextual memory recall. To test cued conditioning, four 30 second tones are presented with 30 second intervals in a novel chamber. Solid surfaces were cleaned with a 10% ethanol solution prior to the first animal and between subsequent animals in each case.

Freezing was scored on video playback by a blinded observer and, after validation in C57Bl6 mice (n = 4/6), the test was performed in TASK-3 KO mice (n = 6) and littermate controls (n = 7). Additionally, the effect of cholinergic blockade on dropbox memory acquisition was tested by pre-treating one group of C57Bl6 mice with 50 mg/kg atropine sulfate i.p. prior to each training day. To confirm that the dropbox environment itself did not elicit freezing, a cohort of mice were placed in the dropbox without the water drop.

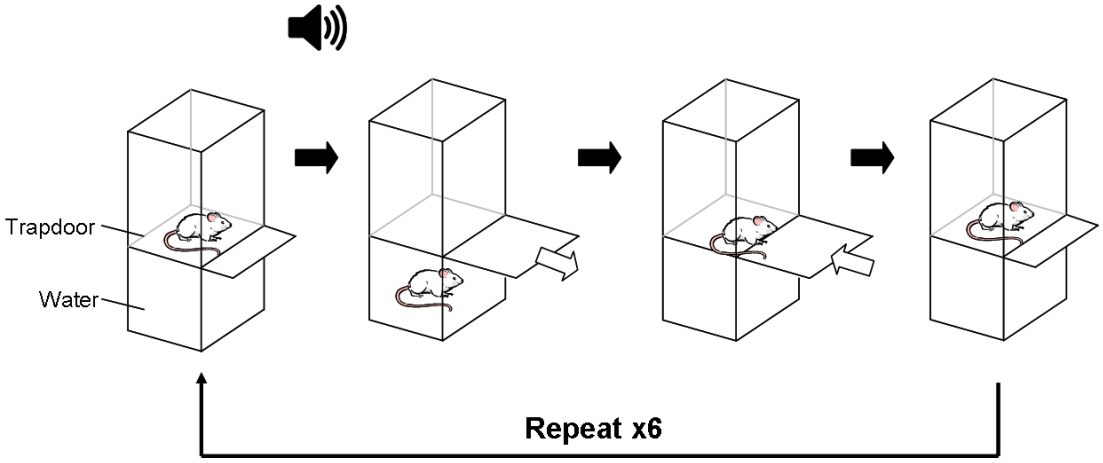

Figure 2.9 The dropbox measures aversive memory behaviour.

A mouse learns to associate a tone and an environmental context with a water-drop and will freeze when placed in the same context or exposed to the tone in expectation (fear) of the aversive stimulus.

2.5.7 Orientation response test

To test the homeostatic orientation response, purported to involve type-2 theta-related processes (Shin, 2010), a bespoke motorised circular platform was made. The platform consisted of a plastic turntable with a diameter of 10 cm, which was driven inside a stationary drum measuring 12 cm high, by a 3 V bi-directional motor.

Mice were habituated to the apparatus for a few minutes on several days before the test and then the platform was rotated at 20 rpm for one minute each in the clockwise and anti-clockwise direction. The extent of the orientation response was measured by the turns in the same direction as the rotation in TASK-3 KO (n = 5) and littermate mice (n = 4). One week later, the same mice were pre-treated with 50 mg/kg atropine sulfate i.p. to elucidate the effect of antagonising cholinergic neurotransmission on turning behaviour.

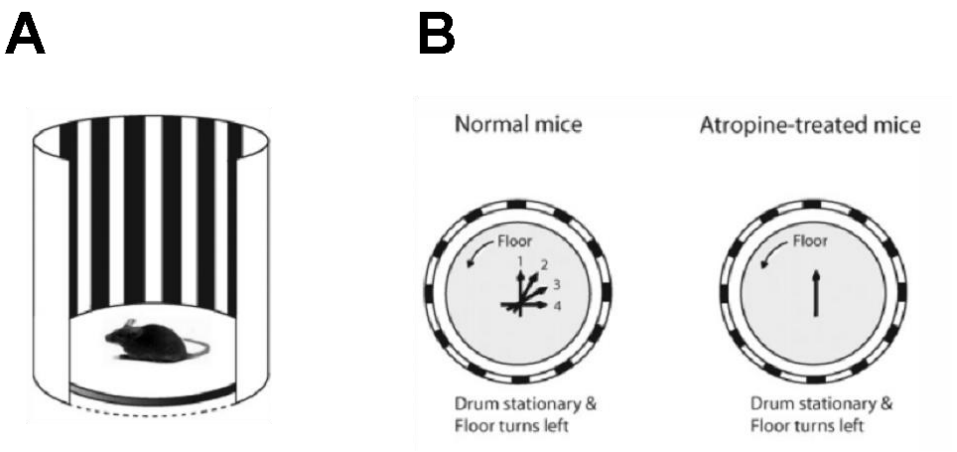

Figure 2.10 The orientation response is a homeostatic behaviour indicative of normal sensorimotor processing.

A – The mouse is placed in a rotating drum and its behaviour is monitored. B – Normal mice will perform an "orientation response" in the direction of the movement, whereas atropine-treated mice lack this behaviour. [Adapted from Shin (2010)]

2.6 Adeno-associated virus production

2.6.1 Overview

To introduce the TASK-3 gene back into discrete regions of the TASK-3 KO mouse brain two recombinant Adeno-associated viruses (rAAVs) were designed and made. One of them would express, under a pan-promoter, the TASK-3 gene and an enhanced green fluorescent protein (eGFP) marker (eGFP-2A-TASK-3 rAAV); the second would contain cyclization recombinase (Cre) and flippase (Flp) transgenic elements that aimed to restore endogenous expression levels (Cre-2A-Flp rAAV).

2.6.2 eGFP-2A-TASK-3 rAAV

Overview

The TASK-3 gene was amplified from a pDNA3 plasmid using polymerase chain reaction (PCR) with primers containing ApaI and HindIII restriction endonuclease (RE) sites and the purified product was digested with the appropriate RE and ligated into a similarly cut plasmid adjoining a 2A co-translation cassette and eGFP. The eGFP-2A-TASK-3 fragment was amplified by PCR using primers with NotI and HindIII sites in the forward and reverse primers, respectively. This fragment was then ligated into an AAV vector between inverted terminal repeat (ITR) motifs.

This new plasmid construct was co-transfected with pFΔ6, pH21 and pRV1 helper plasmids into human embryonic kidney (HEK)-293 cells that act as a "production factory" for the rAAV particles. The cells were harvested, lysed and the rAAV particles were captured on a heparin sulphate column before collection.

TASK-3 amplification

The TASK-3 gene was amplified from a pDNA3 plasmid using PCR with primers containing ApaI and HindIII RE sites.

1µl plasmid template (mTASK-3 in pDNA3) was added to 25 µl "Go Taq Green Master Mix" (Promega, UK), and 10 µM primer mix* in a total volume of 50 µl. DNA was amplified in standard PCR conditions as follows: 5 minutes at 95°C, followed by 30 cycles of 1 minute at 95°C, 1 minute at 55°C and 1.5 minutes at 72°C, then 5 minutes at 72°C and held at 4°C until later use.

5 µl of each sample was then run on a 0.8% agarose gel containing SYBR-Safe (Invitrogen, USA) using 1x TAE running buffer and compared against a 1500 bp DNA ladder (Promega, UK). Gels were run for 1 hour at 90 V and visualised using a Kodak DC290 camera (USA).

The amplified product was purified using MinElute gel extraction kit (Qiagen, Netherlands) and, since Taq polymerase adds an adenine nucleotide onto the PCR product, it was then ligated into TOPO vector (Invitrogen, USA). The TASK-3 TOPO vector was transformed into *E.coli* XL-1 blue competent cells (Agilent Technologies, USA) via the heat shock method (30-60 s at 42°C and 2 minutes on ice) and grown on Luria broth (LB) agar plates with 100µl/ml ampicillin overnight at 37°C. Single colonies were selected and innoculated in LB broth for overnight incubation at 37°C.

Cells were spun down at 4100 rpm, the supernatant was discarded and the vector DNA was collected using Genelute plasmid miniprep kit (Sigma, USA). Correct TASK-3 TOPO vectors were confirmed through gel electrophoresis of ApaI/HindIII double digests and DNA sequencing (Eurofins MWG Operon).

Further details of the TASK-3 gene can be found at:
http://www.ensembl.org/Mus_musculus/Gene/Summary?g=ENSMUSG00000036760;r=15:72342549-72376709;t=ENSMUST00000044624

*TASK-3 amplification primers:

All primers were manufactured by Sigma (USA). The following primers contain the beginning and end of the TASK-3 transcript, as shown by the italicised nucleotides, in the forward and reverse primers, respectively. Emboldened nucleotides represent the ApaI RE site in the forward primer and the HindIII RE site in the reverse primer. Extra A and T nucleotides were added to the extremities to improve RE activity.

Forward primer:

5'-ATA TAT **GGG CCC** *ATG AAG CGG CAG AAC GTG C*-3'

Reverse primer:

5'-ATA TAT **AAG CTT** *TTA GAT GGA CTT GCG ACG GAG GTG C*–3'

TASK-3 sub-cloning

The next step involved sub-cloning the TASK-3 into a vector containing eGFP, to allow for visualisation of expression. This vector, peGFP-2A-$GABA_A$-γ2, was constructed in-house to contain eGFP linked to a 2A co-translation cassette linked to $GABA_A$-γ2. By design, the $GABA_A$-γ2 component contained at its beginning an ApaI RE site and at its end a HindIII RE site to allow for easy sub-cloning.

Two separate digestions, (1) with the TASK-3 TOPO vector and (2) with the peGFP-2A-$GABA_A$-γ2, were carried out under the same conditions. The respective vectors were incubated for 2 hours at 37°C with ApaI and HindIII (NEB, USA) and then the enzymes were inactivated by heating to 65°C for 20 minutes. Then, to prevent re-ligation of the peGFP-2A-$GABA_A$-γ2 with its digestion product, the peGFP-2A-$GABA_A$-γ2 mixture only was dephosphorylated with shrimp alkaline phosphatase (NEB, USA) for 1 hour at 37°C, before another heat inactivation step.

Samples of the mixtures were run on gels to confirm complete digestion and then the digestion products were mixed in a total volume of 10µl ddH_20 in a ratio of 3:1, TASK-3 insert:peGFP-2A backbone, such that the total DNA did not exceed 200ng. T4 ligase was added as part of the "Rapid Ligation Kit" procedure (Roche, Germany) and the mixture was incubated at room temperature (RT) for 20 minutes, before transformation into competent *E.coli* cells. DNA was prepared as discussed previously and correct ligation products confirmed through digestion and sequencing.

eGFP-2A-TASK-3 sub-cloning

The eGFP-2A-TASK-3 fragment was amplified by PCR using primers* containing a NotI RE site in the forward direction and the previously used reverse primer containing a HindIII RE site. After purification, the PCR fragment was ligated into the multiple cloning site of an empty pAM-flex AAV vector (originally provided by K. Deisseroth, Stanford University, USA) following similar procedures as outlined previously and correct ligation products confirmed through digestion and sequencing. The pAM-flex AAV vector contains two loxP sites flanking the transgenes to allow for Cre-based switching. This means that a transgene inserted in the reverse (nonsense) orientation can be turned on conditionally in the presence of Cre (which is itself usually under the control of a cell-specific promoter). Transgenes inserted in the forward (sense) position will be expressed constitutively as per the pAM-flex promoter.

A schematic of the workflow for the eGFP-2A-TASK-3 rAAV can be found in figure 5.2 in the results and discussion section.

* eGFP-2A-TASK-3 amplification primers:

The following primers contain the beginning of the eGFP transcript and the end of the TASK-3 transcript, as shown by the italicised nucleotides, in the forward and reverse primers, respectively. Emboldened nucleotides represent the NotI RE site in the forward primer and the HindIII RE site in the reverse primer. An extra cytosine nucleotide was added to the forward primer to reproduce the Kozac sequence that improves translational recognition. Extra A and T nucleotides were added to the extremities to improve RE activity.

Forward primer:

5’-ATA TAT **GCG GCC GC**C *ATG GTG AGC AAG GGC GAG G*-3’

Reverse primer:

5’-ATA TAT **AAG CTT** *TTA GAT GGA CTT GCG ACG GAG GTG C*–3’

2.6.3 Cre-2A-Flp rAAV

Overview

As an alternative strategy, the nature of the TASK-3 knockout (Figure 2.11) meant that it had the potential to be rescued by Cre and Flp genetic modification; and so, an rAAV containing Cre and Flp was made (See results section for further details). Briefly, an rAAV plasmid containing Cre linked to Venus by a 2A cassette was acquired and the Venus element was excised and replaced by the Flp gene, creating a Cre-2A-Flp rAAV plasmid. Similar methodology was used as for eGFP-2A-TASK-3 rAAV plasmid production and hence some details have been omitted in the following section for the Cre-2A-Flp rAAV production.

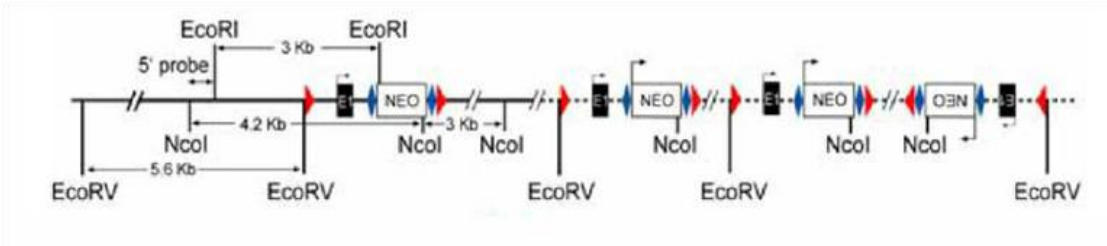

Figure 2.11 TASK-3 gene inactivation in the knockout.

The TASK-3 gene is inactivated by a series of multiple neomycin (NEO) inserts. Serendipitously, the TASK-3 gene can be "activated" through Cre- and Flp- based transgenesis. [Adapted from Sandu (2006)]

Flp amplification

The Flp sequence was amplified from pPGUFLPobpA using primers* with a BamHI restriction site in the forward direction and a NotI restriction site in the reverse direction, using similar PCR conditions as previously. The sample was then digested by both of the enzymes and, after confirmation of the correct product by gel electrophoresis, was purified for subsequent use.

*Flp amplification primers:

Emboldened nucleotides represent the BamHI RE site in the forward primer and the NotI RE site in the reverse primer.

Forward primer:

5'-ATA TAT **GGA TCC** ACC ATG GCT CCT AAG AAG AAG-3'

Reverse primer**:**

5'-ATA TAT **GCG GCC GC**T CAG ATC CGC CTG TTG ATG-3'

Removing Cre-2A

The rAAV plasmid was digested with BamHI for 2 hours at 37°C and then the Cre-2A element was gel purified and stored for later use. The rAAV plasmid was then re-ligated using the Roche kit to form a Venus rAAV, whose integrity was confirmed by gel electrophoresis.

Switching Venus for Flp

The Venus rAAV was digested with NotI and BamHI for 2 hours at 37°C and treated with shrimp alkaline phosphatase to prevent re-ligation. The digestions and the digested Flp PCR product were mixed in a 1:3 vector:insert ratio for the Roche Rapid ligation reaction. After transforming *E. coli* and purifying the amplified plasmids, the correct insertion product was confirmed with gel electrophoresis.

Reinserting Cre-2A

The Flp rAAV plasmid was linearised with BamHI and mixed in a 1:10 vector:insert ratio with the previously purified Cre-2A element for the Roche Rapid ligation reaction. After transforming *E. coli* and purifying the amplified plasmids, the correct insertion product was confirmed with gel electrophoresis.

A schematic of the workflow for the Cre-2A-Flp rAAV can be found in figure 5.4 in the results and discussion section.

2.6.4 Virus production for both rAAVs

To produce the virus particles, the pAM-flex eGFP-2A-TASK-3 rAAV or the Cre-2A-Flp rAAV was co-transfected into HEK-293 cells with pFΔ6, pH21, and pRV1 helper plasmids following the protocol of McClure *et al.* (2011).

Five 200 ml culture flasks were plated with HEK-293 cells and incubated for 24 hours in trypticase soy agar (TSA) media (Dulbecco's Modified Eagles Medium (DMEM) supplemented with 10% heat inactivated foetal bovine serum, 2% 200 mM L-Glu, 1% non-essential amino acid solution, and 1% penicillin-streptomycin) at 37°C. Having reached ~70% confluence, media was removed and replaced with fresh pre-warmed media. Three hours later, a plasmid mixture was made of 62.5 µg eGFP-2A-TASK-3 plasmid, 125 µg pFΔ6, 31.25 µg pH21 and 31.25 µg pRV1 in 1650 µl 2.5 M $CaCl_2$ and 12 ml ddH_20. After filtering through a 0.2 µm syringe filter (Sartorius Stedim, France), 13 ml 2x HEPES-buffered saline (HBS) was added while vortexing. A white precipitate formed after two minutes and 5 ml of the mixture was added to each flask. 16 hours later, the medium was replaced with 25 ml fresh medium and then the cells were incubated for a further 60-65 hours before harvesting.

Media was removed and cells were washed once with warm phosphate-buffered saline (PBS), before detachment in PBS. Cells were centrifuged at 800g for 10 minutes and cell pellets were resuspended in 150 mM NaCl, 20 mM Tris (pH 8.0). Cells were solubilised with 0.5% sodium deoxychloate and 50 U/ml benzonase endonuclease was added to digest RNA. The contents were mixed thoroughly and incubated at 37°C for 1 hour and then centrifuged at 3000g for 15 minutes at 4°C. The supernatant was collected for purification.

A 1 ml HiTrap Heparin column (GE Healthcare, USA) was pre-equilibrated with150 mM NaCl, 20 mM Tris (pH 8.0) and then the supernatant was loaded onto the column at a rate of 1 ml/minute. The coat proteins of the AAV2 allow affinity binding of the virus to the heparin sulphate in the column. The column was washed with 100 mM NaCl, 20 mM Tris (pH 8.0) and then the virus was eluted with increasing salt concentrations, of which the first two eluants were discarded and the last three collected for concentration: 1 ml 200 mM NaCl, 20 mM Tris (pH 8.0); 1 ml 300 mM NaCl, 20 mM Tris (pH 8.0); 1.5 ml 400 mM NaCl, 20 mM Tris (pH 8.0); 3 ml 450 mM NaCl, 20 mM Tris (pH 8.0); 1.5 ml 500 mM NaCl, 20 mM Tris (pH 8.0). The 6 ml sample was centrifuged at 2000g in a concentrator with a 100,000 molecular weight cut-off (Sartorius Stedim, France) to a volume of 250 µl. A further 250 µl PBS

was added before filtration through a 0.2 µm syringe filter and then the sample was aliquoted and stored at -80°C until required.

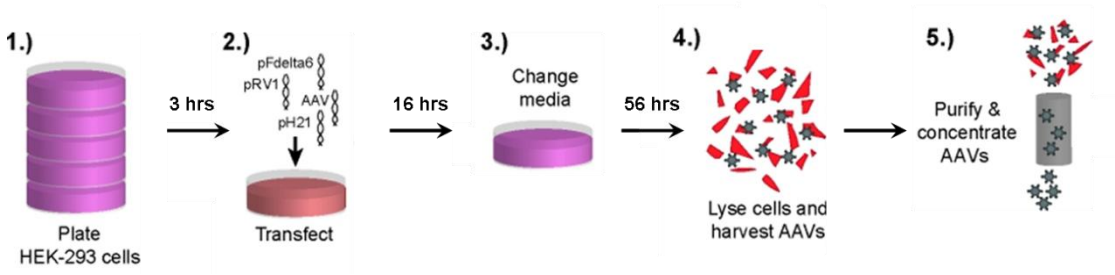

Figure 2.12 rAAV production via a HEK-293 cell "production factory".

1) HEK-293 cells are plated and grown to ~70% confluence and 2) are transfected with the plasmids. 3) Media is changed after 16 hours and the cells are incubated for a further 56 hours. 4) Cells are harvested, lysed and the rAAVs are separated from cell debris by centrifugation. 5) The rAAV particles are purified on a heparin column and concentrated. [Adapted from McClure et al. (2011)]

2.6.5 Expression assays

HEK-293 cell transfection

To verify the expression of the rAAV transgenes, the peGFP-2A-TASK-3 was transfected individually and the pCre-2A-Flp was transfected with a marker plasmid (see Results section). Fluorescence was visualised with a Nikon Eclipse 80i camera (Japan) using QCapture Pro software (QImaging, UK).

The HEK-293 cell line was maintained in TSA media at a constant 37°C and 5% CO_2 in a humidified incubator and plated into 15 mm well plates containing glass coverslips coated with poly-D-lysine (1 mg/ml) to facilitate cell adhesion.

Depending upon the experimental strategy, between 0.1 μg and 1 μg of the plasmids were transfected (or multiply co-transfected) using the calcium phosphate technique. Briefly; 5.6 μl of 2M $CaCl_2$, plasmid cDNA and H_20 (up to 25 μl/15 mm well) were mixed in a sterile Eppendorf tube. To this, an equal volume of HBS plus 45 μl of phosphate was added. The contents of the tube were mixed by gentle agitation and incubated for 20 minutes at room temperature before adding dropwise to the plated cells. Cells were then incubated for 7-9 hours at 37°C and 3% CO_2 before washing twice with PBS. After washing and the addition of fresh culture media, the cells were incubated at 37°C and 5% CO_2 for up to one week.

The expression of the transgenes in the rAAV particles was also confirmed in HEK-293 cells. Briefly, HEK-293 cells were plated as before, and serial dilutions of the eGFP-2A-TASK-3 rAAV and Cre-2A-Flp rAAV were added to duplicate wells. Fluorescence was monitored every few days for the eGFP-2A-TASK-3 rAAV and the cells were fixed in 4% paraformaldehyde for both rAAVs after 5 days.

Cre-2A-Flp rAAV-infected cells were incubated overnight at 4°C with 1:1000 rabbit polyclonal anti-Cre antibody (Novagen, USA) in PBS. The next day, cells were incubated with 1:1000 AlexaFluor 488 goat anti-rabbit secondary antibody (Invitrogen, USA) in PBS, for 2.5 hours at room temperature, before washing and imaging.

Organotypic slices

The expression of the eGFP-2A-TASK-3 rAAV and a control Cre-Venus rAAV were also tested on organotypic hippocampal slices. Briefly, 400 µm thick hippocampal slices of 2-day old mice were attached to a porous membrane and the organotypic cultures were incubated overlying TSA media for 14 days in 5% CO_2 at 37°C. 1 µl of the viruses were added and the slices were monitored for fluorescence for several weeks.

2.6.6 DNA sequencing

Plasmid samples were prepared as 0.1 µg/µl DNA in 15 µl total volume and sequenced by Eurofins MWG Operon. The sequencing primers were designed in-house and are listed below:

TASK-3

1) ATCCGCCACAACATCGAGGA

eGFP-2A-TASK3

1) GCCATACGGGAAGCAATAGC
2) CGTTGGGGTCTTTGCTCAGGGC
3) CAGCGTAGAACATACAGAAGGC
4) GGTTCTGCCGTATTTCCTGAGG

Cre-2A-Flp

1) CCTTCTTCTTTTTCCTACAGCTCC
2) GGAGAATGTGGATGCTGGGGAG
3) AGAGTGGGTGCTGCCAGGGACAT
4) CATCCCTTACAACGGCCAGAAGC
5) CTGAAGAAGAACGCCCCCTACCC

2.7 *Ex vivo* brain analysis

2.7.1 Perfusion fixing

Mice were anaesthetised with pentobarbital (Merial,UK) and, following loss of pedal reflex, the chest cavity was opened to reveal the heart. A needle was inserted into the left ventricle and the right atrium was cut open. Ice cold PBS was infused at 2 ml/min and, when the exsanguinate ran clear, was exchanged for cold 4% paraformaldehyde in PBS. The whole brain was then carefully removed and post-fixed overnight at 4°C in 4% paraformaldehyde in PBS, before cryo-protection in 30% sucrose in PBS at 4°C until the brain sank to the bottom of the vial.

2.7.2 Brain slicing

Fixed and cryo-protected brains were mounted on a pre-chilled platform and snap frozen in dry ice. 40 µm slices were sectioned on a Leica SM microtome (Germany) and stored free-floating in PBS at 4°C.

2.7.3 Immunhistochemistry for GFP

Brain slices were permeabilised in PBS + 0.4% Triton X-100 at RT for 30 mins and then non-specific binding was blocked by incubation in PBS + 4% normal goat serum (NGS) and 0.2% Triton X-100 at RT for 30 mins. Slices were then incubated in PBS + 2% NGS and 0.1% Triton X-100 containing rabbit anti-GFP primary antibody (Invitrogen, 1:1000 dilution) overnight at 4°C.

After overnight incubation, the slices were washed three times in PBS + 1% NGS at RT for 10 minutes each. Then the slices were incubated with PBS containing Alexa Fluor goat anti rabbit 488 secondary antibody (Invitrogen, 1:1000 dilution) at RT for 2.5 hours. Slices were then washed twice in PBS + 1% NGS and once in PBS at RT for 10 minutes before mounting on Superfrost slides (Thermo Scientific, USA).

Fluorescence was imaged on a Nikon Eclipse 80i camera (Japan) using QCapture Pro software (QImaging, UK).

2.8 Graphics and statistics

Graphs were drawn using Microsoft Excel, GraphPad Prism and Systat SigmaPlot. Student's t-test – paired or unpaired as appropriate – was used for statistical comparisons, unless stated otherwise. In such cases, where more than two groups were compared or where there were multiple comparisons, either 1-way or 2-way ANOVAs were used. Where there was significance in the preliminary analyses, Bonferroni or Tukey post hoc tests were performed. Significance is displayed throughout as * = $p < 0.5$, ** = $p < 0.01$, *** = $p < 0.001$.

RESULTS & DISCUSSION

Halothane anaesthesia

3.1 Background

The search for the neural correlates of consciousness (NCC) began formally when Francis Crick joined Christof Koch on a quest to understand human phenomenal consciousness (Crick *et al.*, 1998; 2003). The rubric entailed that even high-level conscious phenomena had their seat in the physical body and, in particular, the brain. Potential explanations of the problem have focused on oscillatory activity of the brain, especially in the gamma range of frequencies (>40 Hz) and specific time-sensitive interactions between different regions of the brain.

Researching anaesthetic mechanisms necessarily takes on parallel questions concerning what brain regions and what brain activity is involved in causing *loss* of consciousness. This study first sought to identify possible neural correlates of *un*consciousness by recording the cortical activity of mice in response to the anaesthetic halothane.

In this study, C57Bl6 mice had cortical screw electrodes and nuchal muscle wire electrodes chronically implanted for ECoG and EMG recording, respectively. The mice were placed in an anaesthetic chamber and exposed to increasing concentrations of halothane at 10 minute intervals. At each concentration, righting reflex was measured and recorded as intact or lost. Electrophysiological data was collected on a tetherless recording device during the entire procedure and the data were analysed by FFT.

3.2 A broad analysis of frequency in halothane anaesthesia

To get a sense for how halothane affects the global activity of the brain, the total power contained in the ECoG in six C57Bl6 mice was plotted as a percentage of initial power over time (and therefore over increasing halothane concentration) in figure 3.1A. The power decreases from 100% at baseline to 40% at the end of the experiment in staggered jumps, but with a linear correlation R^2 of 0.89.

The negative correlation between power and concentration indicates how halothane affects brain activity in at least one of two ways. Firstly, halothane may reduce the frequency of the ongoing electrical activity, consistent with its prolonging the time decay phase at inhibitory synapses (Kitamura *et al.*, 2003); and secondly, halothane might also decrease the number of cells active at any one time, through the same or similar inhibitory mechanisms.

Dividing the power into discrete frequency bands, as in figure 3.1B, shows that at the start of the experiment, with no anaesthetic present, the majority of the power is contained within the theta range: approximately 70% of the power is between 4 Hz and 12 Hz, split between the higher frequency theta range of 8-12 Hz (~30% total) and the lower frequency theta range of 4-8 Hz (~40% total).

When 0.4% halothane is introduced, the dominant power switches to the lower frequency theta band, which possesses approximately 70% of total power. Correspondingly, the power in the higher frequency band decreases to about 15% total power. Interestingly, there is no major change in power distribution after this initial "theta switch" and the power in the delta and alpha frequency bands are constantly low throughout the halothane exposure.

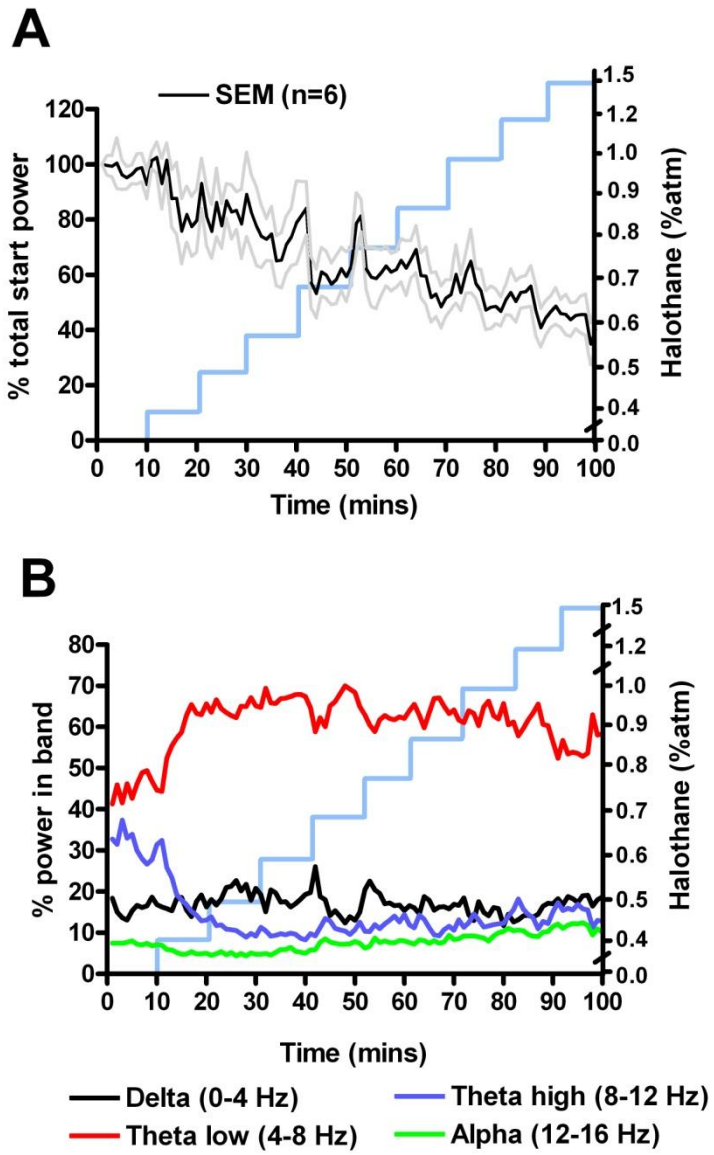

Figure 3.1 The power dynamics contained within the ECoG changes with increasing halothane concentration.

A – Total power up to 25 Hz contained within the ECoG decreased from baseline by in excess of 50% over time, which correlates every 10 minutes with an increase in halothane concentration. B – The contribution to the ECoG of specific frequency bands had moderate changes over time/increasing halothane concentration. The major observation was a switch between the 8-12 Hz band and the 4-8 Hz band after 10 minutes with the introduction of halothane, indicating a shift from type-1 to type-2 theta. The average of six animals without error bars has been shown for clarity. [Halothane steps indicated in blue; n = 6]

3.3 Characterising the spectral power of halothane anaesthesia

To obtain a more detailed profile of the frequency distribution, the power spectra of the FFTs were compared across halothane concentrations. A typical ECoG response for one mouse is shown in figure 3.2. Under baseline conditions – 0.0% halothane – the power spectrum shows low power dispersed over a broad frequency range, with peak power at 7.5 Hz (Figure 3.2A), indicative of a freely behaving animal. The addition of 0.4% halothane to the chamber causes a powerful peak at 6 Hz (Figure 3.2B), which reaches a maximum amplitude at 0.5% halothane (Figure 3.2C), before becoming tuned to lower frequencies up until 1.0% halothane (Figure 3.2D-E). At 1.5% halothane the peak has disappeared, leaving low peak power in the delta range of frequencies (Figure 3.2F).

This prominent oscillation was found to be sensitive to systemic atropine sulfate, indicating the involvement of muscarinic receptors and identifying the activity as a type-2 theta oscillation (Kramis *et al.*, 1975). So, the "theta switch" observed previously is a result of halothane shifting the activity from type-1 to type-2 mechanisms.

The hippocampal theta oscillation has been proposed to act as a conscious window, providing frames of time in which disparate brain processes can bind together as a possible NCC (Doesburg *et al.*, 2009). The type-2 theta oscillation has the interesting property of being present both with anaesthetics and normal behaviour. The oscillation can be provoked by aversive stimuli such as a toe-pinch during halothane and urethane anaesthesia and also during alert immobility (Bland *et al.*, 2001). Could it be that the type-2 theta oscillation present during halothane anaesthesia represents a kind of "alert immobility"? If so, to what extent does the oscillation impinge upon conscious processes; and would modulating the oscillation affect sensitivity to halothane anaesthesia?

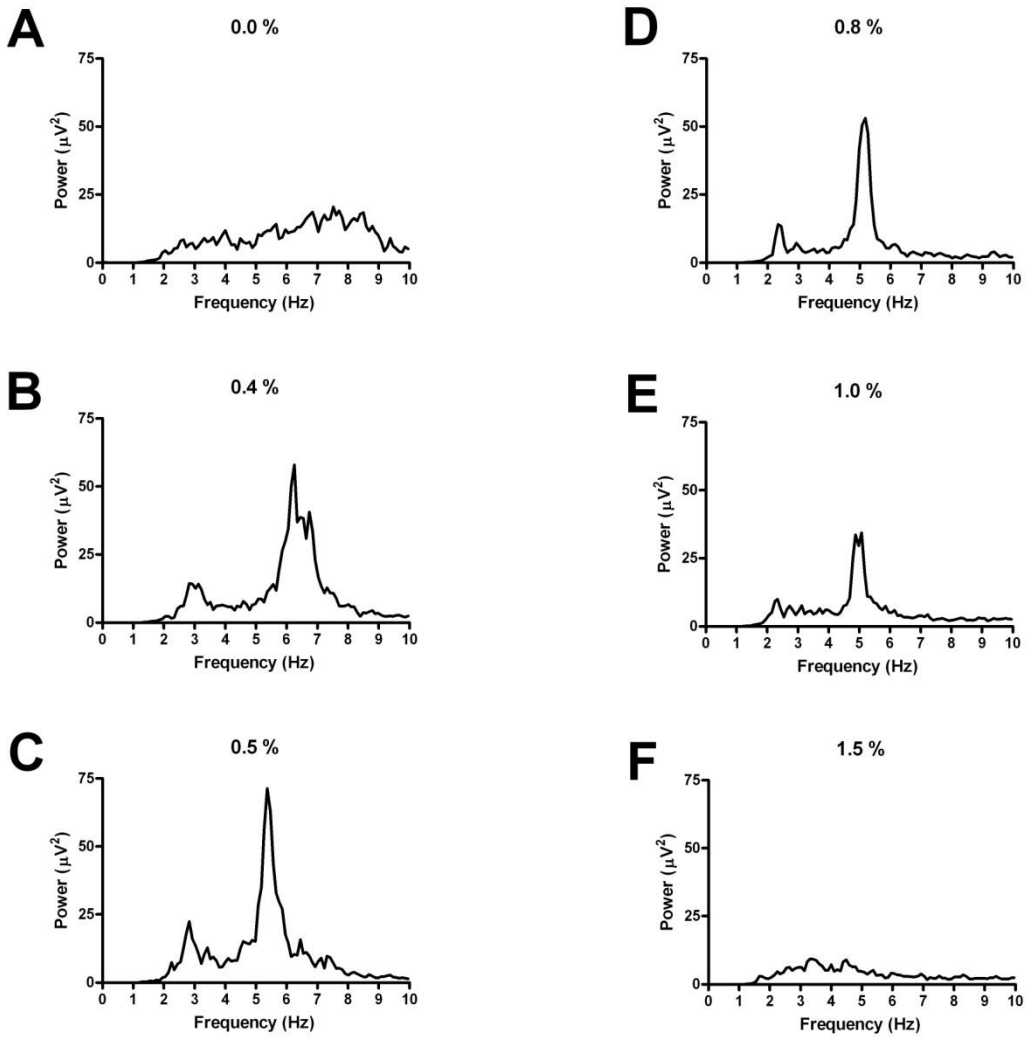

Figure 3.2 The ECoG response to halothane.

The ECoG response of a single C57Bl6 mouse shows a prominent peak in the FFT power spectrum in the theta frequency range that changes with increasing concentrations of halothane. A – Baseline recording in 0.0% halothane shows a broad spectrum with the peak power at 7.5 Hz, typical of behavioural type-1 theta. B-D – Increasing doses of halothane from 0.4% to 0.8% cause a prominent peak in the lower type-2 theta range whose frequency decreases in a dose dependent manner. E-F – The theta peak decreases in intensity and disappears at 1.5% halothane, replaced by desynchronised lower power in the delta range of frequencies.

3.4 Correlating theta peak with anaesthetic sensitivity

To answer whether or not the type-2 theta oscillation correlated with anaesthetic sensitivity, the LORR of six C57Bl6 mice was recorded over increasing halothane concentrations with simultaneous ECoG measurements. The peaks in the power spectra at each anaesthetic concentration were fitted to Lorentzian curves to smooth any noise and calculate the respective peak frequency and Q-factor. Figure 3.3A shows how the peak frequency changes with increasing halothane concentration. At baseline the peak frequency is over 7 Hz, and with each incremental increase in halothane concentration, with the exception of a slight increase at 1.0%, the frequency decreases to less than 5 Hz, following a first-order polynomial fit.

The Q-factor is a measure of peak shape; being the full width of the Lorentzian fit at half maximum amplitude, divided by the maximum frequency. So, the higher the Q-value, the more defined is the peak, which means that a narrow frequency band will have a large associated power. Figure 3.3B shows that the Q-factor increases with each concentration until 0.7% halothane, and then the value dips and rises at higher concentrations, following a fourth-order polynomial. The Q-factors under all concentrations of halothane are greater than baseline, suggesting a more robustly synchronised oscillation with anaesthesia.

Simultaneously with electrophysiological recording, a behavioural correlate of consciousness was measured by testing the righting reflex. At each concentration, the animals were scored as being able to right themselves after being turned onto their backs or not. Quantal analysis (Waud, 1972) of the binary-scored data revealed a curve with a slope of 28.22 ± 12.57 and ED_{50} for LORR of 0.74 ± 0.02 % (Figure 3.3C).

The general trend towards lower frequency oscillations with increasing halothane concentrations and the observation that the maximum Q-factor appears at around the righting reflex switch, was not bourn out in significant correlations between the average peak statistics and group LORR.

However, there is a significant difference between the average of all peak frequencies when the righting reflex is intact and when the righting reflex has been lost ($p < 0.001$). Figure 3.3D shows the frequencies plotted, intact against lost, revealing a threshold zone where certain frequencies are mutually exclusive to an “awake” state (that is, with intact righting reflex) or to an “asleep” state (that is, with a lost righting reflex).

Since there is also a range of frequencies between 5 Hz and 6 Hz when an animal can be in either of the two states, the switch between an intact righting reflex and a lost one is more subtle than an all or nothing phenomenon.

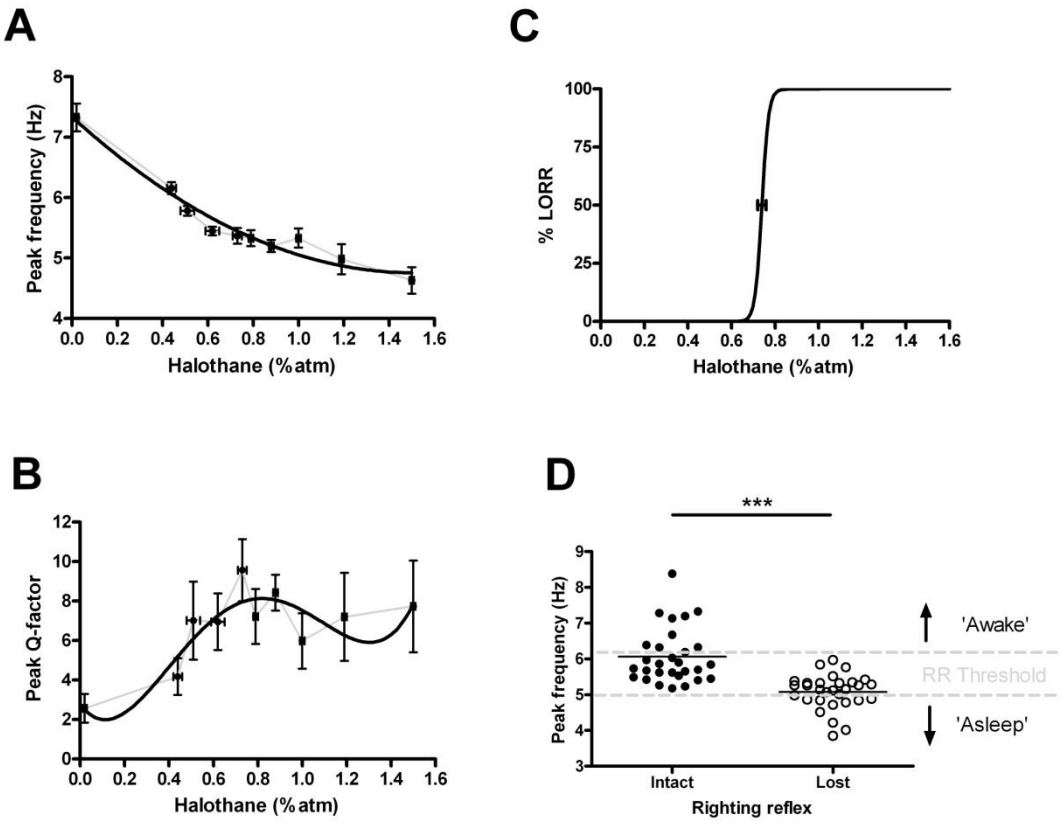

Figure 3.3 Lorentzian analysis shows concentration-dependent changes of the type-2 theta peak in response to halothane.

A – Peak frequency of the halothane-associated type-2 theta oscillation decreases with increasing halothane concentration from 7 Hz at 0.0% halothane to 5 Hz at 1.5% halothane. B – A fourth-order polynomial fit of the Q-value shows peak definition increases to a maximum at 0.7% halothane. C – The righting reflex of the animals was measured at each concentration and Waud analysis revealed an ED_{50} of 0.74% ± 0.02 and slope of 28.22 ± 12.57. D – The peak frequencies when righting reflex was intact is significantly different to the peak frequencies when righting reflex was lost ($p < 0.001$). Thresholds could also be observed for 'awake' and 'asleep' frequencies. [n = 6]

3.5 Continuous spectral analysis as a visual tool

Plotting individual power spectra for discrete time intervals (as in Figure 3.2) has a number of attractive features, but the technique cannot display the temporal dynamics of the ECoG; one of its most advantageous features. Therefore, further methods of analysis and data presentation were sought to fully characterize the changing ECoG in the time domain.

Figure 3.4 shows a matrix of serially plotted 30-second power spectra over 100 minutes of ECoG recording in one representative mouse. The colour-coded z-axis represents the relative powers at each frequency, with warm colours (red) representing high power and cool colours (blue) representing low power. The plot has been smoothed to produce a contour plot that shows how the desynchronised baseline ECoG changes to a highly tuned type-2 theta peak with increasing concentrations of anaesthesia. At the highest concentrations of halothane, the theta power disappears, being replaced by power in the delta range of frequencies (1-4 Hz).

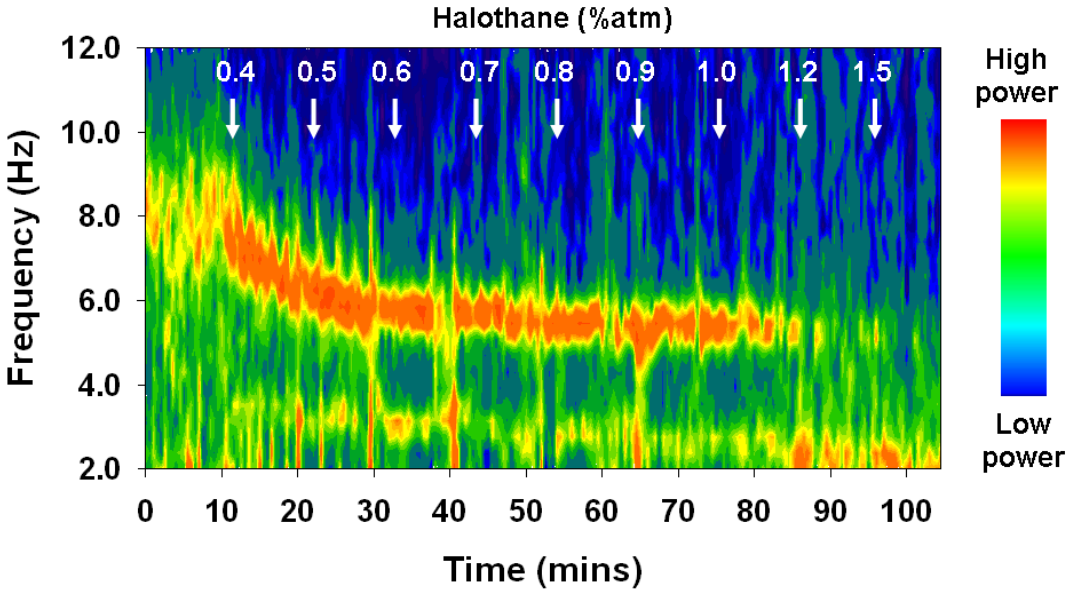

Figure 3.4 Contour plot of serial FFT power spectra.

Contour plotting of serial FFT power spectra shows the frequency and power changes of the ECoG in response to halothane. 30-second FFT power spectra were plotted successively over time for a single C57Bl6 mouse. The z-axis of the matrix shows high power frequencies in red and low power in blue. Note the immediate "tuning" to type-2 theta after halothane introduction and theta "drop-off" at the highest halothane concentrations.

3.6 Systemic cholinergic modulation of theta does not affect LORR

The theta oscillation observed during halothane anaesthesia was found to be sensitive to i.p. injection of 50 mg/kg atropine sulfate (Figure 3.5A). This shows a key role for muscarinic cholinergic neurotransmission in the generation of the oscillation, indicative of the type-2 theta oscillation.

Even though previous results (as in Figure 3.3) demonstrate minimal relationship between theta and LORR, given that the theta oscillation is such a prominent ECoG feature of halothane anaesthesia, the effect of ablating theta through atropine on LORR was investigated. Recall that below a cut-off threshold of 5 Hz, no mouse is judged as conscious by LORR. So, shunting the dominant oscillation from theta towards delta frequencies, while not immediately anaesthetising the animal, might increase its sensitivity to anaesthetics.

Figure 3.5B shows the LORR curves of six C57Bl6 mice, pre-treated with i.p. saline (solid line) or atropine sulfate (dashed line). The LORR curve for saline of 0.78 ± 0.01 % (slope, 342 ± 302) is not significantly different ($p = 0.59$ for EC_{50} & $p = 0.31$ for slope, $n = 6$) to that for atropine sulfate of 0.76 ± 0.03 % (slope, 19 ± 8).

In this case, muscarinic antagonism had no effect on sensitivity to halothane, indicating that the theta oscillation may not have a role in mediating those processes that are inhibited to cause LORR.

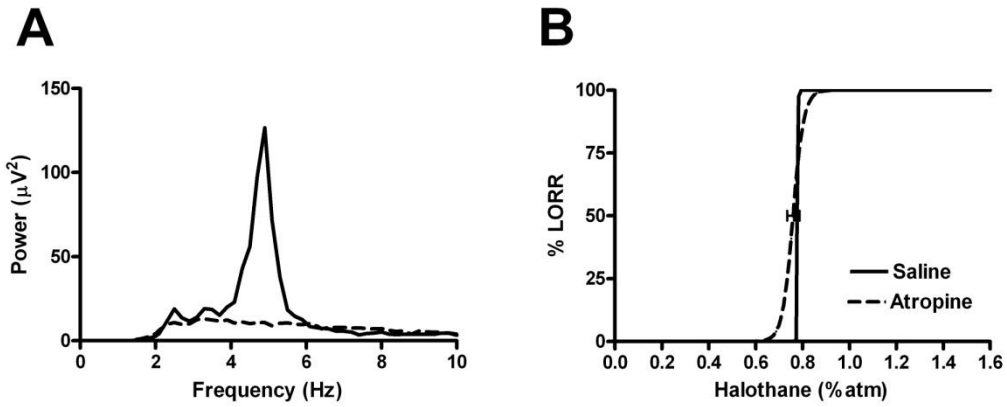

Figure 3.5 Systemic atropine sulfate administration ablates the halothane-associated theta oscillation without affecting halothane sensitivity.

A – The solid line shows a power spectrum of 30-seconds of ECoG recorded in a C57Bl6 mouse during 0.8% halothane exposure. The dashed line shows the same animal exposed the same halothane concentration after pre-administration of 50 mg/kg i.p. atropine sulfate, demonstrating muscarinic sensitivity of the theta oscillation. B – The LORR EC_{50} between saline (solid) and atropine sulfate (dashed) pre-treated mice are not significantly different. [n = 6]

3.7 Blocking cholinergic neurotransmission in the medial septum

The medial septum provides cholinergic and GABAergic input to the hippocampus and is thought to mediate the major component of the type-2 theta oscillation by relaying rhythmic activity from the supramammillary nucleus to the hippocampus (Yoder *et al.*, 2005). The next experiment, in which atropine sulfate was administered directly into the cannulated medial septum of C57Bl6 mice, had two main objectives:

1. To clarify with greater anatomical precision that the theta oscillation observed during the previous studies was due this type-2 mechanism.
2. To test whether a more discrete antagonism would affect sensitivity to halothane anaesthesia.

Halothane, at a concentration of 1.0%, elicited a robust and continuous oscillation in the type-2 theta range, as shown by the representative power spectrum in figure 3.6A and the continuous contour plot in figure 3.7A. Once the oscillation became stable, aCSF alone or aCSF containing 50 μg atropine sulfate was injected into the medial septum. aCSF had no effect on the oscillation (Figure 3.7A), while the atropine sulfate bolus was sufficient to ablate the theta oscillation, as in figure 3.6A and figure 3.7B. Atropine sulfate ablates the theta oscillation, significantly shifting the dominant ECoG frequency from 5.03 ± 0.09 Hz to 2.82 ± 0.09 Hz ($p < 0.05$, $n = 4$); that is, from type-2 theta into the delta range of frequencies. The first objective was thus satisfied; type-2 cholinergic mechanisms are involved in the theta oscillation.

The ablation of the type-2 theta oscillation lasted for over an hour (Figure 3.7B), enabling LORR experiments to be performed on atropine sulfate pre-treated animals. These experiments tested the hypothesis that specific antagonism of medial septum cholinergic neurotransmission would increase the sensitivity to halothane anaesthesia. The EC_{50} for halothane LORR with control aCSF injection was 0.94 ± 0.03 % (slope, 36 ± 21), which was not significantly different ($p = 0.62$ for EC_{50} & $p = 0.21$ for slope, $n = 6$) to that for the atropine sulfate injection EC_{50} of 0.91 ± 0.05 % (slope, 8 ± 2).

It should be noted that the control aCSF EC_{50} appears to be substantially higher than that for the uncannulated mice that received i.p. saline or atropine sulfate in the previous study. It is therefore possible that the arousal of the cannulated mice in this experiment was heightened to a degree that may have masked the true effect of cholinergic antagonism in the medial septum. However, taking the results at face value indicates that, in answer to the second objective of this part of the study,

discrete antagonism of the medial septum cholinergic system does not affect sensitivity to halothane anaesthesia. Further, the type-2 theta oscillation appears to be unrelated to the processes that inhibit the righting reflex.

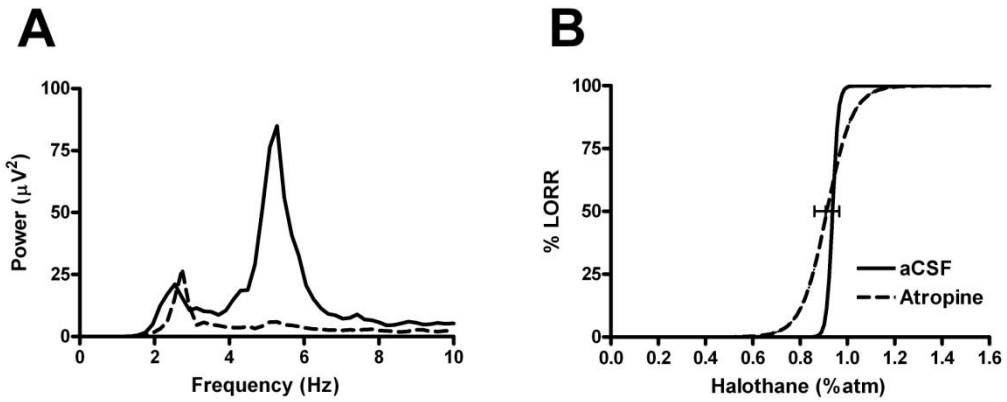

Figure 3.6 Effect of atropine sulfate in the medial septum.

Atropine sulfate administered into the medial septum ablates the halothane associated theta oscillation, but does not affect halothane sensitivity. A – The solid line shows a power spectrum of 30-seconds of ECoG recorded in a C57Bl6 mouse during 1.0% halothane exposure. The dashed line shows the same animal exposed to the same halothane concentration after administration of 50 mg medial septum atropine sulfate. B – The LORR EC_{50} between saline (solid) and atropine sulfate (dashed) pre-treated mice are not significantly different. [n = 6]

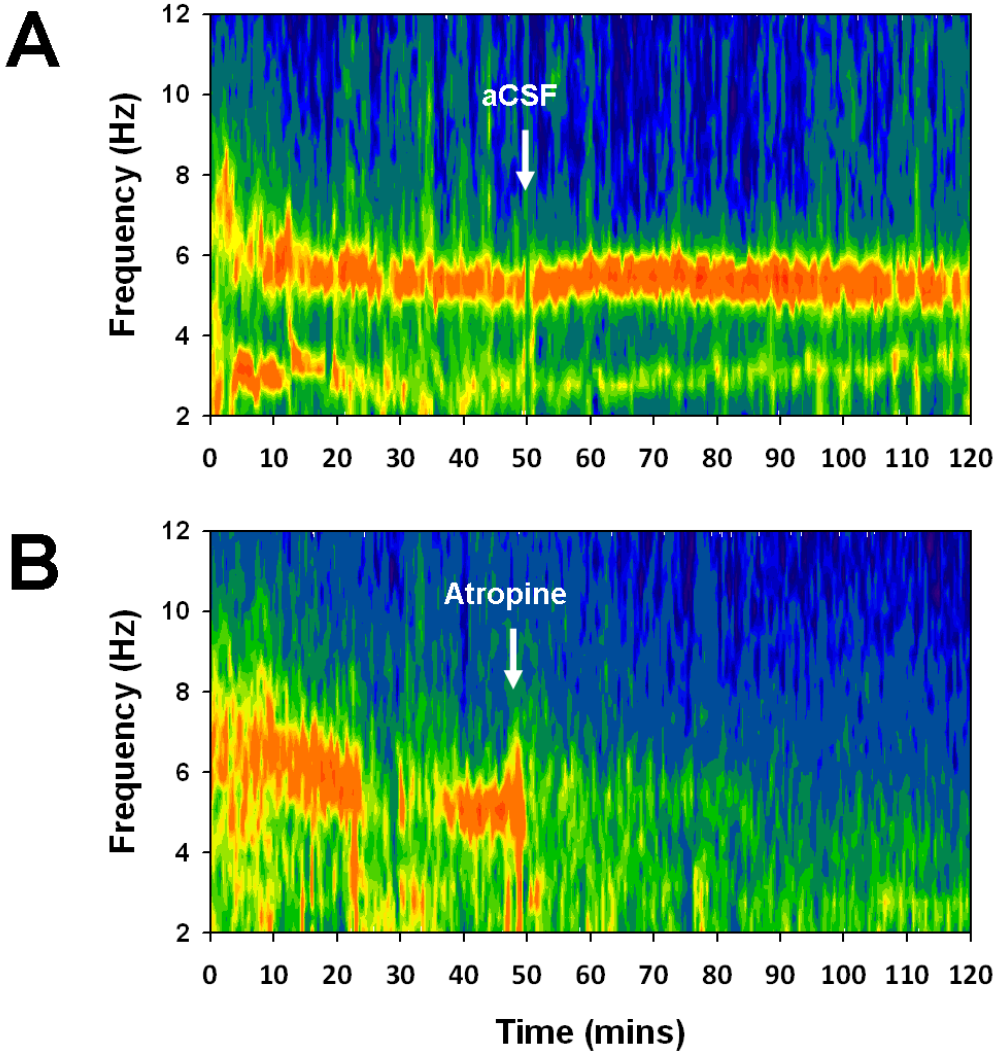

Figure 3.7 Atropine sulfate administered into the medial septum ablates the halothane associated theta oscillation.

A – 1% halothane causes a robust and continuous theta oscillation, unaffected by medial septum injection of aCSF at 50 minutes. B – Atropine sulfate injection into the medial septum causes a complete and long-lasting ablation of the halothane-induced type-2 theta oscillation. The transient theta "drop-out" at around 30 minutes represents a previous unsuccessful injection.

As well as ruling out a possible role in the anaesthetic cascade, the fact that blocking the type-2 theta oscillation had no effect on halothane sensitivity raised the question of what other characteristic of the ECoG might be more relevant. Being such a prominent feature of halothane anaesthesia, theta tends to dominate the ECoG waveform, perhaps masking more relevant signatures of the anaesthetic state. Would removing it uncover another pattern?

Figure 3.8A shows the ECoG response of a mouse pre-administered with aCSF into the medial septum to increasing concentrations of halothane, with the point of LORR indicated by a dashed line. The theta oscillation can clearly be seen to straddle the point of LORR, confirming the finding that it does not act to either impair or induce anaesthesia. In comparison, blocking the type-2 theta oscillation by medial septum atropine sulfate in the same mouse shunted the dominant frequency to the delta range, as in figure 3.8B. The point of LORR, marked with a dashed line, separates a conscious animal from an unconscious one, but in this case there does not appear to be a clear neurophysiological delimiter.

In a few mice, there did seem to be a correlation between LORR and an increase in power in the delta range of frequencies, as represented in figure 3.8C. Here, atropine sulfate has completely ablated theta activity in response to halothane, with no dominant power until the point of LORR, which coincides with an increase in delta power.

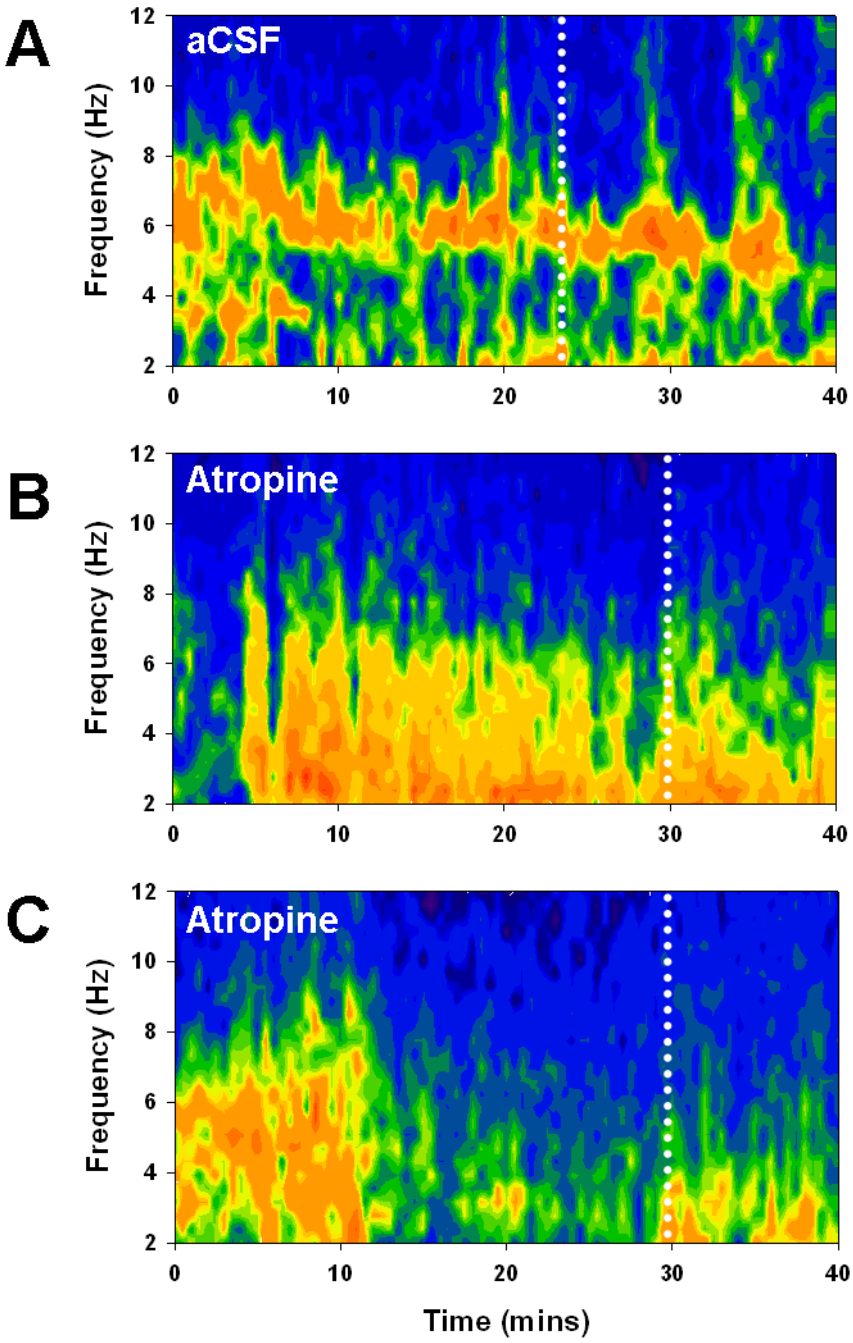

Figure 3.8 Ablating theta oscillation does not affect loss of righting reflex.

Atropine sulfate pre-administered into the medial septum ablates the halothane-associated theta oscillation with no consistent effect on LORR. A – The theta oscillation "straddles" the LORR with medial septum aCSF in mouse #1. B – Medial septum atropine sulfate shunts the dominant ECoG frequency to the delta range without affecting LORR in mouse #1. C – After theta ablation with medial septum atropine sulfate in mouse #2, LORR coincides with an increase in delta-band power.

Atropinization of the medial septum caused an absolute increase in delta power in all mice and a relative increase compared to the theta band at the highest concentrations of halothane ($p < 0.05$), as shown in figure 3.9. However, while there was a trend towards a higher delta/theta (0-4 Hz/4-8 Hz) ratio with increasing anaesthesia, there was not an obvious correlation between the change in delta power and LORR across the group of animals.

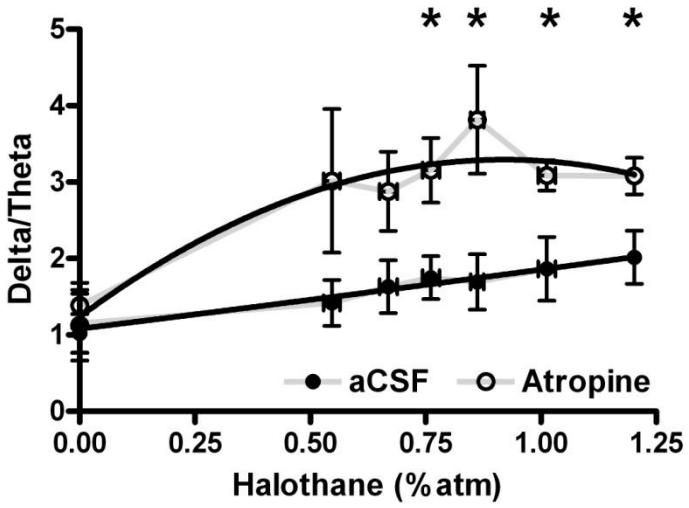

Figure 3.9 Medial septum atropine sulfate increases the delta band power.
The Delta/Theta ratio is significantly increased ($p < 0.05$) with atropine sulfate compared to control over all halothane concentrations. [n = 6]

3.8 Cholinergic modulation of halothane-induced delirium

Prior to its hypnotic effects, halothane induces a transient period of behavioural excitation, correlating to the anaesthetic delirium phase in humans, which is associated with spasmodic movements and incomprehension. Since the cholinergic system has been implicated in mediating some of the delirium symptoms, the next experiments set out to test the effects of inhibiting and potentiating the theta oscillation on halothane-induced delirium. If the type-2 theta oscillation was not relevant to LORR, then it could be involved in mediating some of the cognitive effects of anaesthesia.

Normally, increases in running speed correlate with increases in type-1 theta frequency (Pang *et al.*, 2009), so a mouse running at high speeds as in the excited delirium state should show theta oscillations of high frequency. However, halothane appears to shunt the dominant ECoG frequency from type-1 theta to the lower frequency type-2 theta. The working hypothesis, therefore, was that there would be a functional disjuncture between the internal spatio-temporal dynamics of the hippocampus and the behavioural environment. So, the slower frequency brain state of halothane-induced type-2 theta would be unable to process the fast-moving behaviour, embodying the cognitive impairments of the delirium state.

Eight C57Bl6 mice were given i.p. injections of either saline, atropine sulfate (50 mg/kg) or the acetylcholinesterase inhibitor eserine (0.2 mg/kg), with each treatment separated by one week, and habituated to an activity monitor for 30 minutes. The animals were then exposed to 2% halothane for 10 minutes. Figure 3.10A shows that with saline pre-treatment (in black), the introduction of 2% halothane causes a transient increase in locomotion as recorded by horizontal infra-red beam breaks.

2-way ANOVA revealed a significant effect of drug on the distance travelled ($p < 0.001$). Post hoc Bonferroni's tests showed that mice pre-treated with atropine sulfate, to ablate muscarinic cholinergic neurotransmission, showed a similar activity profile (Figure 3.10A) and total distance travelled was not significantly different compared to saline control in either the 10 minutes before or after halothane exposure (Figure 3.10B). However, eserine reduced the locomotor excitation during halothane compared to both saline ($p < 0.001$) and atropine sulfate ($p < 0.01$), and also prior to halothane exposure ($p < 0.001$), indicating that the drug's action may occur independently of halothane (Figure 3.10A&B).

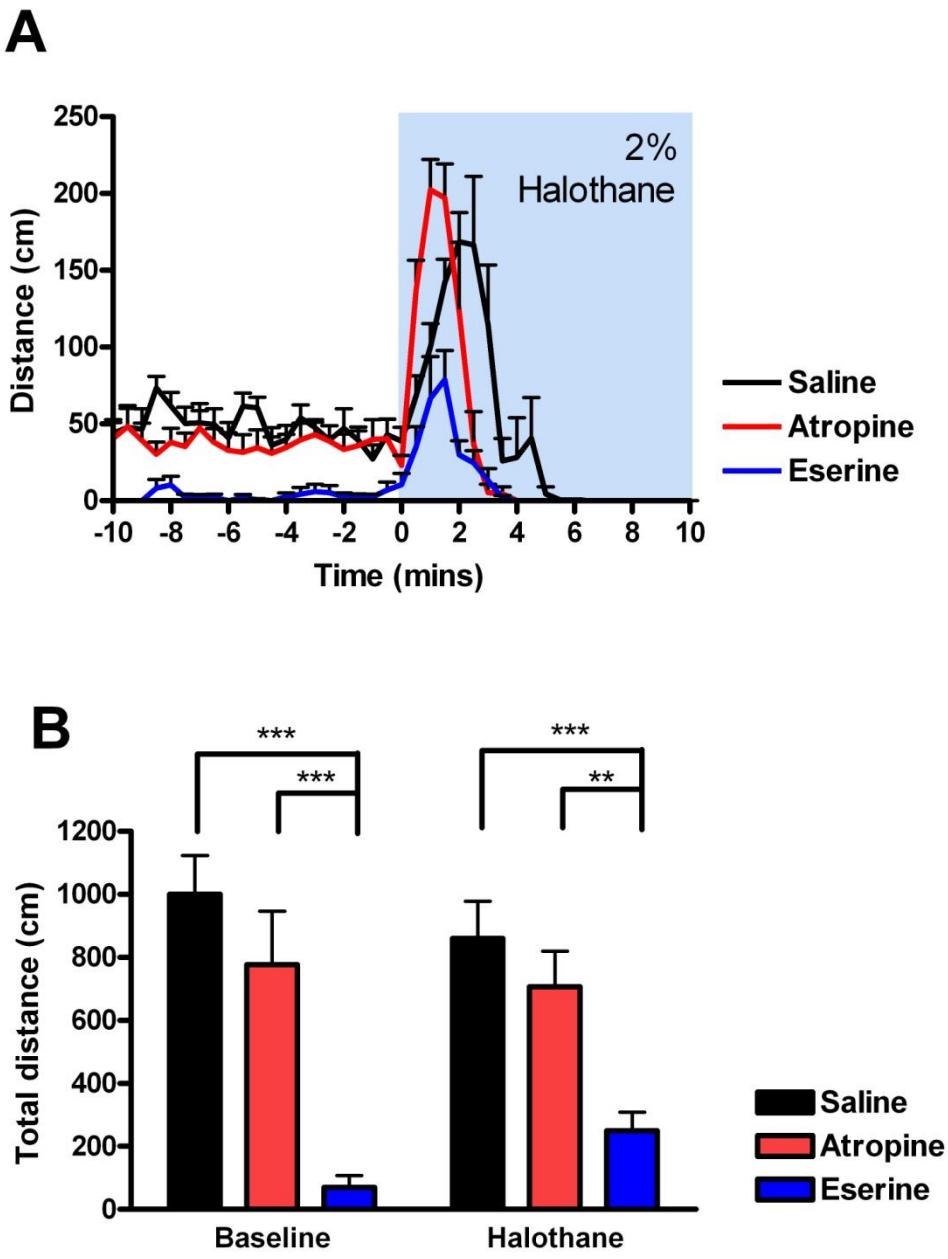

Figure 3.10 Halothane-induced hyper-locomotion is largely resistant to cholinergic modulation.

A - Halothane induces a transient increase in locomotion before sedation, hypnotic anaesthesia and behavioural immobility. B – Atropine sulfate pre-treatment has no effect on locomotion before or during the delirium phase. Eserine pre-treatment reduces locomotor activity prior to halothane exposure compared to both other treatments ($p < 0.001$) and during halothane exposure, compared to saline ($p < 0.001$) and atropine sulfate ($p < 0.01$). [n = 8]

Figure 3.11 shows that the different drug pre-treatments significantly altered the dynamics of the ECoG, with particularly striking effects on the theta oscillation. As expected, in the saline condition the desynchronised frequency spectrum at baseline (0-10 minutes) rapidly tunes to a prominent theta frequency oscillation after introduction of halothane, reaching maximum power at the 15 minute mark (Figure 3.11A).

While atropine sulfate did not significantly affect locomotor activity, it did cause a more desynchronised ECoG profile in the baseline phase, compared to saline, and completely ablated the type-2 theta oscillation normally associated with halothane anaesthesia (Figure 3.11B). Eserine treatment also desynchronised the baseline ECoG, but in contrast to atropine sulfate, the halothane-associated theta oscillation contained much greater power (Figure 3.11C).

Overall, these results indicate that while modulating cholinergic neurotransmission affects the theta oscillation, it is not solely responsible for halothane-induced behavioural excitation.

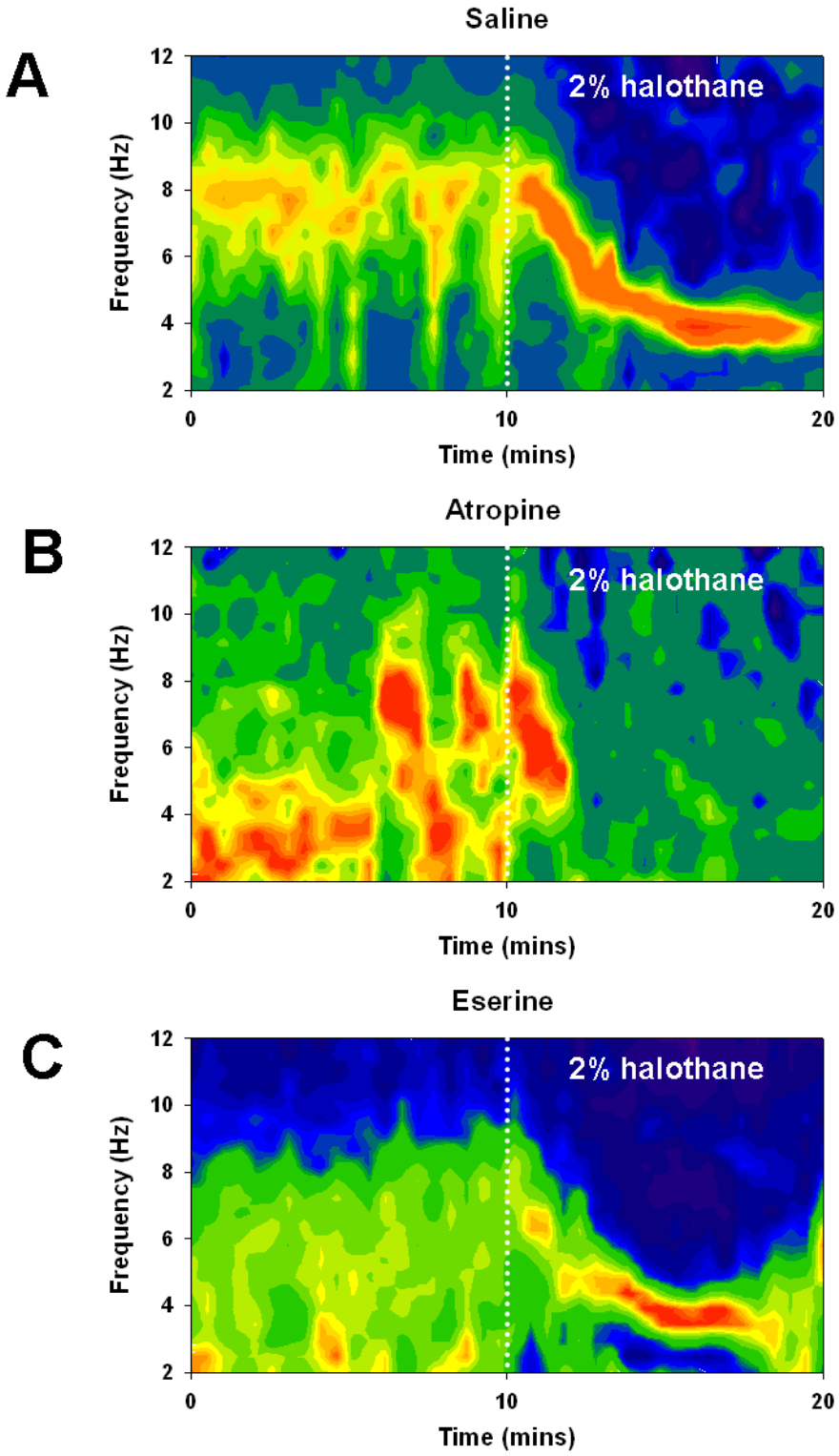

Figure 3.11 Cholinergic modulation of halothane-induced type-2 theta.

The type-2 theta response to halothane is modulated by pre-treatment with atropine sulfate and eserine. A – A typical ECoG response to halothane after pre-treatment with saline. B – Atropine sulfate ablates the type-2 theta oscillation. C – Eserine potentiates the type-2 theta oscillation in response to halothane.

3.9 Discussion

The preceding experiments sought to understand whether the type-2 theta oscillation had a role in mediating LORR in response to halothane anaesthesia. After characterising the power and frequency dynamics of the ECoG in response to increasing doses of halothane, a clear correlation between type-2 theta and LORR could not be observed. However, since the oscillation was such a prominent feature of halothane anaesthesia – being variously described as "anaesthetic-resistant", "anaesthetic-associated" and "anaesthetic-induced" – it was tantalising to suggest that modulating the oscillation would affect anaesthetic sensitivity. Further, type-2 theta oscillations are also present during paralysis with neuromuscular blockers (Whishaw, 1976) and can be enhanced with tail-pinch during halothane (Bland *et al.*, 2003) and urethane anaesthesia (Clement *et al.*, 2008), hinting at a possible role for theta and cholinergic processes in sensory processing and movement intention, key components of the righting reflex (Kandel *et al.*, 2000).

In the next part of this study, systemic atropine sulfate successfully ablated the theta oscillation without affecting the concentration of halothane required to induce LORR. The centrality of medial septum cholinergic activity to the theta oscillation was then confirmed through ablating type-2 theta with atropine sulfate in this area. Since systemic drug administration can have off-target effects, atropine sulfate was then delivered directly to the medial septum prior to a second analysis of halothane sensitivity. This treatment had no affect compared to a vehicle injection, supporting the previous finding that the type-2 theta oscillation is not involved in LORR. So what does it do?

Type-2 theta is usually described in physiological and behavioural terms: it is sensitive to muscarinic antagonism and occurs during type-2 behaviours such as alert immobility (Kramis *et al.*, 1975). Since the theta observed in this study is blocked by atropine sulfate, it is presumably an active process involving cholinergic neurotransmission and not simply a trend to lower frequency oscillations as the concentration of halothane increases. But is the animal also in the alert immobile state?

Since the type-2 theta oscillation bridges both the LORR and LOTW thresholds, occurring with aversive stimuli even at concentrations of halothane that induce immobility (Bland *et al.*, 2003), it is likely that it contains a sensory component of some kind. Bland *et al.* (2001) suggest that type-2 theta represents a

mode of sensory integration. As they see it, ascending pathways from the reticularis pontis oralis and the pedunculopontine tegmentum provide tonic type-2 sensory inputs to the posterior hypothalamus and supramammillary nucleus which synergise with type-1 inputs in the medial septum before transfer to the hippocampus. Here, type-2 theta is proposed to modulate sensory input, especially when a motor response is anticipated.

Another theory suggests that theta acts as a filter for relevant information by suppressing non-relevant sensory processes (Sainsbury, 1998). This inhibitory interpretation views theta as essentially a static oscillation – exponential increases in running speed only change the frequency by a few hertz – which is unable to process large amounts of information. And, in addition, it can explain how the two types of theta could combine onto the same neurons to mediate a cohesive output.

Either of these theories would be satisfied – but no one preferred – if habituation of the theta oscillation was observed after a long or repeated halothane exposure. For the sensory integration theory, type-2 theta would disappear because there is no successive motor output; and for the sensory inhibition theory, type-2 theta would disappear because there are no changes in the external environment. It would also be interesting to determine the concentration at which aversive stimulation fails to induce type-2 theta under halothane anaesthesia in a similar way to the use of evoked potentials for monitoring anaesthetic depth.

However, even if the animal is in sensory processing state, the fact that even very small decreases in theta frequency have been shown to cause amnesia (Perouansky *et al.*, 2010) means that there is little conscious activity.

In this study, LORR was used as a surrogate for LOC, based primarily on the pharmacological correlation between the two parameters over a variety of anaesthetics (Franks, 2008). The experiments here show that the type-2 theta oscillation plays no role in either maintenance of consciousness or loss of consciousness, as judged by LORR and therefore can be ruled out as a *de facto* neural correlate of consciousness.[8]

In comparison, the pioneers of hippocampal theta research Kramis, Vanderwolf and Bland (1975) argued that type-1 theta might be more important,

[8] However, high doses of atropine can produce unconsciousness, highlighting the cholinergic system as a whole as a possible NCC (Gadecki W, Majewski J (1969). New observations on atropine coma treatment in psychoses. *Pol Med J* **8**(6)**:** 1515-1517.).

saying that "[their] data raise the intriguing possibility that depression of the system producing atropine-resistant theta activity may be largely responsible for the production of the anaesthetic state." However, although blocking type-1 theta is a necessary feature of anaesthesia, it is clearly not sufficient; otherwise, animals would fall asleep as soon as they stopped moving. But, if the two types of theta are more interdependent than the separatist schools imagine, there is the possibility of shutting them down at the same point with a forced walking test, which provides a new metric for analysing the point of LOC in mice (Hwang *et al.*, 2010).

In this test, trained mice are suspended on a moving treadmill during anaesthetic exposure, with the loss of movement (LOM) classified by an accelerometer-based motion detection system. LOM has a good pharmacological correlation with LORR, and has the potential advantage in the context of this study to ask whether the type-2 theta oscillation is a sensory product after the "depression of the system producing atropine-resistant theta activity", which is necessarily active during movement (Hwang *et al.*, 2010).

There were several other reasons for choosing to investigate cholinergic modulation of halothane anaesthesia, and specifically the role of the medial septum. Firstly, cholinergic systems modulate during sleep and wake states (Lydic *et al.*, 2005) and thus could mediate sleep-like states of anaesthesia; secondly, halothane anaesthesia affects the cholinergic system (Keifer *et al.*, 1994); and thirdly, inactivation of the medial septum increases sensitivity to anaesthetics (Ma *et al.*, 2002).

The cholinergic system is one component of the multiple arousal systems of the brain stem that control states of wakefulness over the circadian rhythm. More or less every neurotransmitter has a role in either promoting or maintaining REM, NREM or wake activity, as the list below shows.

	NEUROTRANSMITTER	BRAIN REGION
Wake active	noradrenaline	locus coeruleus (pontine brainstem)
	neuropeptide S	neuropeptide S cells (pontine brainstem)
	serotonin	raphe neurons (medial brainstem)
	dopamine	midbrain and brainstem
	histamine	TMN (posterior hypothalamus)
	hypocretin/orexin	lateral hypothalamus
	acetylcholine	basal forebrain and pontine brainstem
Sleep active	GABA	VLPO (preoptic area)
	GABA	MnPO (preoptic area)

Cholinergic neurons in the pedunculopontine and laterodorsal tegmental nuclei (PPT and LTD, respectively) project widely throughout the entire brain, innervating the thalamus, lateral hypothalamus, basal forebrain and prefrontal cortex (Saper *et al.*, 2010). PPT/LTD neurons are most active during wakefulness and REM sleep, and less so during NREM sleep, indicative of a role in maintaining cortical arousal (Steriade, 1993). However, that cholinergic neurons in the LTD increase their firing rates just before the transition from slow waves to faster frequencies (Boucetta *et al.*, 2009) suggests that these neurons might also play a causal role in sleep-to-wake transitions.

The activity of LDT/PPT neurons is also reduced under halothane anaesthesia (Lydic *et al.*, 1993), a phenomenon that is also accompanied by a decrease in acetylcholine levels in the pontine reticular formation (Keifer *et al.*, 1994) and one that is vital for the production of NREM-like spindles (Keifer *et al.*, 1996). Cholinergic basal forebrain neurons also play a role in sleep-like spontaneous alternations under urethane anaesthesia (Clement *et al.*, 2008), again illustrating possible overlap between sleep and anaesthetic mechanisms. During the course of this study, both cyclic alternations and spindle activity were isolated in response to halothane anaesthesia, as shown in figure 3.12.

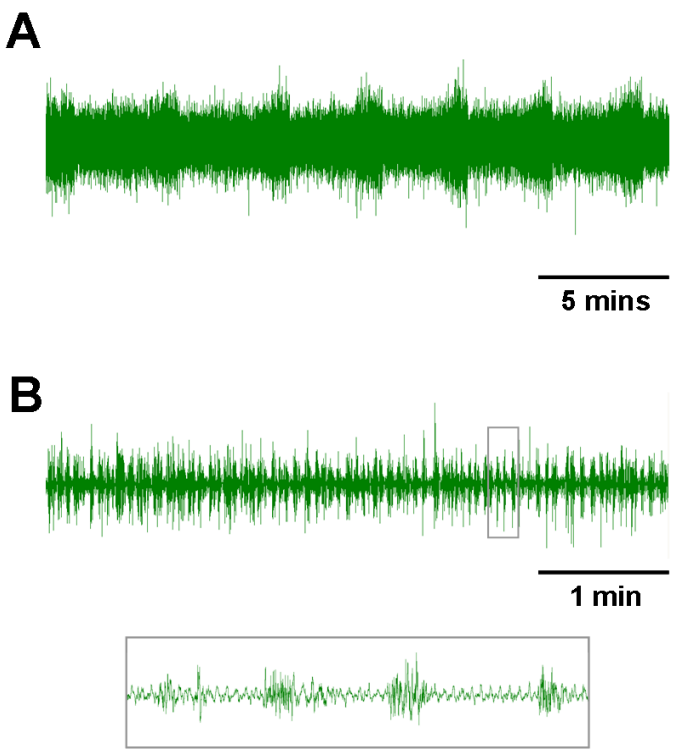

Figure 3.12 Signs of cholinergic activity under halothane anaesthesia.
A – Sleep-like spontaneous alternations are observed under halothane anaesthesia with a cycle of approximately 4 minutes. B – Spindling activity observed at 2% halothane. The boxed area and insert show three clear spindle waveforms.

Since much anaesthetic research is focused on what occurs at the surgical plane, many experiments investigating the role of the cholinergic system in anaesthesia measure endpoints that are more relevant for their needs, such as MAC. In this context, systemic blockade of both nicotinic and muscarinic acetylcholine receptors had no effect on the concentration of the volatile anaesthetic isoflurane (Eger *et al.*, 2002) or the intravenous drug etomidate (Zhang *et al.*, 2007) needed to produce immobility in rats in response to tail clamp. However, there is some evidence that manipulating cholinergic neurotransmission changes anaesthetic sensitivity, although results seem to differ depending upon the method of drug delivery.

Activation of the cholinergic system with systemic eserine reduced the duration of ketamine anaesthesia in rats (Mimura *et al.*, 1990), antagonised halothane anaesthesia in dogs (Roy *et al.*, 1981), and also increased the dose of propofol to induce unconsciousness in humans (Fassoulaki *et al.*, 1997).

Central administration of cholinergic drugs had contradictory results depending upon the location. Intracerebroventricular (ICV) injections of eserine

increased the MAC for isoflurane (Zucker, 1991), but the blocker atropine sulfate had no effect. In another study, injection of the muscarinic agonist carbachol into the pontine reticular nucleus actually reduced halothane MAC, an effect that was reversed by atropine sulfate (Ishizawa, 2000).

Other, lesion-based studies, showed that inactivating the basal forebrain increased the potency of propofol anaesthesia, in correspondence with decreased acetylcholinesterase staining in either the hippocampus (Laalou *et al.*, 2008) or the frontal cortex (Leung *et al.*, 2011).

A similar result was also found by inactivating the hippocampus directly: muscimol injection into the hippocampus increased the duration of LORR and LOTW for propofol, isoflurane and halothane (Ma *et al.*, 2002). And, in the same study, inactivation of the medial septum had the same affect. A broader analysis later identified the entire limbic system as being important in anaesthesia (Ma *et al.*, 2006): inactivating those areas that activate the limbic cortices – the SUM and the VTA – or that mediate output of the hippocampus – NAc and ventral pallidum – all enhanced the effect of halothane and pentobarbital.

The experiments in this study challenged the hypothesis that either cholinergic neurotransmission in general, or in particular to the type-2 theta oscillation, is important for LORR. This measure of anaesthesia has a strong relationship (simply in terms of pharmacological correlation) to human LOC; therefore, any understanding of the former will aid the understanding of the fundamental nature of the awake human brain and the behaving individual. As such, the study had two parallel aims: (i) to uncover a possible NCC, and (ii) to elucidate brain regions involved in anaesthetic action. Since systemic administration and medial septum delivery of atropine sulfate failed to change the point of LORR, the theta oscillation could be ruled out as a major NCC and it was deemed unnecessary to complement the analysis with the delivery of eserine before a LORR assay. The duration of LORR was not measured since by its very nature it involves excretory and metabolic processes, largely a factor of respiration, that may change independent of the central affects that mediate consciousness. Attempts to correlate the point of gain of righting reflex with ECoG signals were unsuccessful (data not shown), primarily because of the non-uniform hysteresis in anaesthetic emergence (Aouad *et al.*, 2005). Thus only the use of LORR,

and therefore the experiments in this study, can adequately represent the transition to and the mechanisms that cause anaesthetic-induced unconsciousness.

Medial septum-specific atropinization had the advantage over lesion studies in that only the type-2 theta system was affected. This acute and selective strategy avoided the damage to unrelated systems that can occur with brain lesioning approaches. It also had the advantage of testing only cholinergic neurotransmission through a pure antagonism. This is in contrast to the studies above that inactivated various regions of the brain with a GABAergic agonist (Ma *et al.*, 2006). The word "inactivation" implies simply a cessation of firing, however, since muscimol actively inhibits a variety of cell types there can be a number of possible outcomes. For instance, GABAergic neurons downstream of the inactivated pathway might be disinhibited, meaning that the actual site of inhibition could be further away from the intended site. Another problem with this method is that halothane and propofol potentiate GABA neurotransmission themselves, so in combination with GABA agonists, the additive affects may well be non-specific (Kitamura *et al.*, 2003).

By blocking type-2 theta, judged to be an epiphenomenal event for halothane actions at LORR, the lesser power of the delta oscillation was found to increase with anaesthetic concentration (Figure 3.9), whereas in the control groups the ECoG signature was dominated by theta, with no obvious change in delta over the halothane ramp (Figure 3.1B). Present during anaesthesia and NREM sleep (Franks, 2008), these slower delta frequencies are thought to result from interactions between the thalamus and the cortex (Steriade *et al.*, 1993). A complete analysis of the mechanisms involved in delta wave generation is beyond the scope of this report; however, that activating the thalamus directly by potassium channel inactivation (Alkire *et al.*, 2009) or nicotinic stimulation (Alkire *et al.*, 2007) reverses anaesthesia points towards a possible common mechanism of anaesthesia involving the thalamus and delta frequencies.

It should be noted that this study acquired its electrophysiological data from a pair of cortical screw electrodes. This technique is sufficient for analysing the general state of the brain and, in combination with monitoring muscle tone, is the prime method for scoring sleep states, making it quite amenable to measuring similar behavioural transitions between consciousness and unconsciousness. However, one electrode can only provide so much detail and the technique is therefore limited to making fairly

gross statements about the activity of the brain. And even here, brain activity alone cannot be used to delineate states of consciousness with complete confidence, as several studies have reported neocortical slow wave activity without behavioural signs of anaesthesia (Leung *et al.*, 2011; Vanderwolf, 1988).

Ongoing global oscillations are indicative of phase-locked synchronously fluctuating membrane potentials, but are also reciprocally modulated by single cell firing (Buzsaki, 2002; 2012). The theta oscillation, therefore, is regulated not only at a relatively large-grained level via cholinergic and GABAergic burst firing in the medial septum, but also at a fine-grained cellular level in the hippocampus. Place cells, for instance, fire at specific locations in the animal's environment and are temporally organised by phase precession (Jones *et al.*, 2005). The precise timing dynamics of these, and other, cells is important for ongoing behaviour, but they are transparent to ECoG techniques.

Suggestions for possible NCC have included interactions at the whole-brain level (Edelman *et al.*, 2011) to the molecular level (Hameroff, 2006); but, more likely, the NCC exist as co-dependent processes at multiple hierarchical levels and so complementary strategies, including ECoG, are necessary for research to progress in this area.

While the hypothesis that cholinergic pathways have a role in anaesthetic actions that induce LORR was now ruled out, there remained the possibility that they were involved in other aspects of the anaesthetic cascade. Other work by Ma and Leung (2002) has indicated a role for the medial septum and the theta oscillation in the excitation induced by anaesthetic induction. They found that muscimol injections into the medial septum or hippocampus attenuated both type-2 theta oscillations and this behavioural excitation.

Studies in this report recapitulated halothane-induced delirium, with C57Bl6 mice exhibiting exaggerated locomotion during anaesthetic induction (Figure 3.10). This effect was attenuated by eserine pre-administration (which also decreased baseline activity), suggesting that cholinergic facilitation of type-2 theta oscillations, rather than their ablation was responsible for blunting locomotor hyperactivity.

In addition to the behavioural excitation caused during induction of anaesthesia, hyperactivity was also observed during emergence from anaesthesia, as shown in an activity trace of three mice over the entire recording period (Figure

3.13A). Additionally, the longer it took for this phase to occur, the less extreme was the hyperactivity.

Under baseline conditions, the median frequency of the ECoG was found to positively correlate with running speed up until a maximum resonant frequency (R^2 = 0.60; second-order polynomial). High running speeds in the induction excitation phase fit this distribution, whereas low and high running speeds during emergence excitation were consistently lower than normal (Figure 3.13A).

Referring back to the original hypothesis, it appears that the hyperactivity associated with anaesthetic induction operates under normal type-1 theta dynamics. That is, locomotion speed positively correlates with theta frequency during delirium. Then, if normal theta activity persists during this phase, can it really be delirium? If this heightened activity is correlated to the confusional states in human delirium, then another mechanism must be more relevant. How, for instance, might hippocampal-cortical transfer operate under these conditions?

Complementary to this, the hyperactivity observed in the emergence phase more closely fits with the confusional hypothesis. On these terms, the reduced theta frequencies cannot support the ongoing integration of environmental and sensorimotor processing, leading to confusional states that might correlate with the anaesthetic phenomenon of emergence agitation. This is particularly problematic in children, who often wake confused and extremely distressed, and is becoming increasingly common with the use of modern anaesthetics like sevoflurane and desflurane that have rapid excretion rates (Cravero *et al.*, 2000). Qualitatively, this emergence confusion has been compared to the inconsolable crying that often accompanies waking from night terrors in the developing child (Johr, 1999), which again fits with possible overlapping mechanisms between sleep and anaesthesia (Franks, 2008).

Confusional states like these – and indeed also Alzheimer's disease, itself a risk-factor for emergence agitation – have been linked to a cholinergic deficit (Chaput *et al.*, 2012), with cholinesterase inhibitors proving promising pharmacological tools (Field *et al.*, 2012), although no direct mechanism has been found. It is possible then, that they could also be explained by a disjuncture in theta oscillation dynamics, be it either type-1 theta, type-2 theta, or most likely a combination of both.

As the animals in these confused and hyperactive states will have an intact righting reflex, by the demarcation of LORR, they would be conscious. Similarly a child or adult in a state of delirium might react with intention to push someone away

or remove their anaesthetic mask in a meaningful gesture indicative of awareness. But how relevant is this to the consciousness sought-after in a description of the NCC? If aberrant hippocampal oscillatory dynamics are important in these states then Kramis, Vanderwolf and Bland might be right after all, and the hippocampal type-1 theta oscillation may well be an NCC.

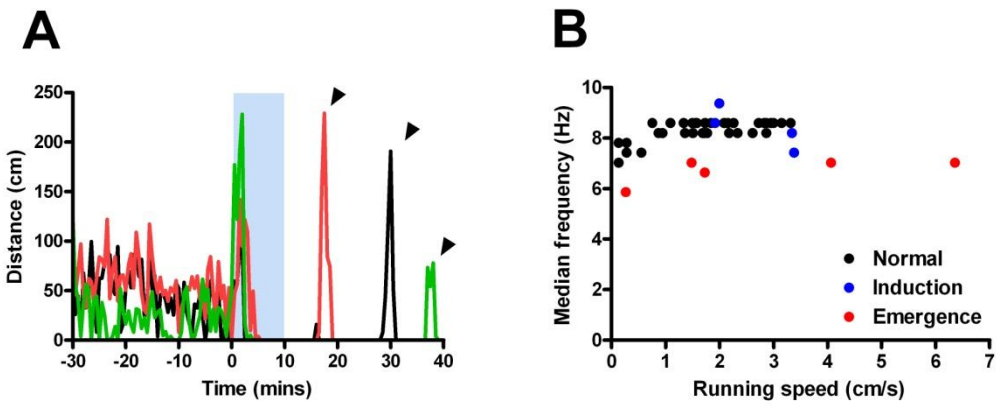

Figure 3.13 Emergence agitation correlates with theta frequency impairment. *A – The response to 10 minutes exposure to 2% halothane (marked by the blue box) is shown in three C57Bl6 mice. Notice the large increase in activity at the onset of anaesthetic exposure, indicative of pre-hypnotic delirium, and the later increased activity when the animals emerge from the anaesthesia in a state of agitation (arrowheads). B – A representative example of one C57Bl6 mouse. Median theta frequency correlated with running speed in the anaesthetic chamber before halothane was introduced (Normal: black). Increased movement during induction was associated with a similar frequency distribution (Induction: blue), but theta frequency in the emergence state was lower than predicted by the model distribution (Emergence: red).*

Behavioural experiments

4.1 Background

Previous studies have indicated a diverse array of mild to moderate behavioural phenotypes in TASK-3 KO mice. Compared to control mice, TASK-3 KOs have impaired performance in spontaneous alternation and in the Morris water maze (Linden *et al.*, 2007). The finding that TASK-3 KO mice have aberrant type-2 theta oscillations (4-7 Hz) could explain the impaired performance in these hippocampal-dependent cognitive tests. Further investigations, therefore, set out to (i) examine the behavioural type-2 theta in TASK-3 KO mice and (ii) examine other cognitive behaviours in TASK-3 KO mice.

During the course of the studies well-described behavioural tests were performed as well as more experimental and completely new paradigms. The T-maze investigates working memory, a fundamental process involving important interactions between the prefrontal cortex and the hippocampus (Jones *et al.*, 2005). The object recognition test analyses the explicit memory over both short (minutes to hours) and long (days) time periods (Bevins *et al.*, 2006). Hippocampal-dependent fear memory was investigated using an adaptation of traditional foot shock conditioning paradigms, the dropbox.

4.2 Eliciting alert immobility in the rat exposure test

To discover if TASK-3 KO mice were able to produce type-2 theta activity during natural behaviour, a version of the rat exposure test was validated that should induce the freezing behaviour associated with the type-2 theta oscillation. Developed to investigate defensive behaviours in mice with a view to testing anxiety levels, the rat exposure test elicits robust freezing behaviour, as well as other mouse defensive activity like the stretch attend posture and digging behaviour (Yang *et al.*, 2004).

The original design consisted of a home chamber connected by a tunnel to an exposure chamber in which a rat was housed behind a wire mesh. Since this study was primarily concerned with freezing behaviour, the chamber was modified to a single exposure chamber with a small boxed-in "safe-zone", separated from the rat by a wire mesh.

Freezing behaviour was scored using a video recording and EMG analysis, in response to the sight and smell of a rat. The test was validated in C57Bl6 mice, which froze for an average of 24.1 ± 4.1 s (n = 9) and, importantly, this freezing behaviour co-occurred with an oscillation in the type-2 frequency range.

TASK-3 KO mice showed a similar degree of freezing to littermate controls, both in terms of the number of separate freezing events and their duration ($p = 0.20$ and $p = 0.50$, respectively). However, 2-way ANOVA of the ECoG revealed differences between the genotypes in the power spectra associated with both movement and freezing. Figure 4.1A shows the considerable overlap in the movement power spectra between genotypes and, correspondingly, post hoc Bonferroni's tests comparing each 0.78 Hz bin up to 25 Hz showed that TASK-3 KOs had only a subtle increase in power during movement compared to littermates at 7.81 Hz ($p < 0.05$), In contrast, the power of the theta oscillation during freezing was deemed significantly lower ($p < 0.001$) in TASK-3 KO mice than in littermates for a much larger frequency range, between 6.25 Hz and 8.59 Hz (Figure 4.1B).

These results indicate that as well as having aberrant type-2 theta oscillations with halothane anaesthesia, TASK-3 KO mice also have reduced power in type-2 theta in a natural behavioural setting, while, as for the halothane condition, peak frequency remains unchanged ($p = 0.53$).

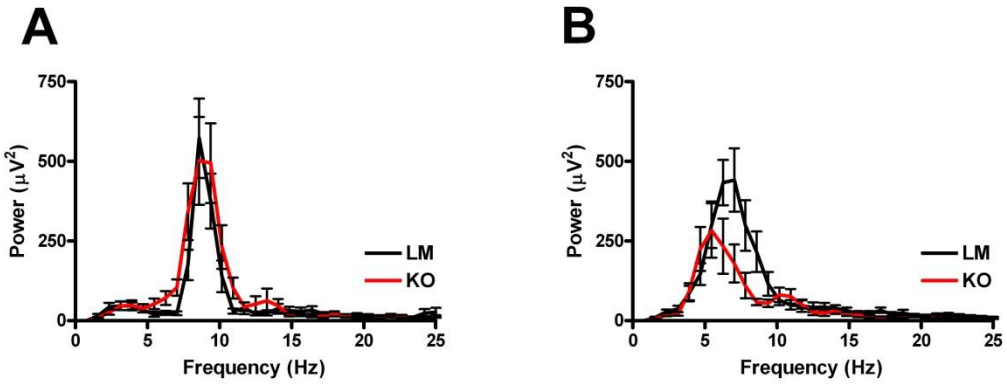

Figure 4.1 Type-2, but not type-1, theta power is reduced in TASK-3 KOs.

A – Power spectral analysis of locomotion speeds above 2cm/s reveals that TASK-3 KO mice have intact movement-related type-1 theta, compared to littermates. B – TASK-3 KO mice have reduced power in the type-2 theta oscillation during alert immobility induced by the rat exposure test. (For clarity, significance levels are not shown on graph)

4.3 Testing working memory in the spontaneous alternation T-maze

Previous studies have shown that TASK-3 KO mice have impaired performance in the spontaneous alternation version of the T-maze (Linden *et al.*, 2007). The T-maze is classically used to measure working memory performance in rodents: a mouse or rat placed into the trunk of a "walled-in" T-shape will choose to enter one of the arms of the T; after returning to the start – following an innate predisposition to explore novelty – the animal will, more often than not, enter the other previously blocked arm. Additional rewards and punishments can be added to probe motivational and other learning and attentional processes; however, the version of the test used in this study intended to exclusively explore working memory.

A modified version of the continuous alternation T-maze, first described by Gerlai (1998), was used in which, except on the first trial where one of the goal arms was blocked-off, the animals were free to choose either arm once they had returned to the start position. Since the animals make this return journey under their own volition, there is minimal interference by the investigator.

The test, with alternation scored as a percentage "correct" choice in a total of ten trials, was first validated in C57Bl6 mice, which showed an average of 80 ± 6 % correct choices, significantly different to a hypothetical mean of 50%, that for a random decision making process ($p < 0.05$).

TASK-3 KO mice ($n = 11$) had an average of 60 ± 7 % correct choices, which was not significantly different to LM controls ($n = 9$), which had a slightly better performance with an average of 64 ± 6 % correct choices ($p = 0.62$). However, when the separate groups were compared to the hypothetical mean of 50%, the TASK-3 KO mice were not significantly different to chance ($p = 0.19$), whereas the LMs performed better than chance ($p < 0.05$). These divergent results can perhaps be explained by the increased spread of the TASK-3 KO data, as shown by the individual data points plotted in figure 4.2A, but taken together they show that TASK-3 KO mice have impaired performance in the T-maze.

To test whether basal activity of the mice could have been a confounding factor, the latency to complete the ten trials was also compared between the two genotypes. As shown in figure 4.2B, there was no difference between the two groups ($p = 0.65$). Additionally, there was no correlation between the time it took to complete the ten trials and the percentage of correct choices for either genotype, with R^2 of 0.03 for TASK-3 KOs and R^2 of 0.02 for littermates.

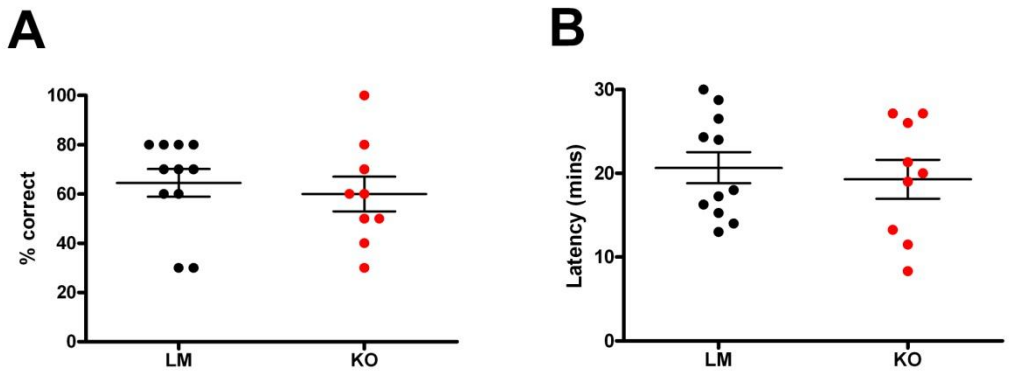

Figure 4.2 TASK-3 KO mice perform similarly to littermates in the T-maze.

A – On average, TASK-3 KO mice perform the same number of "correct" choices in the alternation T-maze, but not significantly different to chance. B – The latency to complete 10 alternation trials is the same for TASK-3 KO and littermates.

4.4 Testing object recognition memory

A role for the type-2 theta oscillation has been implicated in novelty detection (Myhrer *et al.*, 1988) so any changes in this oscillation in TASK-3 KO mice might impair novelty salience and subsequent novelty recognition. To test this hypothesis, the object recognition test was validated in C57Bl6 mice and then performed on TASK-3 KO and control mice.

C57Bl6 mice were habituated to a novel open field environment for 10 minutes and then, after a further 10 minute inter-trial period, they were exposed to two identical objects in a 10 minute training phase. Interaction time was scored as the time the mice spent with their noses touching the objects. Figure 4.3A shows that in the training phase the mice had no preference for either object ($p = 0.36$), spending an average of 16.8 ± 8.1 s interacting with the left object and 11.8 ± 4.0 s interacting with the right object.

After a second inter-trial period of 10 minutes, one object was swapped for a novel object and the mice were allowed 10 minutes of exploration in the new environment. In this test for short-term memory, the novel object should evoke a greater amount of interest and interaction. In this phase, the mice showed a significant preference for the novel object ($p < 0.05$), exploring the novelty for 22.5 ± 2.9 s, twice as much as the familiar one, which attracted only 11.3 ± 3.6 s of interaction (Figure 4.3B).

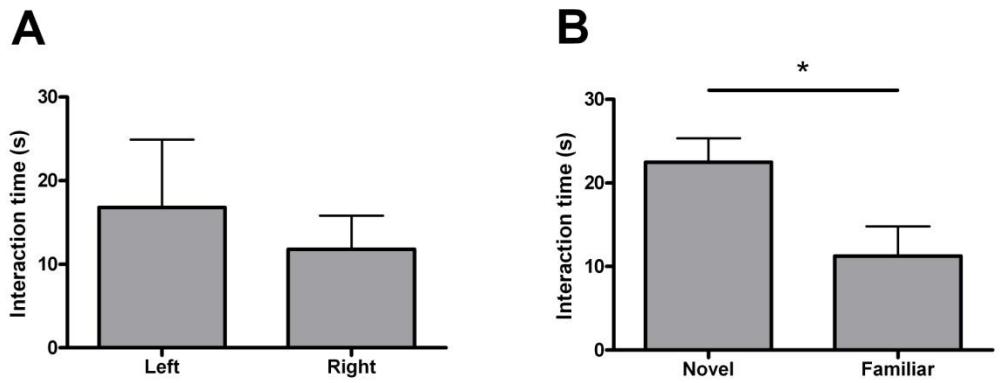

Figure 4.3 C57Bl6 mice recognise a novel object 10 minutes after exposure to two identical objects.

*A – Mice have no preference for either of two identical objects in the 10-minute trial phase of the object recognition test. B – A significant increase in interaction with the novel object in the test phase indicates intact object memory. (*p < 0.05)*

Once the procedure was validated, TASK-3 KO and littermate controls (n = 14 and n = 10, respectively) were run through the test. In the training phase, littermates interacted with both objects equally (20.2 ± 2.6 s vs. 20.4 ± 2.9 s; p = 0.91), as did TASK-3 KOs (26.1 ± 3.3 s vs. 25.1 ± 3.8 s; p = 0.68), as reflected in figure 4.4A. Although TASK-3 KO mice had a tendency for greater interaction, there was no significant difference between the genotypes (p = 0.26).

After one object was swapped for the novel object, the mice were allowed 10 minutes of exploration in the new environment. In this phase, shown in figure 4.4B, the animals in both groups showed a statistically significant preference for the novel object, with littermates preferring the novel object to the familiar one by 22.4 ± 3.4 s to 13.6 ± 3.5 s, and TASK-3 KOs by 22.5 ± 2.8 s to 14.3 ± 3.1 s (p < 0.05 for both). The interaction score was not significantly different between genotypes (p = 0.81).

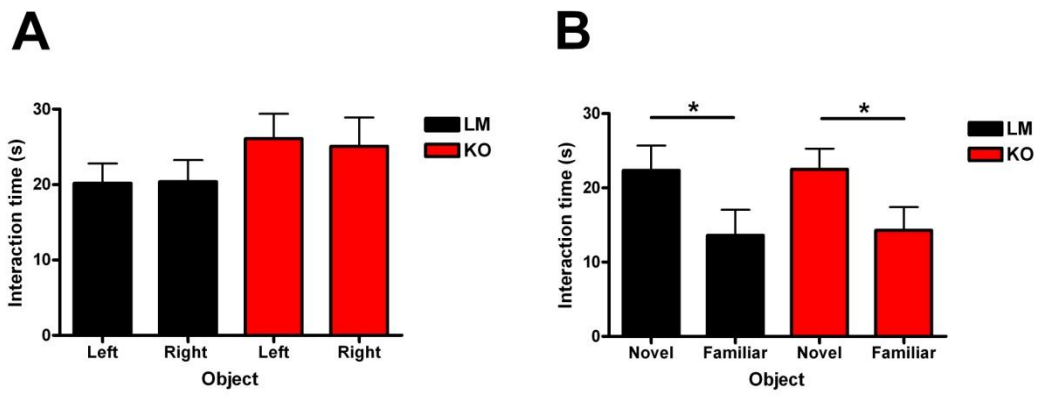

Figure 4.4 TASK-3 KO mice perform normally in the short-term object recognition test.

*A – In the training phase TASK-3 KO mice and littermate controls explore two identical objects equally. B – Both genotypes have a similar preference for a novel object, indicating similarly intact object recognition memory. (*p < 0.05)*

Further to this short-term test, long-term memory retention was investigated by exposing the mice to a second novel object 24 hours later, with the results in figure 4.5. TASK-3 KO mice (n = 8) preferred the novel object by an average of 46.6 ± 3.5 s to 12.6 ± 2.8 s for the familiar object ($p < 0.01$). Littermates (n = 5) also showed a significant preference for the novel object (38.6 ± 6.8 s vs. 12.0 ± 2.2 s; $p < 0.05$). The interaction score was not different between the two genotypes ($p = 0.50$).

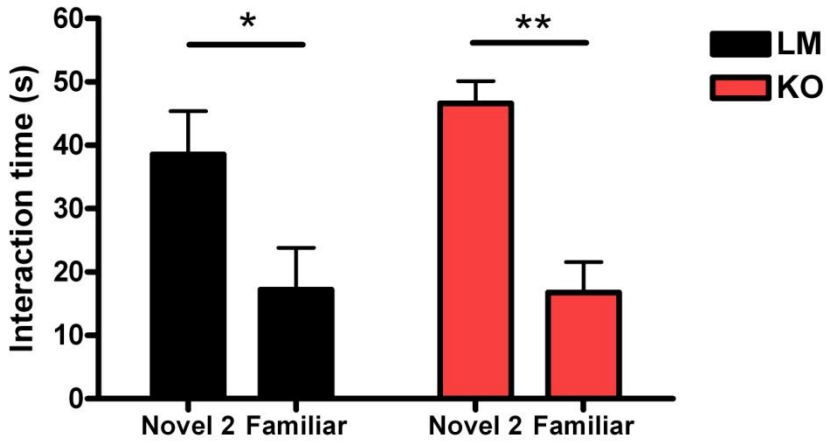

Figure 4.5 TASK-3 KO mice perform normally in the long-term object recognition test.

*TASK-3 KO mice perform equally to littermates in recognising a second novel object 24 hours after the first presentation. (*p < 0.05; **p < 0.01)*

4.5 Testing spatial recognition memory

The spatial recognition test measures the ability of an animal to recognise its spatial surroundings. The test was validated in C57Bl6 mice (n = 4), which were habituated to five fixed objects over three 10 minute sessions. 1-way ANOVA revealed a significant effect of habituation session on object interaction ($p < 0.001$), as shown in figure 4.6A. Bonferroni's test was then used to analyse significance between sessions. In the first session, the animals interact with the five objects an average of 41.5 ± 3.1 s, significantly more than in the second session, with 18.1 ± 2.7 s total interaction ($p < 0.001$), and the third session, with 10.6 ± 1.4 s interaction ($p < 0.001$). There was no significant decrease in interaction between the second and the third session ($p > 0.05$). This habituation of interaction time indicates intact object-place learning. Importantly, there was no difference in the interaction times between the objects, meaning that none of the objects was inherently more interesting that the others, a fundamental consideration for object preference studies.

After habituation, two of the objects were placed in new spatial locations and the animals were tested for their recognition of the change; evidenced by an increased interaction time with the displaced objects. Figure 4.6B shows that the animals favoured the displaced objects by interacting with them over 60% more than the non-displaced objects ($p < 0.01$).

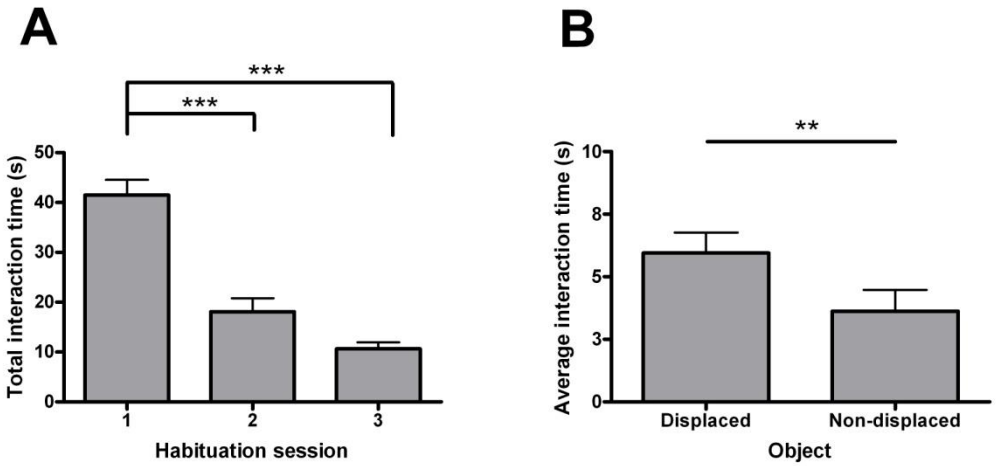

Figure 4.6 The spatial recognition test is validated in C57Bl6 mice.

*A – Over three exposure sessions the mice explore the 5 objects less, indicating habituation and learning. B – In the test phase the mice recognise the new spatial arrangement with increased preference for the displaced objects. (**p < 0.01; ***p < 0.001)*

TASK-3 KOs and littermate controls (n = 7) were then run through the spatial recognition test, with both genotypes showing significant modulation of interaction in the habituation phase ($p < 0.01$ for littermate and $p < 0.05$ for KOs; 1-way ANOVA). Littermates showed a significant reduction in object interaction in the second and third sessions compared to the first session, as judged by Bonferroni's post hoc tests ($p < 0.05$), while there was only a significant reduction between the first and third sessions for TASK-3 KOs ($p < 0.05$), as shown in figure 4.7A.

In the test phase, two objects were moved into new spatial locations and the time spent interacting with the displaced objects was compared to that for the non-displaced objects. Figure 4.7B shows that neither genotype had a significant preference for the displaced objects ($p = 0.71$ for littermates and $p = 0.49$ for TASK-3 KOs). Despite the TASK-3 KOs showing a slightly longer interaction time throughout the four sessions, there was no significant difference between the genotypes (e.g., $p = 0.46$ for the test phase). Here, short-term recognition of the displaced spatial environment seems to be similarly impaired in both genotypes (interaction scores are no different, $p = 0.57$). Since a long-term consolidation test 24 hours later in C57Bl6 mice revealed no significant preference for displaced objects ($p = 0.48$), a long-term test was not performed on TASK-3 KOs and littermates.

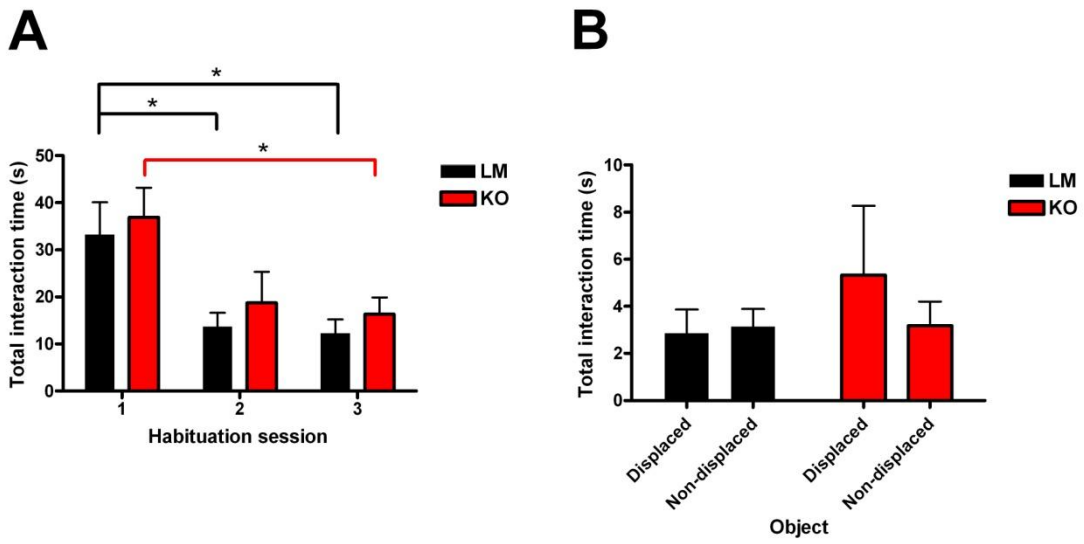

Figure 4.7 TASK-3 KO mice perform equally to littermates in the spatial recognition test.

*A – In the habituation phase, littermate mice have significantly reduced object interaction by the second session, whereas TASK-3 KO mice take until the third session. B – In the test phase, neither genotype interacts with the displaced objects for longer than the non-displaced objects. (*p < 0.05)*

4.6 Testing emotional memory in the dropbox

A novel Pavlovian conditioning paradigm was developed using the naturalistic fear of water instead of an electric shock. After habituation to the dropbox environment on the first day, a trace conditioning procedure was performed on two consecutive days where the unconditioned stimulus (dropping into water) was separated by a trace interval from the conditioned stimulus (10,000 Hz tone). On the fourth day, the mice were returned to the dropbox and contextual memory was assessed by the amount of freezing.

The test was validated in three test groups of C57Bl6 mice (n = 4/6). Two of the groups were administered either saline vehicle or 50 mg/kg atropine sulfate prior to each conditioning session and a third group was subjected to the tone but no water drop. 1-way ANOVA of the data revealed a significant drug effect on freezing ($p < 0.01$).

Figure 4.8, and associated Tukey's tests, show that when the mice are placed back into the context, the unconditioned control group, which had no previous water drop, show little freezing behaviour (11.8 ± 2.7 s). Dropbox conditioning causes a significant freezing phenotype (49.7 ± 7.5 s, $p < 0.01$), an effect that is sensitive to muscarinic antagonism by atropine sulfate (23.0 ± 6.7 s, $p < 0.05$). Further, there is no difference between the unconditioned control group and the atropine treated group ($p = 0.20$), suggesting complete dependence for memory acquisition on muscarinic-cholinergic neurotransmission.

When freezing was tested in response to the tone in a neutral context, there was no difference in freezing between the saline and the atropine sulfate-treated group (data not shown; $p = 0.36$).

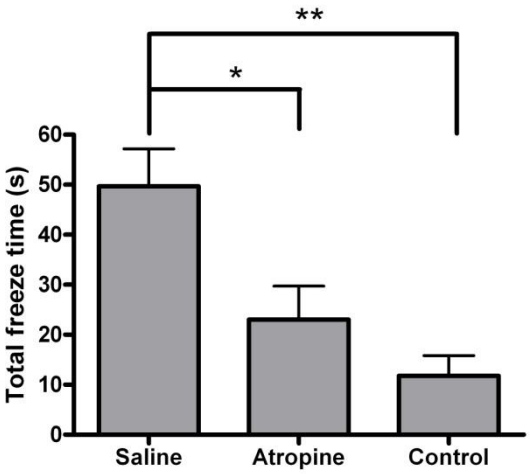

Figure 4.8 C57Bl6 mice show significant freezing in the dropbox.

*The freezing response after aversive memory conditioning is attenuated with systemic atropine sulfate during the acquisition phase. (*p < 0.05; **p < 0.01)*

The test was repeated in TASK-3 KO mice (n = 6) and littermate controls (n = 7), with the results shown in figure 4.9. Both genotypes displayed freezing behaviour when replaced in the conditioned context of the dropbox after training, TASK-3 KOs froze for an average of 34.5 ± 8.7 s, much less than littermates, which froze for an average of 55.4 ± 8.2 s. However, this difference was not statistically significant (p = 0.11). TASK-3 KOs also spent less time exploring the environment during the trial phase, as in figure 4.9B, but again this difference was not statistically significant (p = 0.10). Therefore, TASK-3 KO mice have a statistically normal freezing response to dropbox conditioning.

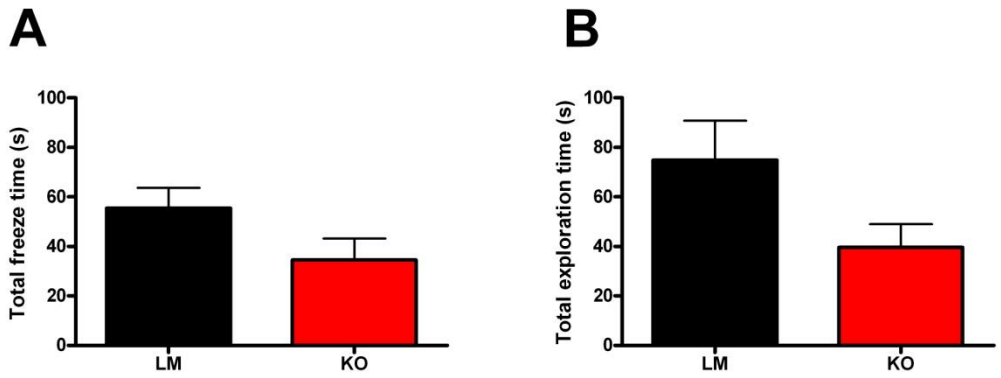

Figure 4.9 TASK-3 KO mice perform similarly to littermates in the dropbox.
A – The aversive conditioning of the dropbox elicits robust freezing in both genotypes. B – TASK-3 KOs have a non-significant trend towards lower exploration in the context of aversive conditioning.

4.7 Testing the homeostatic orientation response

The ability for an animal to orient itself in space upon external dislocation has been associated with the vestibular system and the hippocampus (Tai *et al.*, 2012). Specifically, the homeostatic orientation response has been shown to depend upon the type-2 theta oscillations (Shin, 2010). This ability was tested in TASK-3 KO mice in comparison to littermate controls.

The number of rotations in the same direction of the rotation was quantified during 2 minutes of rotation. With saline injection, TASK-3 KO mice (n = 5) performed 21 ± 2 rotations, which was not significantly different (p = 0.59) to littermate controls (n = 4), with 19 ± 4 rotations (Figure 4.10). Atropine sulfate had no effect on the orientation response in either genotype (p = 0.96 for littermates and p = 0.34 for TASK-3 KOs), with TASK-3 KOs performing 18 ± 2 rotations and littermates 18 ± 4 rotations.

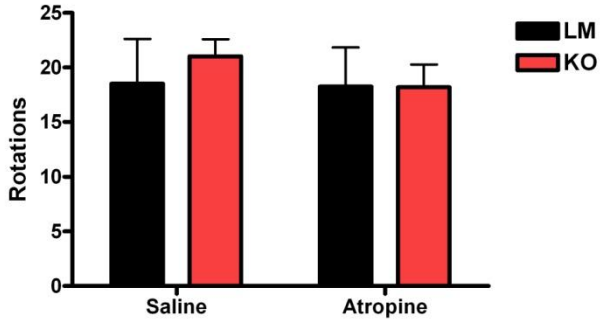

Figure 4.10 TASK-3 KO mice have intact orientation response.

TASK-3 KO mice have no deficits in the orientation response and none of the genotypes are affected by atropine sulfate pre-administration.

4.8 Discussion

These studies first sought to clarify whether the type-2 theta impairments in TASK-3 KO mice were limited to the anaesthetic condition. Previous studies had shown that TASK-3 deletion ablates the type-2 theta oscillation usually found in response to halothane anaesthesia, and that this oscillation was unaffected by atropine sulphate or eserine (Pang *et al.*, 2009), suggesting serious deficits in the cholinergic system that mediates type-2 theta activity. In addition, it was possible that the sequelae of cognitive impairments suffered by TASK-3 KO mice could be explained by a type-2 theta impairment during natural behaviours.

The type-2 theta oscillation was identified in a series of seminal experiments along with the type-1 theta rhythm (Kramis *et al.*, 1975; Usui *et al.*, 1977). Recorded from the hippocampus of rodents, the theta rhythm is an oscillation of between 4 and 12 Hz that changes depending upon the ongoing behaviour of the animal. The type-1 theta oscillation results from glutamatergic and serotonergic inputs from the entorhinal cortex and predominates at the higher range of frequencies. The frequency also positively correlates with running speed of the animal and hippocampal place cells, which fire at a precise location in the spatial field of the animal, have been shown to be modulated by the hippocampal theta rhythm (Hasselmo, 2005).

The type-2 theta oscillation is readily observed in rodents during anaesthesia with various drugs, including urethane and halothane (Bland *et al.*, 2003; Clement *et al.*, 2008), and less so during certain behavioural routines (Kramis *et al.*, 1975; Sainsbury *et al.*, 1987). Rabbits produce relatively long trains of type-2 theta activity in response to a wide range of sensory stimulations (Bland *et al.*, 1981) and guinea pigs display type-2 theta in response to stimulation during situations of heightened arousal in the presence of predators such as snakes (Sainsbury *et al.*, 1984). Rats also produce type-2 theta in the presence of predators such as the cat and ferret, and previously neutral stimuli can elicit type-2 theta oscillations during predator exposure, leading to the hypothesis that type-2 theta only occurs during sensory processing when the animal is in an aroused state (Sainsbury *et al.*, 1987). There is also evidence that immobility-related type-2 theta occurs during wider-scale environmental processing and initiation of motor programs (Oddie *et al.*, 1997), as well as memory processing in fear conditioning paradigms (Seidenbecher *et al.*, 2003). Other type-2 behaviours such as the automatic motor activities associated with eating and

copulating occur with a desynchronised brain activity with large irregular amplitude (LIA) when the animals presumably interact less with the wider environment.

Different rodent species, therefore, have broadly similar type-2 theta stimulants, with the main difference appearing to be the arousal threshold. While rabbits have a well-known propensity to freeze with unpredictable but non-specific stimuli – even vehicle headlights will do, for example – in studying the mouse it became apparent that robust freezing behaviour could not simply be caused by unpredictable and aversive stimuli. Although there is some evidence that type-2 theta oscillations may be important in the freezing behaviour used as a measure of fear memory in Pavlovian conditioning paradigms, the finding that inescapable shock – essentially the definition of the foot-shock fear memory paradigm – is associated with a specific ablation of the type-2 theta oscillation (Balleine *et al.*, 1991) contraindicates shock tactics.

Therefore, the approach focused on more naturalistic ways to induce alert immobility, such as exposing the test subject to evidence of a predator. Fox odour, and its artificial analogue trimethylthiazoline (TMT), for instance, has been used to induce freezing behaviour in mice (Fendt *et al.*, 2005). Interestingly, inactivation of the lateral septum, a structure adjoining the type-2 theta-related medial septum, blocks fox odour-induced fear behaviour (Endres *et al.*, 2008). Evidence that the pertinent odour-processing oscillatory frequencies are in the beta range (Fendt *et al.*, 2005) does not rule out the involvement of type-2 theta in the actual freezing behaviour. The simplicity of this test was an attractive feature, but the chemicals involved are extremely potent and have the potential to cause lasting effects in animals that are not involved in the study.

Efforts then narrowed to the rat exposure test (Yang *et al.*, 2004). This model of mouse defensive behaviours causes robust freezing behaviour among other threat-related activity such as the stretch attend posture, stretch approach and threat contact reduction. The apparatus was modified to exclude the central tunnel and home area to maximize contact with the rat, and to counteract the possibility of ablating type-2 theta, as occurs in inescapable conditions, a small “safe-zone” was created to which the mice could retreat.

The test elicited robust freezing behaviour associated with type-2 theta in C57Bl6 mice, and also in TASK-3 KO mice and littermate controls. While the peak frequency of the theta oscillation was unchanged, the power of the theta frequency

was significantly reduced in the TASK-3 KOs. It has been proposed that the frequency of the oscillation is set by GABAergic projections into the hippocampus, with inhibitory interneurons more able to regulate timing of pyramidal cell firing, while the power of the oscillation is controlled by cholinergic projections, with muscarinic receptors more suited to slower state changes (Hasselmo *et al.*, 2001). This is consistent with the previously proposed cholinergic system deficit in TASK-3 KO mice.

The next studies sought to investigate a possible link between the cognitive impairments of TASK-3 KO mice and the newly described behavioural type-2 theta impairment. Previous studies had found memory impairments in TASK-3 KO mice in the T-maze and the Morris water maze (Linden *et al.*, 2007).

In the Morris water maze TASK-3 KO mice were slower to find the platform throughout the training phase, but only TASK-3 KO females showed fewer platform crosses during the probe trial (Linden *et al.*, 2007). No such sex differences were found in the T-maze and, overall, TASK-3 KO mice showed a working memory deficit as judged by a lower alternation rate compared to littermates.

The study in this report, however, showed that TASK-3 KO mice performed with equal alternation rates to littermate controls. The different findings here can be explained by the time of day that the experiment was completed: Linden *et al.*'s (2007) study was performed during the light phase of the diurnal cycle, whereas the study reported here was performed in the dark phase. Being the active phase of the rodent circadian rhythm, the dark phase is cognitively more relevant, given the evolutionarily-disposed behavioural demands of a nocturnal species.

Further studies by Gotter *et al.* (2011) add complexity to the situation with results indicating working memory deficits in the Y-maze in TASK-3 KO mice in the inactive phase but not in the active phase. A point worth noting is that few studies compare their alternation rates to the hypothetical null-hypothesis mean of 50%; so, in fact, it is not clear if even the control animals alternate at rates above chance. When this measure was taken in this study, littermates alternated at above chance level but TASK-3 KOs did not. Taken together, the data from three separate groups indicates that TASK-3 KO mice have subtle impairments in working memory in the active (wake) phase, which are accentuated in the inactive (sleep) phase, suggesting sleep-

related cognitive bias. A direct comparison in working memory performance between controls in the active and inactive phase has not yet been made.

Alternation rate in the T-maze has been variously impaired by hippocampal (Johnson *et al.*, 1977) and septal lesions (Clody *et al.*, 1969), consistent with a role for the septohippocampal system in mediating novelty-related working memory. A specific role for the cholinergic system is shown by anatgonism in the medial septum reducing alternation rates (Givens *et al.*, 1995), whereas eserine enhances alternation (Egger *et al.*, 1973). Complementary to this, lesions of the basal forebrain, which provides cholinergic input to the prefrontal cortex, also reduces alternation rate (Murray *et al.*, 1986). The importance of this dual cholinergic system is also supported by a coupling of theta oscillations between the hippocampus (via medial septum) and the prefrontal cortex (via basal forebrain) during successful memory performances (Hyman *et al.*, 2005; 2010).

A specific role for medial septum-regulated type-2 theta in alternation working memory is highlighted by cholinergic antagonism reducing choice accuracy in the T-maze (Givens *et al.*, 1990). Here, the change in theta frequency correlated with the deficit in choice accuracy, but further studies showed that rather than a decrease in frequency, blocking muscarinic neurotransmission by intra-septal scopolamine caused in increase in theta frequency (Givens *et al.*, 1995).

While TASK-3 channels are widely expressed in the hippocampus (Talley *et al.*, 2001; Torborg *et al.*, 2006) and have a role in muscarinic neurotransmission in the thalamus (Meuth *et al.*, 2003), the exact role of TASK-3 conductances in the septo-hippocampal system in relation to theta activity and working memory is unknown. The relatively intact working memory of TASK-3 KO mice in this study could therefore be due to the pseudo-normal theta frequency dynamics in both moving (type-1 theta) and immobility (type-2 theta).

A role for type-2 theta in environmental and sensory processing in states of high arousal has already been explicated (Bland *et al.*, 2001; Oddie *et al.*, 1998; Sainsbury, 1998). It therefore follows that type-2 theta might also have a role in novel situations where the animal must be alert and ready to respond to potential threats. In an early study in this regard, when rats were exposed to a novel smell they exhibited oscillatory activity in the high theta frequency range, usually indicative of the type-1 oscillation (Myhrer *et al.*, 1988). However, since the animals were perfectly still at

this time, and although the response was only non-specifically blocked by atropine sulfate, the case was made for it being of the type-2 variety.

More recently, there has been some controversy as to which facet of the theta oscillation is more important in processing novelty. Jewajee *et al.* (2008) showed that, over several days of habituation to a novel environment, the frequency of the theta oscillation increased and then decreased sharply again with unexpected novelty. These findings were directly questioned by Sambeth *et al.* (2009), who argued that using foraging food-deprived rats undermined the study since food consumption and reinforcement increases hippocampal acetylcholine levels (Ghiani *et al.*, 1998). Additionally, the Sambeth *et al.* study (2009) found novelty to correlate with an increase in power of the theta oscillation rather than a decrease in frequency. However, they were unable to replicate a positive correlation between running speed and theta frequency, which puts their own data into question.

Within the context of this relatively ambiguous situation, it made sense to test the ability of TASK-3 KOs to recognise novelty. Would a deficit in theta power translate to novelty recognition impairments in TASK-3 KO mice?

In fact, TASK-3 KO mice showed similar behaviour to littermate controls firstly in response to novelty, and then in subsequent recognition of novelty over the short-term and long-term. In the first object exposure, both genotypes showed little signs of anxiety and interacted with both novel objects equally. When one object was replaced for another, TASK-3 KOs and littermates both showed a significant preference for the novel object, with no difference between the genotypes as judged by the interaction ratio, which normalises for individual differences in activity.

As TASK-3 KO mice show sleep differences compared to controls (Pang *et al.*, 2009), it was reasonable to predict that memory consolidation during sleep, and therefore retention of the object-memory, might be affected. Specifically, TASK-3 KO mice show significantly reduced sleep in the first two hours of the lights-on sleep phase of their diurnal cycle and a fragmented sleep pattern when they finally do sleep. That is, they have more numerous but shorter length episodes of sleep, and they appear to be less able to support long trains of REM sleep (Pang, 2010). Other work, however, suggests that TASK-3 KOs have exaggerated nocturnal locomotor activity (Gotter *et al.*, 2011; Linden *et al.*, 2007), and a less, rather than a more, fragmented sleep pattern (Gotter *et al.*, 2011).

A point worth mentioning here though is that polysomnographic sleep scoring uses a template based on ECoG and EMG derivatives, which, if animals have inherently different neuronal oscillations – as TASK-3 KOs appear to have – may skew the interpretation of results. Therefore, any sleep stage scoring should also be accompanied by ECoG frequency distributions to clarify that the same sleep stage is being compared between animals.

When the TASK-3 KO mice were tested for object recognition 24 hours after training they performed as well as littermates. Moreover, the recognition appeared to be enhanced in TASK-3 KO mice as they, but not littermates, showed a significant increase ($p < 0.01$) in interaction score between the 10 minutes test and the 24 hour test, suggesting facilitated long-term (and sleep-dependent) memory consolidation.

Gotter *et al.* (2011) tested novelty recognition 3 hours after acquisition and also found a facilitation of object-memory in TASK-3 KO mice over controls. The authors make an attempt to explain this phenomenon through the trend towards increased interaction time in the acquisition phase for TASK-3 KO mice, consistent with a facilitatory role of novelty-induced immobility-related theta (Myhrer *et al.*, 1988). It is not stated whether the animals in Gotter *et al.*'s study (2011) slept between the two exposures, but the inter-trial period is consistent with medium to long-term memory consolidation that can be enhanced by sleep (Binder *et al.*, 2012). In fact, there is a reciprocal relationship between sleep and novelty recognition: novel object presentation increases the amount of REM sleep, and therefore theta frequency activity (Schiffelholz *et al.*, 2002), and is impaired by sleep deprivation (Palchykova *et al.*, 2006). So it possible that the fragmented REM sleep baseline in TASK-3 KO mice is more labile to the effects of novelty, leading to an enhanced memory consolidation. In any case, the sleep deficits in TASK-3 KO mice do not appear to impair object-memory.

To probe the memory of TASK-3 KOs further, their performance in a spatial recognition paradigm was measured. Performance in this version of the test has also been linked to the septohippocampal system and concurrent theta activity (Okada *et al.*, 2010). The hippocampus has a long-known role in spatial memory, both in reinforced tests such as the Morris water maze and unreinforced tests like spatial recognition (Gerlai, 2001). Place cells, that fire in specific locations of the animals' spatial field, are also linked to the theta oscillation (O'Keefe *et al.*, 1978).

The mice in this study were exposed to five objects over three habituation sessions, before two of the objects were displaced in a fourth trial (Save *et al.*, 1992). If the mice recognised the change then they should spend more time interacting with the displaced objects. Both littermates and TASK-3 KOs showed habituation to the objects as measured by a decrease in interaction time over the course of the first three object exposures indicating intact object-place memory. The difference between the first two sessions for TASK-3 KO mice was not significantly different, possibly due to the tendency for increased exploration compared to littermates.

In the probe test, neither genotype showed a preference for the displaced object, indicating that spatial recognition memory is impaired in both littermates and TASK-3 KO mice. However, a more likely explanation is that the test suffered from methodological problems. Despite the fact that the test was validated in this laboratory in C57Bl6 mice, with a significant preference for the displaced objects in the probe test, this was only in four individuals. Previous work using this five object format has been performed in rats rather than mice, and even then the effect was on the order of a few seconds of preference for the displaced object (Okada *et al.*, 2010). Mouse studies have usually opted for using fewer objects to test spatial memory. Indeed, several studies use only two identical objects over the three habituation sessions, one of which is moved to a new location in the probe test (Florian *et al.*, 2011; Palchykova *et al.*, 2006). While overall the objects in this study elicited no group preference, some individual animals did appear to have a preference for one particular object, which they would favour even in the presence of an object in a novel spatial location. Future tests of this sort should be based on simplified versions of the spatial recognition test that may more precisely delineate any impairment in theta-dependent memory encoding.

The next experiments sought to measure the emotional memory in TASK-3 KO mice. This is often tested in rodents using Pavlovian fear conditioning paradigms (Maren *et al.*, 2004), which consist of a box that delivers a series of electric shocks to the animal, sometimes associated with a tone. When the animal is placed back into the box or hears the tone, even in a different context, the animal will have a freezing response in expectation of being shocked. The amount of freezing is suggested to act as a marker for emotional memory.

The neuronal circuits involved in mediating this fear response include the amygdala, a part of the evolutionarily ancient limbic system of the brain (Kapp *et al.*, 1979) and the hippocampus (Berry *et al.*, 2001). Conditioning to the tone stimulus itself is primarily associated with activity in the lateral amygdala (Quirk *et al.*, 1995), whereas fear memory based on contextual (spatial) cues involves the hippocampus (Vazdarjanova *et al.*, 1998).

Further, cholinergic neurotransmission and the theta oscillation have been implicated in the hippocampal processing relevant to fear memory acquisition and retrieval. Blocking muscarinic neurotransmission through systemic scopolamine dose-dependently reduced freezing in the acquisition phase, retrieval to context phase and retrieval to tone phase (Anagnostaras *et al.*, 1999). More refined cholinergic antagonism in the rat hippocampus generally (Gale *et al.*, 2001), and the CA3 region more specifically (Rogers *et al.*, 2004), caused reduced freezing in the acquisition phase of the test and also when the animals were returned to the fear context 24 hours later. In addition, fear responses to tone conditioning were unchanged. These findings fit with computational models suggesting that enhanced cholinergic signalling is important for the acquisition of contextual fear memory (Hasselmo *et al.*, 1995).

In addition, that the cued conditioning was similar in saline and atropine-treated groups indicates that the effect was specific to context conditioning and hippocampal processing (Vazdarjanova *et al.*, 1998).

A potential confound to these data is that the reduced freezing behaviour in the acquisition phase of the test raises the question of whether the drug affects (i) freezing behaviour or (ii) memory formation. As far as these studies report, they have not performed the retrieval test under drugged conditions, so it is not clear whether scopolamine reduces (i) the ability to freeze or (ii) mnemonic freezing behaviour. A corollary question, so far unanswered, is whether freezing itself – and increased type-2 theta – enhances memory acquisition.

Despite these ambiguities, to get a full memory profile, TASK-3 KO mice – having potential functional impairments in the type-2 theta oscillation – were tested in a novel fear conditioning paradigm. The dropbox was developed to avoid some of the facets of the traditional foot-shock that might confound the mechanism under investigation. The dropbox, fully described in Methods & Materials, consisted of a box with a platform over a pool of water. The platform could be rapidly removed

sending the mouse into the water below. After a brief swim, the mouse could be rescued by replacing the platform into its original position.

The dropbox elicited a robust freezing response when the conditioned animals were replaced in the context, suggesting that the test functioned well to condition animals to an aversive stimulus. Atropinization prior to training caused a reduction in freezing behaviour in the off-drug context test 24 hours later, indicating that acquisition in the dropbox conditioning depends upon cholinergic neurotransmission, just like in traditional foot-shock paradigms (see above).

TASK-3 KO mice showed less freezing on average than littermate controls, however, the difference did not reach significance. Exploratory behaviour during the retrieval phase was also not significantly different between the genotypes. While this study shows that TASK-3 KO mice have intact fear memory, any future experiments should investigate the relative effect of atropinization on the acquisition of dropbox fear memory between genotypes.

Overall, the dropbox provides a novel and robust way of measuring fear behaviour in mice and has the potential to be improved from this developmental phase. While fear conditioning using electric shocks can elicit in excess of 70% freezing, the dropbox currently causes a more subtle effect (~20% freezing). Perhaps longer swim times or colder water might increase the aversive nature of the drop. Other issues might be harder to solve though: for example, freezing behaviour during the acquisition was difficult to measure since the animals spent much of the time grooming because they were wet.

The dropbox has numerous advantages over traditional foot-shock methods, both for this study in particular and more generally speaking: the dropbox incorporates several key features of the alert immobile state as the animals process the environment and conditioned cues, retrieve memories, and prepare to execute an escape movement; the dropbox provides an escapable environment so, even though type-2 theta oscillations have been implicated in foot-shock conditioning (Narayanan *et al.*, 2007; Pape *et al.*, 2005; Seidenbecher *et al.*, 2003), possible conditioned ablation of the theta oscillation is prevented (Balleine *et al.*, 1991; Bland *et al.*, 2007b); the dropbox dissociates fear from pain (caused by electric shocks) meaning that the test could have value for testing emotional memory in depression or disease when pain thresholds can be changed (Robinson *et al.*, 2009).

The final test measuring the effect of TASK-3 deletion on behaviour was the orientation response test. When turned in the horizontal plane, animals, including humans, will often turn towards the direction of motion in a homeostatic orientation response (Lackner *et al.*, 2000a; 2000b). Studies have shown that passive rotation – when the animal is immobile in a sling – causes type-2 theta and, further, that ablating type-2 theta with atropine sulfate blocks the orientation response in mice (Shin, 2010).

In the study in this report, atropine sulfate pre-treatment failed to abolish the orientation response in either genotype and there was no difference between TASK-3 KO and littermate performance, with or without the drug. This is consistent with work implicating type-1 theta oscillations as more relevant to the response, since the frequency of the oscillation during rotation tends to be in the higher frequency range (Gavrilov *et al.*, 1995). Indeed, other work shows that atropine sulfate has no effect on the theta oscillation during passive translation (Xie *et al.*, 2012), indicating that it is type-1 theta that processes motion.

Interestingly, mice lacking the phospholipase C (PLC) β4 or β1subunit share a similar neuronal phenotype to TASK-3 KO mice in that they both lack a normal type-2 theta oscillation in response to anaesthetics (Shin *et al.*, 2009; 2005). PLC β4 KOs also have a reduced type-2 theta oscillation in response to passive rotation, which can be restored by cholinergic enhancer rivastigmine (Shin *et al.*, 2009). It is not reported whether either PLC mutant has an intact orientation response, or if they were affected behaviourally by cholinergic modulation. However, the associated activities of PLC and TASK-3 channels in muscarinic neurotransmission (Mathie, 2007) points towards a common molecular mechanism for the generation of type-2 theta oscillations (see figure 4.11).

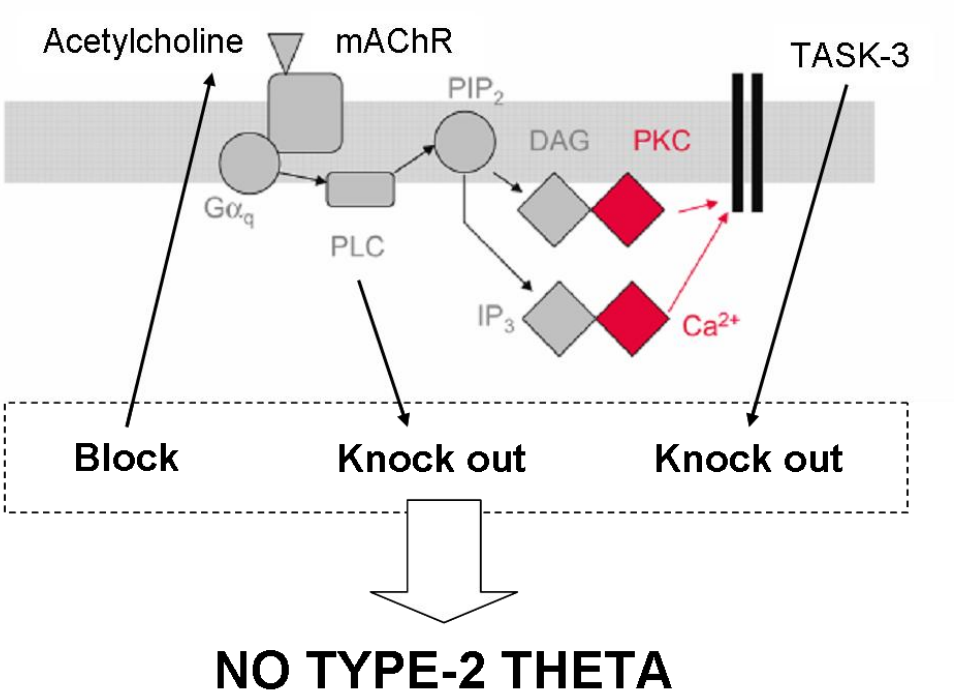

Figure 4.11 A molecular mechanism for the type-2 theta oscillation.

The type-2 theta oscillation depends upon intact muscarinic neurotransmission since blocking mAChRs with atropine sulfate ablates theta. Knock out of other components of the metabotropic signalling pathway – PLC β or TASK-3 – also ablates type-2 theta. [Adapted from Mathie, 2007]

Adeno-associated virus (AAV) experiments

5.1 Background

The first step in understanding the role of a protein in the live animal is often to observe the phenotypic effects in an animal knockout of the coding gene sequence. Indeed, since 2004, there has been an attempt to create null mutants for every gene in the mouse (Knockout Mouse Project). While some developmental genes are fundamental to life and their removal results in a non-viable foetus or severe health problems, many genes can be deleted without major physiological consequences, and therefore their specific function can be dissected with the right barrage of tests.

To this end, the TASK-3 allele was targeted for homologous recombination in mouse embryonic cells. Although the outcome was not exactly according to plan, a null mutant for TASK-3 was created (See Methods & Materials). The TASK-3 KO mouse showed a range of deficits, including a reduced sensitivity to anaesthetics (Pang *et al.*, 2009). An unexpected finding was impairment in the hippocampal type-2 theta oscillation that might explain some of the other cognitive deficits.

The regulation of the type-2 theta oscillation is dependent upon an intact septohippocampal network so, presumably, halothane-induced activation of TASK-3 channels is important in this region. Further investigation into understanding the role of TASK-3 in type-2 theta oscillations could follow several approaches.

Molecular agonism or antagonism provides a useful way to acutely manipulate the action of a receptor or channel both *in vitro* and *in vivo*. If TASK-3 channels could be blocked in specific regions of the brain, such as the medial septum or hippocampus, its role in type-2 theta might be uncovered. However, the range of TASK-3 channel blockers which are freely available, such as zinc, are rather non-specific and a recently discovered series of TASK-3 channel blockers based on a 5,6,7,8-tetrahydropyrido[4,3-*d*]pyrimidine high-throughput screening are not commercially available (Coburn *et al.*, 2012).

Another option would be to delete TASK-3 channels from specific regions of the brain. This conditional knockout technique has the added benefit that any off-target effects are neutralised, while also sparing possible expression changes in other genes that may occur through developmental compensation. Typically, the gene of interest (or a single exon of the gene) is flanked by locus of crossover (lox) sites, creating a floxed allele. When this mouse is mated with another mouse that expresses cyclization recombinase (Cre) under a cell-specific promotor, the floxed allele will be excised and expression of the gene of interest ablated only in those cells (Wisden, 2010). Advances in transgenesis also allow genes to be turned off at a temporal as well as a spatial dimension, using drug-activated gene deletion any time in the adult animal so as to avoid any developmental effects.

This study utilised another method of manipulating gene expression in the adult mouse: Adeno-associated virus (AAV)-mediated gene transfer.

AAVs have a single-stranded DNA genome of about 4.7 kb contained within a non-enveloped capsid, measuring 20 nm in diameter. Highly endemic among human, primate and other animal species, these viruses belong to the genus *Dependovirus*, a name that hints at their reliance on other helper viruses, such as adenoviruses or the herpes simplex virus, for replication of their genome.

The AAV genome consists of two genes, rep and cap, flanked by 145 nucleotide palindromic sequences, called inverted terminal repeats (ITRs), which contain the *cis*-acting sequences vital for virus packaging, replication and integration. The rep gene codes for four non-structural Rep proteins, Rep78, Rep68, Rep72 and Rep40, that regulate replication, viral transcription, packaging of the AAV genomes and site-specific integration. The cap gene codes for three structural virion proteins, VP1, VP2 and VP3, which form the capsid of the virus (Osten *et al.*, 2007).

Upon AAV infection in humans, the AAV genome either stays episomal or integrates into a specific locus on the human chromosome 19, where it remains in a repressed state until super-infection with a helper virus.

Despite their limited genome capacity, their non-pathogenicity – insertional mutagenesis being highly unlikely (Daya *et al.*, 2008) – makes AAVs a promising vehicle for gene therapy, and there have been many efforts in the clinic to cure diseases using recombinant versions (rAAVs) (Bartel *et al.*, 2012). The use of rAAVs

is most common in basic research, particularly in brain sciences where site-specific infection can aid the dissection of neuronal circuitry.

Using a helper plasmid expression system, containing the rep and cap portion of the AAV genome, as well as the accessory adenoviral genes, exogenous DNA sequences of up to 5 kb can be introduced between the ITR sites for subsequent gene transfer.

In trying to find out where the expression of TASK-3 is important for mediating type-2 theta oscillations, AAVs were constructed with the view to reinsert TASK-3 in specific brain regions of the TASK-3 KO. If these regions were important in the TASK-3-mediated oscillations, then theta would be restored. On the other hand, it might be possible to restore the oscillation via a secondary ectopic pathway, where the channels are not usually expressed.

5.2 Making the rAAV plasmids

eGFP-2A-TASK-3 rAAV

One of the AAVs contained the TASK-3 coding sequence and a GFP sequence to act as a marker of expression, with the two linked by a 2A co-translation cassette. The TASK-3 sequence was successfully amplified from pDNA3 containing mouse TASK-3 using primers that contained an ApaI restriction site in the forward direction and an HindIII restriction site in the reverse direction (Figure 5.1A). A possible strategy here could have been to digest the purified PCR product and immediately ligate into the plasmid containing GFP. However, initial attempts in this vein were unsuccessful, possibly because the short overhangs at the restriction sites prevented efficient digestion. Instead, at each amplification step, the DNA proof-reading capability of polymerases like Pfu was sacrificed for a unique feature of TAq polymerase, which adds an adenylated tail at the terminals. The purified PCR product could then be ligated relatively simply into the TOPO vector for convenient storage. Out of nine TOPO reactions, one contained the TASK-3 insert as shown by complete digestion with ApaI and HindIII (Figure 5.1B).

It is a good idea to have some kind of reporter construct to confirm expression of the gene of interest. One way to do this is to directly tag the protein with a fluorescent marker such as GFP; however, the large size of the concatomer may interfere with the endogenous activity of the protein. Smaller peptide tags that act as specific antibody epitopes, such as the His-tag and AU1, can also be used; however, confirmation of expression relies on immunohistochemical techniques.

To circumvent these issues the plan was to link the TASK-3 element to a fluorescent marker via a short co-translation cassette. In this way, two separate proteins would be produced, hypothetically in a 1:1 ratio, without affecting the activity of the TASK-3 channel. A plasmid containing eGFP linked to another gene by a 2A sequence, peGFP-2A-$GABA_A$-γ2, was acquired for this purpose. The 2A sequence is a viral co-translation cassette of about 20 amino acids, with the consensus motif Asp-Val/Ile-Glu-X-Asn-Pro-Gly-Pro, which allows transcription of the full-length sequence, but during translation prevents the formation of a peptide bond between the last glycine and proline. The resulting ribosome skipping creates two separate proteins; in this case, eGFP and TASK-3 (Donnelly *et al.*, 1997; Trichas *et al.*, 2008).

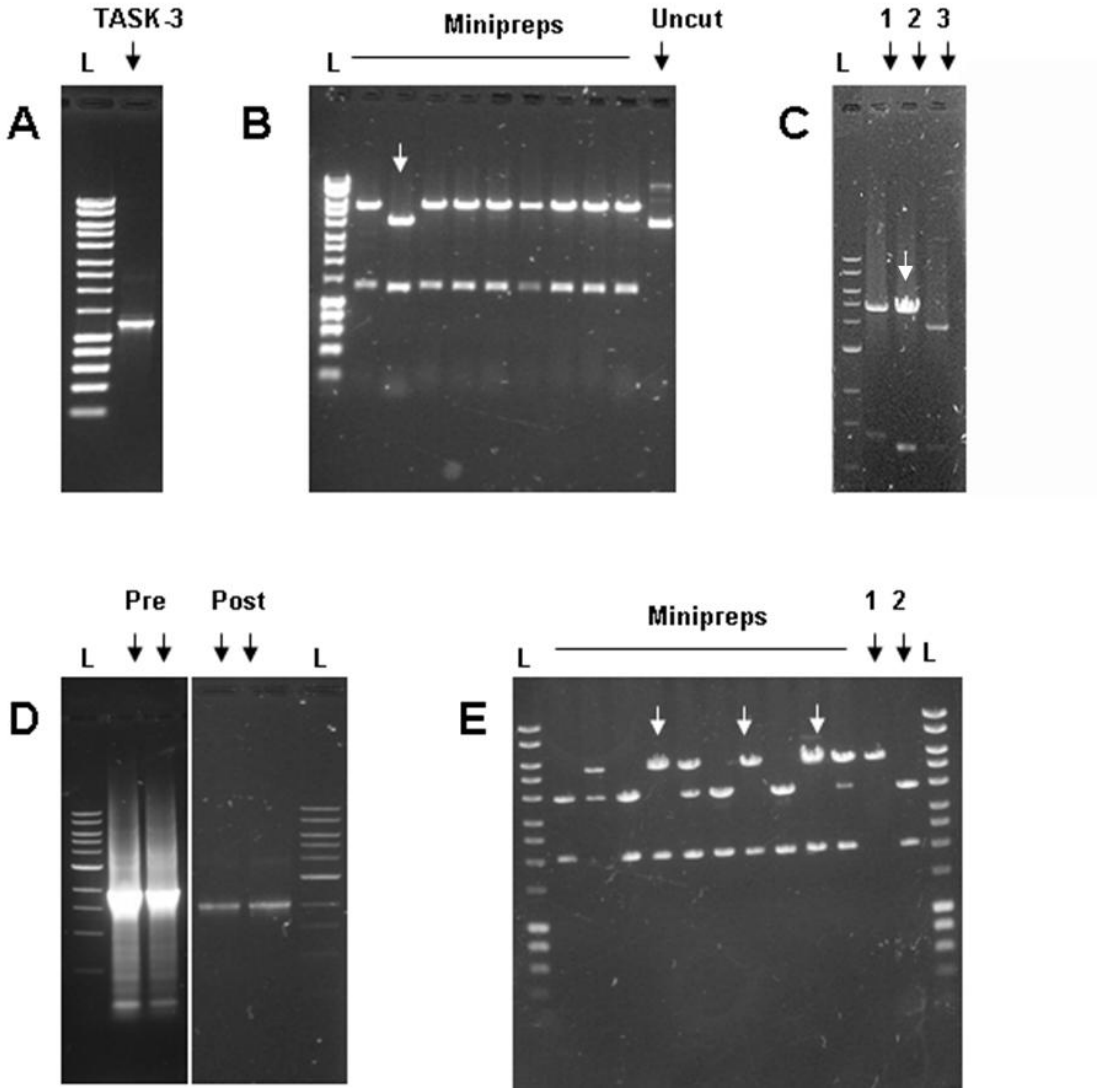

Figure 5.1 eGFP-2A-TASK-3 molecular biology.

A – The mouse TASK-3 gene amplicon at ~1200bp was amplified from pDNA3 with primers containing ApaI and HindIII restriction sites. B – One of twelve minipreps, marked with an arrow, contained the TOPO vector backbone (~4000bp) and the TASK-3 insert (~1200bp). C – ApaI and HindII double digests of peGFP-2A- $GABA_A$-γ2 (sample 1), TASK-3 TOPO (sample 3) and the required ligation product peGFP-2A-TASK-3, marked with an arrow in sample 2. D – A ~2000bp amplicon of two PCR reactions for eGFP-2A-TASK-3 before and after gel purification. E – Three ligation minipreps, with arrows, contain the pAM-flex band (sample 1) and the eGFP-2A-TASK-3 band, in sample 2. [L = DNA ladder.]

To subclone the TASK-3 element into the GFP-2A plasmid, the TOPO vector containing TASK-3 and peGFP-2A-GABA$_A$-γ2 were digested with complementary restriction enzymes and the two digestion mixes were ligated using T4 ligase in a rapid ligation protocol.

Here, certain precautions were taken to ensure successful ligation. Efforts to gel purify the required backbone and insert before ligation, a procedure that also removes restriction enzymes and other contaminants that may affect the reaction, resulted in low DNA yields and were largely unsuccessful. Instead, restriction enzymes were inactivated by heating to 65°C and one of the digestion mixtures was treated with shrimp alkaline phosphatase. This would dephosphorylate the digested DNA terminals, preventing re-circularisation of one of the original plasmids (though the other would remain labile to self-ligation), thus increasing the probability of a correct insertion. Since this strategy appeared to be the most efficient, it was followed throughout.

Figure 5.1C shows the digestion product of peGFP-2A-GABA$_A$-γ2 as sample 1 and the digestion product of TASK-3 TOPO as sample 3. After transfection and DNA purification three peGFP-2A-TASK-3 positive clones out of twelve were identified, an example of which is shown as sample 2 of figure 5.1C. The top band corresponds to the peGFP-2A backbone and the bottom band corresponds to the TASK-3 insert, a result confirmed by DNA sequencing.

The next step was to subclone the eGFP-2A-TASK-3 sequence into a suitable AAV vector. This was achieved by firstly amplifying the entire eGFP-2A-TASK-3 sequence by PCR while simultaneously adding restriction sites for future ligation. The full sequence was amplified successfully and purified as shown in figure 5.1D. Again the product was ligated into TOPO before digestion and ligation into the pAM-flex AAV plasmid.

The pAM flex contains elongation factor (EF)-2 alpha as a constitutive promoter and woodchuck hepatitis virus post-transcriptional regulatory element (WPRE) which improves intron-free transcription. In figure 5.1E, sample 1 shows the empty pAM-flex digested with NotI and HindIII while sample 2 shows a similarly digested eGFP-2A-TASK-3 TOPO. Three out of ten of the transfected ligation mixtures were positive for the pAM-flex backbone and the eGFP-2A-TASK-3 insert. After the sequences were confirmed, these plasmids could be taken forward to producing the rAAV particles. The entire strategy is laid out in figure 5.2.

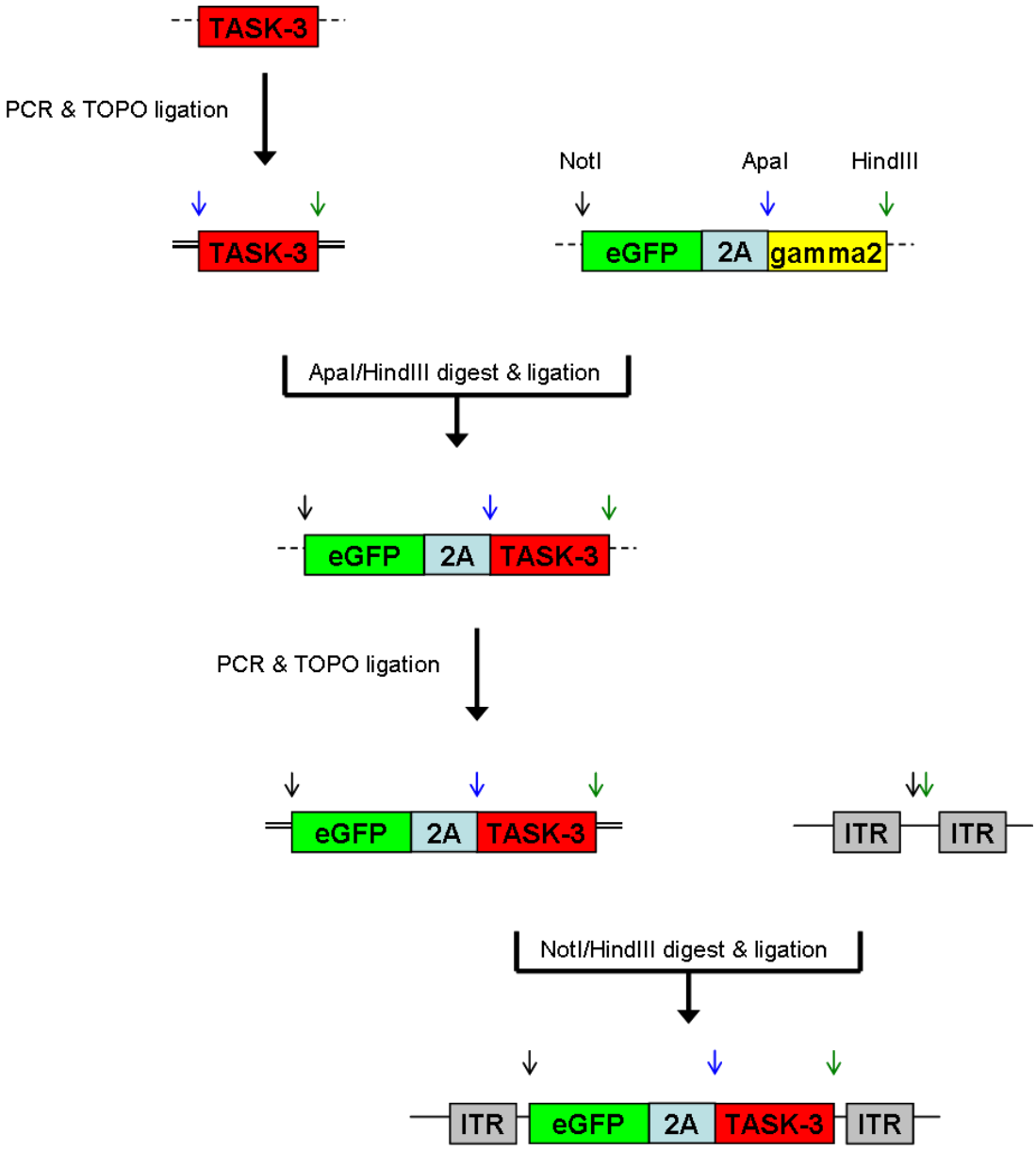

Figure 5.2 Making the eGFP-2A-TASK-3 rAAV plasmid.

TASK-3 was amplified and ligated into TOPO vector before subsequent digestion and ligation with similarly digested peGFP-2A- $GABA_A$-γ2. This construct was then amplified to include compatible restriction sites for ligation between the ITR sites of the pAM-flex AAV vector.

Cre-2A-Flp rAAV

During the construction of the TASK-3 KO it was realised that the TASK-3 allele was multiply reintegrated, but was ultimately and fortuitously not expressed. The manner of the genetic manipulations meant that crossing the TASK-3 KOs with a Cre-deletor mouse and then a flp mouse can turn on the TASK-3 gene and restore normal expression. Taking advantage of this, it might be possible to selectively restore TASK-3 expression in specific brain regions, such as the hippocampus or medial septum, by injecting rAAVs containing the Cre and Flp genes directly into these regions.

This type of gene manipulation has several benefits over the first non-selective method. If an rAAV cassette containing Cre and Flp was viable, the TASK-3 gene would be switched on only in those cells where it would normally be expressed. With the eGFP-TASK-3 rAAV, TASK-3 channels would be expressed in any cell that the virus infects, whether or not the cell-type would normally do so. This ectopic expression could have unknown effects on the physiology of the cell and in the cellular network. And since the eGFP-TASK-3 rAAV contains a constitutive promotor, expression levels could be far greater than normal. On the other hand, through Cre-Flp-mediated switching of the TASK-3 gene into the correct orientation, endogenous promotors would act to transcribe the gene as they would if it had never been modified; hypothetically to the correct mRNA expression levels.

To this end, a Cre-2A-Flp rAAV plasmid containing the CMV enhancer and the chicken beta actin (CBA) promoter was made. Since a Cre-2A-Venus rAAV plasmid was available, the plan was to replace the Venus element with the Flp gene. However, the construct was not designed to easily excise and replace the Venus gene, which would normally be used as the expression marker, since one of the restriction sites flanking the Venus gene was not unique. So, in a more complex subcloning procedure, the Cre-2A segment was temporarily removed through digestion with BamH1 and the resulting plasmid re-ligated and subcloned in *E. coli*. Sample 1 in figure 5.3A shows a BamH1 and NotI digested plasmid containing the Venus gene but not the Cre-2A segment shown in sample 2. The Cre-2A segment was gel purified for later use.

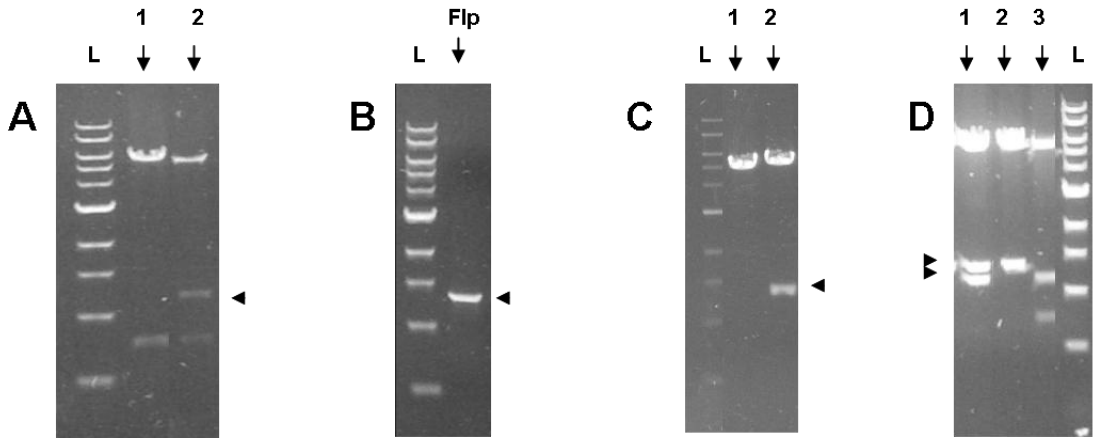

Figure 5.3 Molecular biology of the Cre-2A-Flp rAAV plasmid.

A – The Cre-2A portion of the original plasmid, shown by the arrowhead in sample 2, has been removed from sample 1, where only the Venus gene is present. B – The Flp gene is shown successfully amplified, marked with the arrowhead. C – The Flp fragment has replaced the Venus gene in the CMV plasmid, marked with the arrowhead in sample 2. D – The Cre-2A fragment (as in sample 3) has successfully ligated to the CMV Flp plasmid (as in sample 2) to form the double band of the digested pCre-2A-Flp in sample 1. [L = DNA ladder.]

The Flp gene was amplified from pPGUFLPobpA with primers containing BamH1 and NotI restriction sites and digested with those enzymes, as shown in figure 5.3B. The Flp fragment was then ligated with a similarly digested and phosphatase-treated Venus plasmid, with the intention of replacing the Venus gene with the Flp gene. Figure 5.3C shows an "empty" plasmid in sample 1 and the plasmid with Flp in sample 2.

At this point, the purified Cre-2A fragment could be re-introduced by ligating it with BamH1-cut Flp plasmid. Figure 5.3D shows both the Cre-2A digestion fragment (sample 3) and the Flp fragment (sample 2) together in sample 1, indicating ligation of the Cre-2A into the Flp plasmid. However, since the restriction sites flanking the Cre-2A were the same (BamHI), the ligation reaction could occur in either the correct (forward) orientation or the incorrect (reverse) orientation. Out of six samples sent for sequencing, three were positive for the correct orientation and one of these had no mutations; and hence, was used to make the virus. The strategy is laid out in figure 5.4.

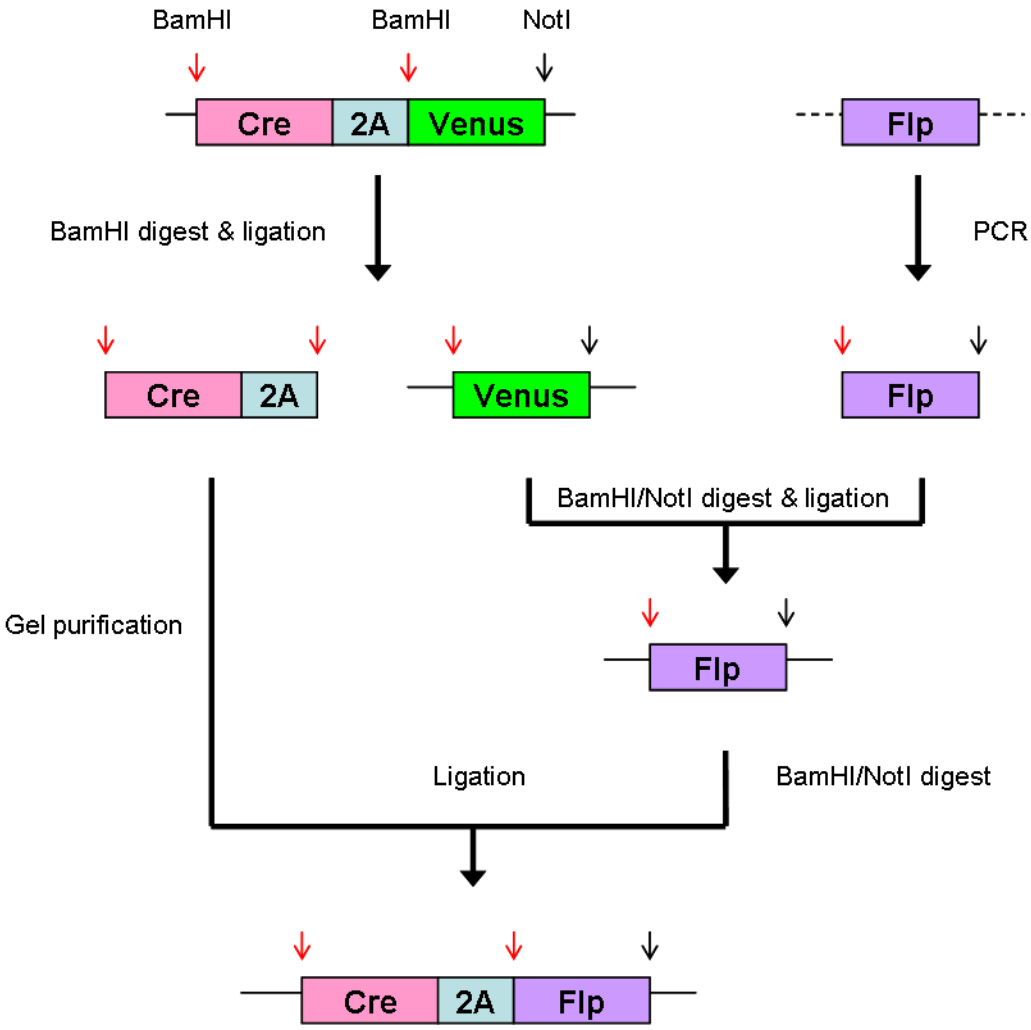

Figure 5.4 Strategy for the Cre-2A-Flp rAAV plasmid construction.

The Cre-2A segment was excised and the Venus gene was swapped for the PCR-amplified Flp gene. The Cre-2A segment was then ligated to the Flp plasmid to form the required pCre-2A-Flp vector.

5.3 Validating the rAAV plasmids

eGFP-2A-TASK-3 rAAV

The design of the eGFP-2A-TASK-3 rAAV plasmid incorporated an eGFP element to aid visual detection of gene expression. HEK-293 cells were transfected with the eGFP-2A-TASK-3 rAAV plasmid using the calcium chloride method and the cells were assessed for fluorescence after three days, revealing strong expression of eGFP, as shown in figure 5.5A. The endogenous fluorescent marker had the added advantage that cells could be checked for fluorescence each day to observe the time course of expression.

Assuming that the 2A co-translation element acts as required the presence of fluorescence in the transfected cells should also confirm expression of the TASK-3 gene. However, it is possible that only one of the transgenes would be expressed, in this case just the eGFP as this is the first gene to be transcribed. One way to circumvent this issue would have been to design the plasmid with the TASK-3 element first, followed by the 2A sequence and then the eGFP. Fluorescence in those conditions would certainly indicate the faithful transcription of TASK-3. In any case, further characterisation of TASK-3 expression was required.

To this end, HEK-293 cells were transfected with either the eGFP-2A-TASK-3 rAAV plasmid or a control plasmid expressing GFP alone. The following day, whole-cell voltage clamp recording revealed a considerably higher outward current in the eGFP-2A-TASK-3 rAAV plasmid-transfected cells compared to control cells (Figure 5.5B; Electrophysiology performed by T. McGee). This result suggested that TASK-3 channels were expressed in transfected cells and correctly targeted to the plasma membrane, where they make a major contribution to cell permeability.

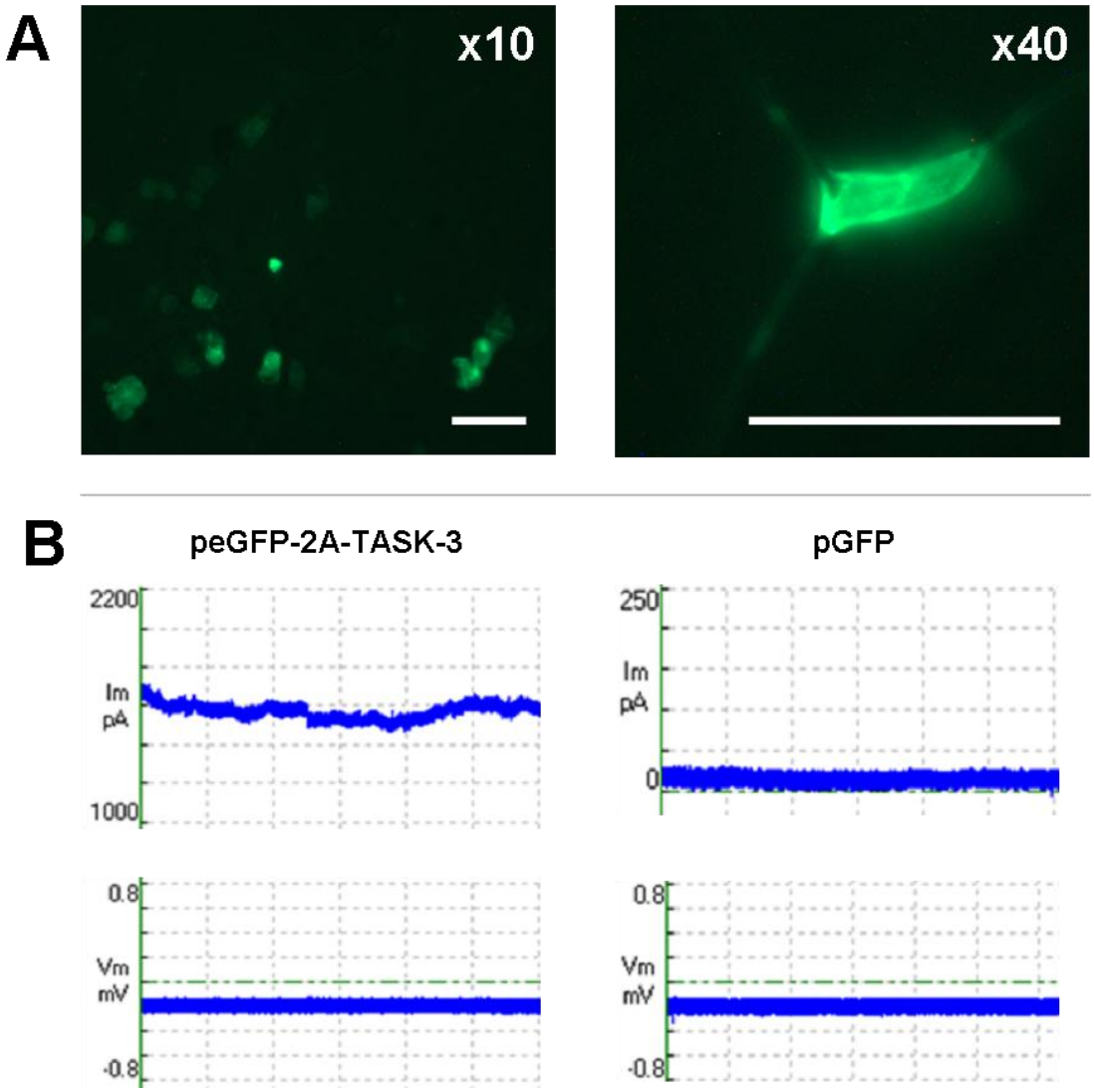

Figure 5.5 eGFP-2A-TASK-3 plasmid expression.

A – Primary fluorescence from the eGFP reporter indicates robust expression of the eGFP-2A-TASK-2 plasmid in HEK-293 cells. [Scale bars = 0.1 mm] B – eGFP-2A-TASK-3 expression causes a depolarisation in the holding current compared with GFP expression in HEK-293 cells. [Electrophysiology performed by T. McGee]

Cre-2A-Flp rAAV plasmid

That the Cre-2A-Flp rAAV plasmid did not contain an endogenous marker of expression presented more of a problem for validation. Immunological staining provided one option, but since the two elements have transgenic functions, the activity of Cre and Flp were tested separately at a functional level.

To assess Cre function, the Cre-2A-Flp rAAV plasmid was co-transfected in HEK-293 cells with a plasmid that contained a dsRed element in the reverse direction between loxP sites. dsRed is a red fluorescent protein, that is not expressed in this native plasmid due to its reversed orientation. On being exposed to Cre, the floxed gene will be switched into the correct orientation and the gene will be expressed. The results of the co-transfection can be seen in figure 5.6A. There is no red fluorescence when the floxed and reversed dsRed plasmid is transfected alone, whereas when the Cre-2A-Flp rAAV plasmid is added, red fluorescence is strong in the majority of cells, indicating effective Cre activity.

Flp function was assessed through a second double transfection. The Cre-2A-Flp rAAV plasmid was transfected with a plasmid that contained GFP between frt sites (LCMV:GFP(FRT)MCS: 5333 bp). This time, the native test plasmid would express GFP and fluoresce green in HEK-293 cells. Then, on the addition of the Cre-2A-Flp rAAV plasmid, the Flp should inactivate the GFP gene by acting on the surrounding frt sites to reverse its orientation. Figure 5.6B shows that the Flp element of the Cre-2A-Flp rAAV plasmid worked exactly as planned. The possibility that the Cre-2A-Flp rAAV plasmid disrupted GFP expression merely through competition or a non-specific mechanism was ruled out through a control transfection of the GFP test plasmid and another plasmid, where fluorescence was unaffected (data not shown).

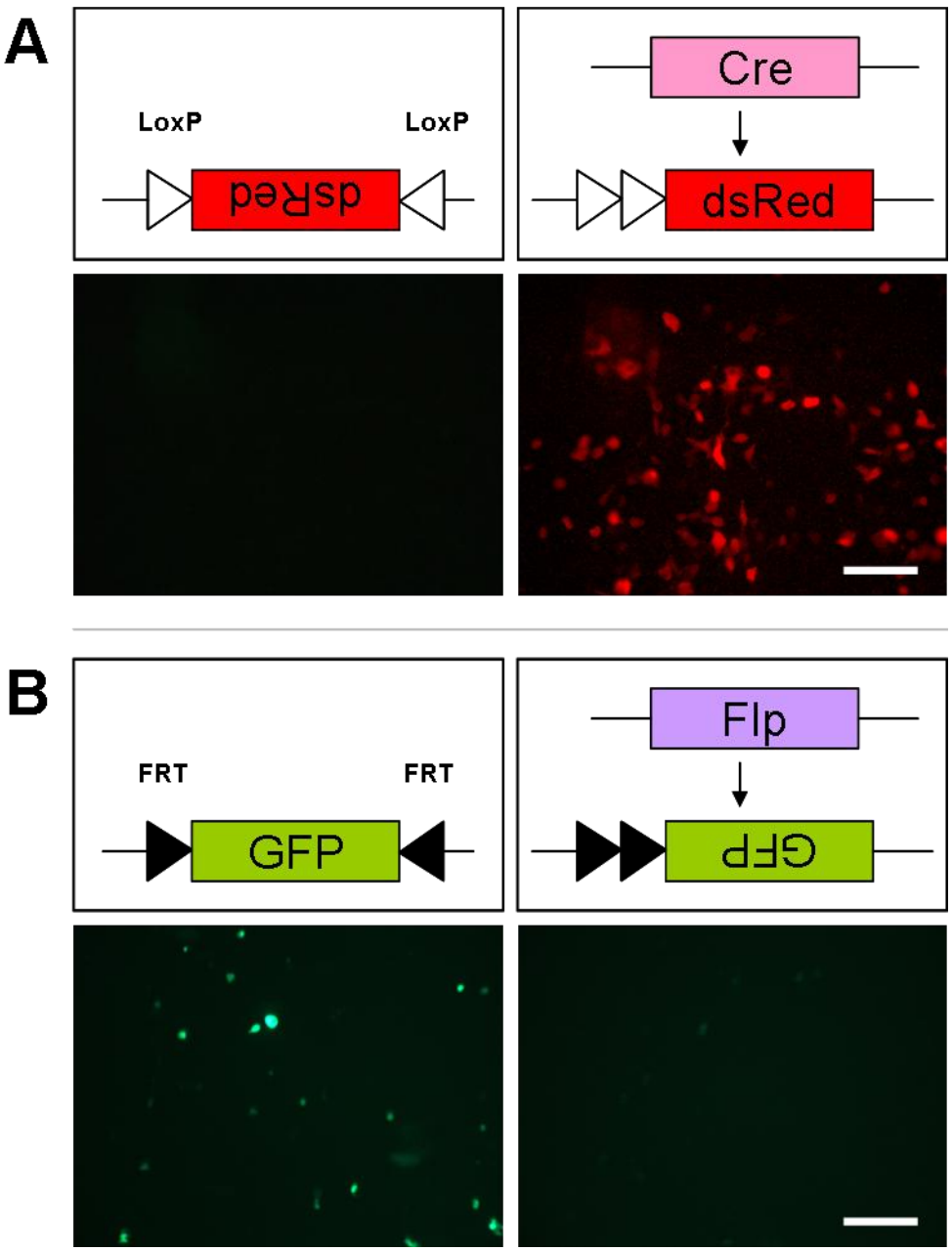

Figure 5.6 Testing the function of the Cre-2A-Flp plasmid.

A – The Cre-recombinase component of the Cre-2A-Flp plasmid switches on dsRed expression in another co-transfected plasmid. B – The Flp element of the Cre-2A-Flp plasmid turns off expression of FRT-flanked GFP from another co-transfected plasmid. [Scale bars = 0.1 mm]

5.4 Making the viral particles

A helper plasmid expression system, containing the rep and cap portion of the AAV genome, as well as the accessory adenoviral genes, was used to produce a chimeric virion particle that would encapsulate the genetic elements of the eGFP-2A-TASK-3 or Cre-2A-Flp plasmid between the ITRs.

For each rAAV the capsid consisted of a chimera of AAV1 serotype and AAV2 serotype. AAV2 based vectors have the advantage of being readily purified by a heparin column (McClure *et al.*, 2011); a much simpler procedure compared to purification via caesium chloride gradient. AAV1 vectors, on the other hand, have the advantage of robust infectivity of neuronal tissue (Royo *et al.*, 2008). In order to generate this chimeric vector, two different helper plasmids were acquired: pRV1 carries the *cap* and *rep* genes for AAV2; and pH21 carries the *cap* and *rep* genes for AAV1. Since HEK-293 cells already contain the adenoviral genes for E1A and E1B, a mini-adenovirus helper plasmid, pFΔ6, was sufficient to add the other adenoviral functions (E2A, E4ORF6 and VA RNAs).

These plasmids were amplified using an *E. coli* expression system and then purified. Integrity of the plasmids was confirmed by restriction digestion, which produced the expected band pattern (Figure 5.7A). Virus production proceeded as in Methods & Materials and, after denaturing with heat and SDS, the viral coat proteins for each rAAV were run on an SDS-PAGE gel.

Each AAV serotype has three structural proteins, with estimated molecular weights of 87,000 Da, 73,000 Da and 62,000 Da and a stoichiometry of 50:5:5, respectively (Rose *et al.*, 1971). However, the denatured samples shown in figure 5.7B do not recapitulate the expected results. Sample 1, eGFP-2A-TASK-3 rAAV, shows strongly staining bands at >100,000 Da and <60,000 Da, vastly different to those expected, while sample 2, Cre-2A-Flp rAAV, show only light staining of one unexpected band.

For further characterisation, the protein and DNA composition of the viral particles was estimated by the relative UV absorbance (at 260nm and 280 nm) of purified and denatured rAAV samples as in Sommer *et al.* (2003). The purified eGFP-2A-TASK-3 rAAV sample contained 4.0×10^{11} viral genomes per ml and the Cre-2A-Flp rAAV contained 1.8×10^{12} viral genomes per ml. The analysis also revealed capsid:genome ratios of 5.7:1 for eGFP-2A-TASK-3 rAAV and 2.4:1 for Cre-2A-Flp rAAV, reflective of the relative abundance of empty capsids in the purified viruses. Despite this, the rAAVs were taken on for further validation.

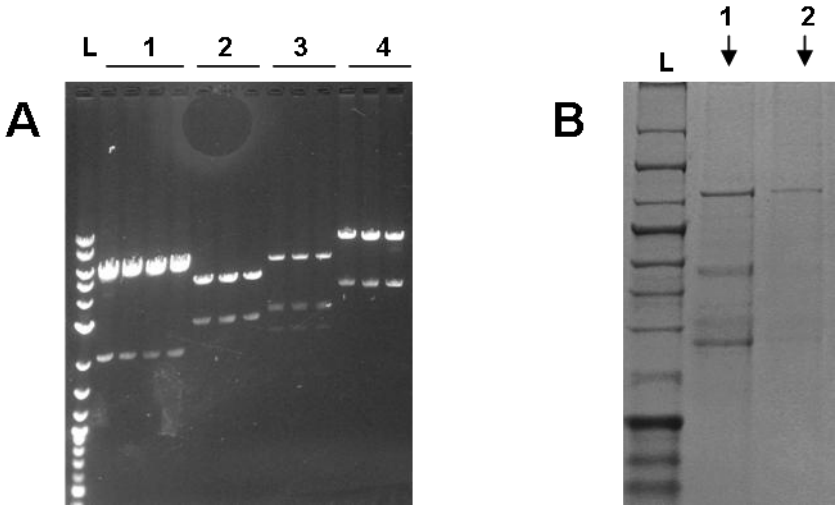

Figure 5.7 Making the rAAVs.

A – The integrity of the helper plasmids needed for rAAV production is confirmed through restriction digestion. Sample 1 is NotI & HindIII-digested eGFP-2A-TASK-3 plasmid, sample 2 is EcoRI-digested pH21, sample 3 is HindIII-digested pFΔ6, and sample 4 is XbaI-digested pRV1. [L = DNA ladder] B – SDS-PAGE analysis of the purified viruses – eGFP-2A-TASK-3 rAAV in sample 1 and Cre-2A-Flp rAAV in sample 2 – gives ambiguous results. [L = Protein ladder]

5.5 Validating the viral particles

HEK-293 cell infection

Activity of the viral particles was checked by infection in HEK-293 cells. Here, the infectivity of eGFP-2A-TASK-3 rAAV could be analysed by fluorescence of the endogenous eGFP marker, whereas the Cre-2A-Flp rAAV required a secondary marker.

Serial dilutions of the viruses were added to HEK-293 cells and, in the case of the eGFP-2A-TASK-3 rAAV, were checked every few days for fluorescence, with maximum expression at five days post-infection. At this point, cells were fixed and analysed. Based on maximum expression of this virus, the Cre-2A-Flp rAAV-infected cells were also fixed and analysed at one time-point, five days after the original infection.

Cells infected with eGFP-2A-TASK-3 rAAV showed modest fluorescence in the cell body that varied in a dose-dependent manner, with the more dilute samples showing comparably less fluorescence than the maximum (data not shown; but see figure 5.9).

The activity of Cre-2A-Flp rAAV was measured by anti-Cre immunocytochemistry with a fluorescent secondary antibody. Robust nuclear staining was observed, with fluorescence, and therefore the number of infected cells, scaling in a dose-dependent manner (Figure 5.8).

The number of infected cells was calculated using ImageJ software (NIH) and viral titers were determined by multiplying the number of fluorescent cells (the average of two wells) by the dilution factor of the rAAV. The eGFP-2A-TASK-3 rAAV titer was 2.0×10^5 infectious particles per ml and the Cre-2A-Flp rAAV titer was 1.1×10^7 infectious particles per ml, reflecting the differences in the earlier protein/DNA analysis.

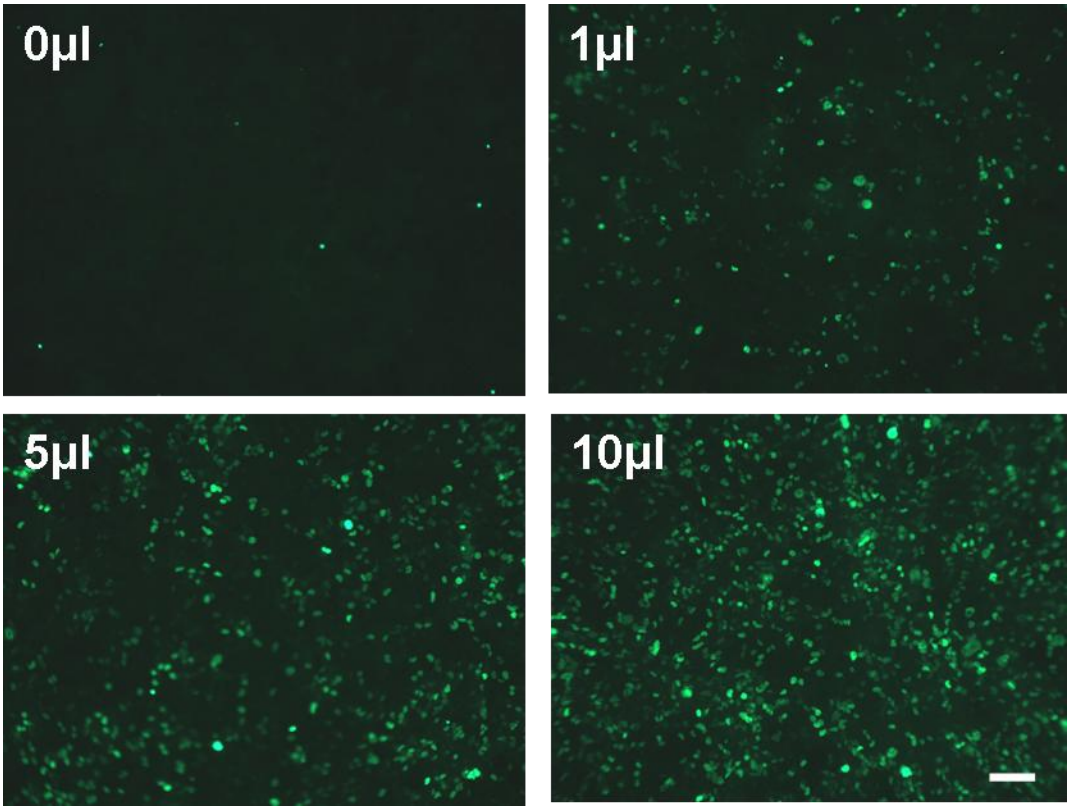

Figure 5.8 Cre-2A-Flp rAAV expression.

Cre-2A-Flp rAAV expression in HEK-293 cells is verified by anti-Cre immunocytochemistry. Nuclear staining increases as the amount of virus infected increases. [Scale bar = 0.1 mm]

Organotypic slice infection

HEK-293 cell cultures are relatively short lived as the cells quickly become confluent and multiple fresh media changes decrease the health of the cells. This means that expression assays are limited to only a few days and positive results do not necessarily predict the long-term and stable expression of the rAAV transgenes. This process, which may take in excess of two weeks (Ehrengruber *et al.*, 2001), must ultimately be tested by *in vivo* infection. Prior to taking the virus into the live animal though, the infectivity of the eGFP-2A-TASK-3 rAAV was assessed in organotypic hippocampal slices from 15 day-old mouse pups (p15). These cultures can be maintained healthily for up to two weeks, where pseudo-normal cellular morphology is retained and differentiation processes occur as in the live animal (Stoppini *et al.*, 1991).

Figure 5.9 shows examples of control non-infected hippocampal slices and slices infected with eGFP-2A-TASK-3 rAAV or Cre-Venus rAAV (a high titer control virus). The Cre-Venus rAAV-infected slice shows robust expression of Venus (a yellow fluorescent protein) increasing in intensity up to 12 days post-infection, consistent with other work (Ehrengruber *et al.*, 2001). Slices infected with eGFP-2A-TASK-3 rAAV show a lesser degree of fluorescence, possibly due to the lower titer of this virus.

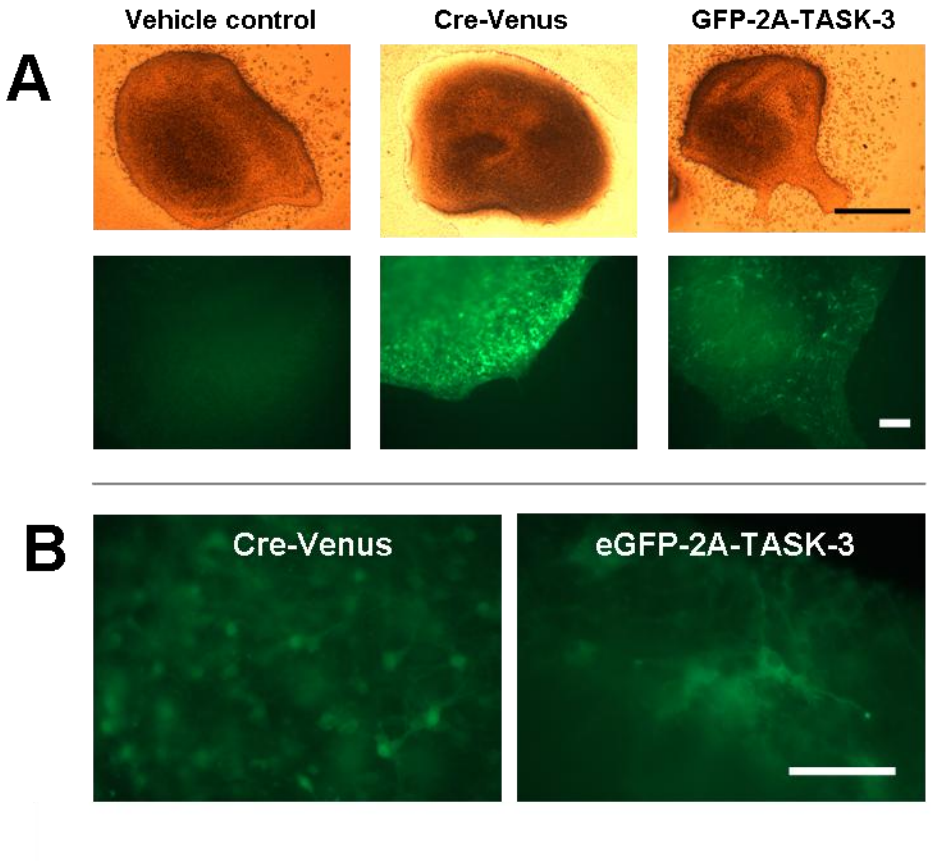

Figure 5.9 Organotypic hippocampal slices validate rAAV expression.

A – The top panel shows bright-field images of the hippocampal slice and the bottom panel shows the green channel images. No fluorescence is observed in the control, while Cre-Venus rAAV infection causes strong fluorescent signal and eGFP-2A-TASK-3 rAAV causes a moderate fluorescent signal. [Scale bars = 1 mm] B – Cre-Venus expresses in the nucleus, whereas the tips of the cellular processes express strong fluorescence in the eGFP-2A-TASK-3 rAAV-infected slice. [Scale bar = 0.1 mm]

In vivo *infection*

As a first step, only the eGFP-2A-TASK-3 rAAV was taken on to *in vivo* studies. After confirming that it could be expressed in HEK-293 cells and organotypic slices, its infectivity was tested *in vivo*. The rAAV samples were prepared as in the methods, injected into the mouse brain and, three weeks later, expression was assessed through primary fluorescence of eGFP or secondary fluorescence of anti-GFP antibodies after immunohistochemistry.

Figure 5.10 shows a successful injection into the medial septum. The injection tract can be seen in figure 5.10A under the red filter, representative of a small amount of scar tissue. GFP expression is high in the medial septum (Figure 5.10B), with fluorescence in the soma and projections of neurons, as in figure 5.10C.

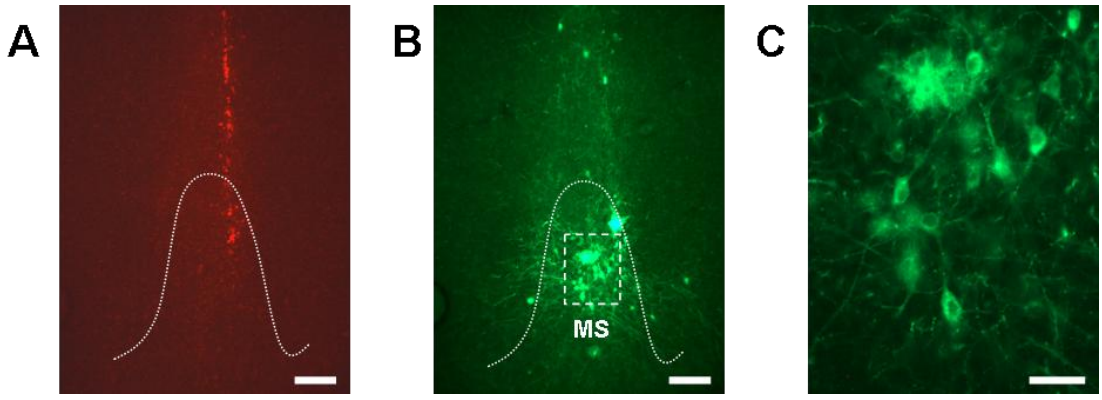

Figure 5.10 Fluorescent microscopy of the eGFP-2A-TASK-3 rAAV in the medial septum.

A – The injection tract is observable under the red filter as a line of scar tissue. [Scale bar = 1 mm] B – Cells in the medial septum – marked with the dotted line – appear to express eGFP. [Scale bar = 1 mm] C – A magnification of the square in the previous micrograph showing eGFP expression in the cell bodies and projections. [Scale bar = 0.1 mm]

eGFP-2A-TASK-3 rAAV injections into the hippocampus were unsuccessful, even after several attempts. Methodological problems concerning the correct placement of the injections could be ruled out because Cre-Venus rAAV showed excellent expression in this area, as in figure 5.11. Referring back to the hippocampal organotypic slices, where expression of the eGFP-2A-TASK-3 rAAV is markedly lower than that for the Cre-Venus rAAV, it could be that the viral titer was simply not high enough to infect these cells. Infectivity *per se* should not be compromised in the eGFP-2A-TASK-3 rAAV compared to the Cre-Venus rAAV, since both of these viruses use the same coat proteins.

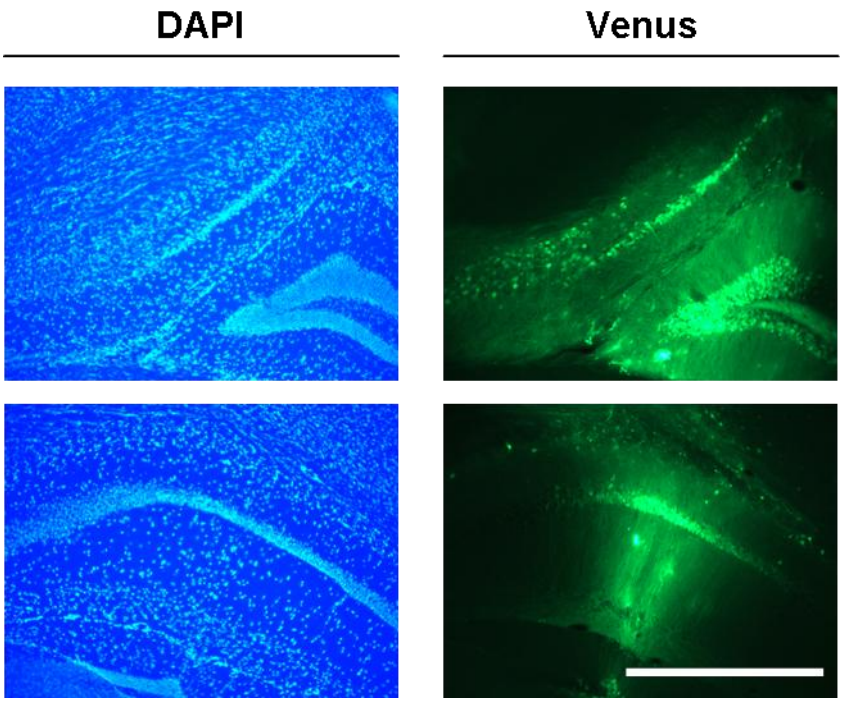

Figure 5.11 The Cre-Venus rAAV expresses strongly in the hippocampus.
The left-panel shows nuclear staining by DAPI, highlighting the different cellular layers of the hippocampus. On the right, Venus fluoresces strongly in the dentate gyrus (top) and CA3 (bottom). [Scale bar = 1 mm]

5.6 Functional effect of TASK-3 channel AAV transfer

Simultaneously with viral injections, littermate and TASK-3 KO mice were instrumented with ECoG/EMG recording electrodes. The animals were exposed to increasing concentrations of halothane and their brain activity was monitored using the Neurologger.

Lorentzian curves fitted to the FFT power spectra at each halothane concentration revealed an increasing Q-factor with increasing anaesthetic in sham-littermate mice (n = 4), as in figure 5.12A. By contrast, sham-TASK-3 KOs (n = 6) showed a flat response; that is, the Q-factor did not change in response to increasing concentrations of halothane (Figure 5.12A). This vastly reduced type-2 theta oscillation compared to littermate, as analysed by 2-way ANOVA and Bonferroni's test ($p < 0.001$ at 1.5% and 2.0%), is reflective of the deficit described previously (Pang *et al.*, 2009).

With successful medial septum eGFP-2A-TASK-3 rAAV infection (n = 2), the Q-factor showed a significant increase from 7 days after infection to 21 days after infection, as in figure 5.12B, presumably as the rAAV reached full expression ($p < 0.05$ at 1.5% and 2.0%). Medial septum TASK-3 channels are thus able to functionally restore, at least in part, the type-2 theta oscillation.

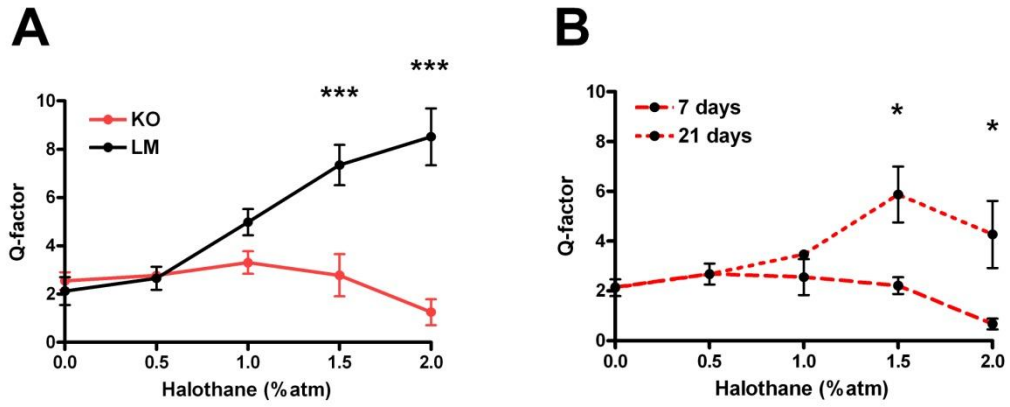

Figure 5.12 eGFP-2A-TASK-3 rAAV infection partially restores the type-2 theta oscillation.

*A – TASK-3 KO mice lack the Q-factor modulation induced by halothane in littermates. B – 21-days after rAAV infection, the Q-factor is significantly increased compared to baseline at 7-days. (*p < 0.05; ***p < 0.001)*

5.7 Discussion

AAV-mediated genetic and functional rescue has proven to be a powerful technique for dissecting the structures and mechanisms important in a variety of physical processes and behaviours (Gerstein *et al.*, 2012; Guillem *et al.*, 2011). A particularly interesting use of this approach was able to restore normal attentional performance in nicotinic acetylcholine receptor (nAChR) β2-subunit KO mice by re-expression in the prelimbic area of the prefrontal cortex (Guillem *et al.*, 2011). That study used a lentiviral expression system to restore acetylcholine sensitivity to this specific region only, proving that cholinergic tone in this area was sufficient to mediate normal performance in an attentional task.

TASK-3 KOs also have altered neuronal function, which manifests at the physiological level in an absence of type-2 theta oscillations (Pang *et al.*, 2009) and at the behavioural level in impaired sleep and memory processes (Linden *et al.*, 2007; Pang *et al.*, 2009). TASK-3 channels are widely expressed through the brain, including the CA1 and dentate granule cell region of hippocampus (Brickley *et al.*, 2007), which is critically involved in mediating theta oscillations. Therefore, it was possible that impaired hippocampal function could explain the type-2 deficit in TASK-3 KO mice.

Work in this laboratory has indeed shown subtle changes in the electrophysiological characteristics of TASK-3 KO hippocampal pyramidal cells (Pang, 2010). While resting membrane potential was unchanged in TASK-3 KOs compared to controls, the action potential characteristics were modulated by halothane in controls but not in TASK-3 KOs. Specifically, control cells had a greater ability to sustain action potential firing than TASK-3 KOs during halothane exposure, consistent with work in cerebellar granule cells (Brickley *et al.*, 2007). However, in addition to an impaired response to halothane in those cells (Brickley *et al.*, 2007) and in motoneurons (Lazarenko *et al.*, 2010), the resting membrane potential was found to be depolarized in TASK-3 KOs. Therefore, altered pyramidal cell characteristics in the TASK-3 KO probably play a limited role in the network impairment that causes reduced type-2 theta oscillations.

TASK-3 channels are also highly expressed in parvalbumin-positive (parv) GABAergic interneurons in the CA1 region of the hippocampus (Talley *et al.*, 2001; Torborg *et al.*, 2006). These cells, which include axo-axonic, basket, bistratified, and oriens-lacunosum moleculare interneurons, have all been implicated in theta

oscillations (Klausberger *et al.*, 2008). So, perhaps the lack of TASK-3 channels in these cells is responsible for the network impairments of TASK-3 KO mice.

Ongoing work in our lab aims to use Cre-based "flex switching" to generate transgenic mice that have (i) TASK-3 channels deleted from only parv-interneurons, or (ii) TASK-3 channels selectively restored in parv-interneurons. Similar approaches have been used to ablate GABA receptor γ2-subunits from parv-interneurons which interfered with theta-gamma rhythm coupling (Wulff *et al.*, 2009). And, other viral-based strategies ablated parv-interneuron output in the CA1 region of the hippocampus, causing working memory deficits (Murray *et al.*, 2011).

The hippocampus was therefore the primary target for TASK-3 rescue in this study. However, expression of the eGFP marker in this region could not be detected, even with secondary anti-GFP immunohistochemical labelling. These results are at odds with the expression observed in organotypic hippocampal slices, and work is ongoing to find a satisfactory explanation. It is possible that the rAAV injections were themselves unsuccessful; however, hippocampal cells were successfully infected with another virus using exactly the same technique.

The secondary target was the medial septum, a region that provides a theta "pacemaker" through burst firing of GABAergic and cholinergic neurons into the hippocampus (Smythe *et al.*, 1991). While TASK-3 expression is not particularly strong here, the fact that atropinization of this region affects the type-2 theta oscillation in the same way as TASK-3 deletion, was reason enough to suspect that TASK-3-dependent muscarinic neurotransmission might nevertheless be important.

After *in vivo* expression of eGFP-2A-TASK-3 in the medial septum was confirmed in a cohort of mice, a second group, consisting of littermate mice with sham injections, TASK-3 KO mice with sham injections, and TASK-3 KO mice with medial septum eGFP-2A-TASK-3 rAAV injections, were instrumented for ECoG/EMG recording. Their response to halothane was measured one and three weeks after surgery; the latter when transgene expression is maximal. The TASK-3 KO shams showed no ECoG modulation of the theta oscillation in response to halothane, while the littermate shams had a strongly tuned peak as evidenced by an increased Q-factor. TASK-3 KO mice with medial septum eGFP-2A-TASK-3 rAAV injections showed a significant increase in the Q-factor between 7 days and 21 days post-infection, indicating enhancement and partial rescue of the type-2 theta oscillation (Figure 5.12).

As the eGFP-2A-TASK-3 rAAV uses a pan-promoter, the transgenes could be expressed in any type of neuronal cell. This is a potential drawback for several reasons: firstly, at a glance, the identity of the cell-type is unknown; and secondly, the rAAV may infect cells unrelated to the study in question. However, while limited to a post-hoc evaluation, the first problem can be solved by co-labelling brain sections with neuronal markers such as cholineacetyltransferase, parvalbumin, calmodulin, etc. The second problem, on the other hand, may actually have its own advantages.

Rescuing a (cellular or physiological) phenotype by introducing a gene back into one particular area rather than another where it would usually be expressed certainly provides quite specific mechanistic information, as in the β2-subunit study (Guillem *et al.*, 2011). However, at a conceptual level, there is an argument that, of course, returning a gene into a hypothetically relevant brain circuit will restore normal function. But, if the function could be restored through a secondary route, to compensate indirectly for the deficit, then a novel mechanism might be unveiled, potentially identifying new therapeutic targets. Just recently, for example, a deficit in sodium channel function that caused various cognitive abnormalities could be reversed by treatment with a positive allosteric modulator of $GABA_A$ receptors (Han *et al.*, 2012).

The medial septum modestly expresses TASK-3 transcripts and strongly expresses TASK-1, as in figure 5.13, potentially forming homodimeric channels (Bayliss *et al.*, 2003). However, it would appear that in the case of TASK-3 deletion, TASK-1 homodimers are unable to compensate for even the relatively low expression levels of TASK-3 required to maintain septohippocampal function and type-2 theta oscillations.

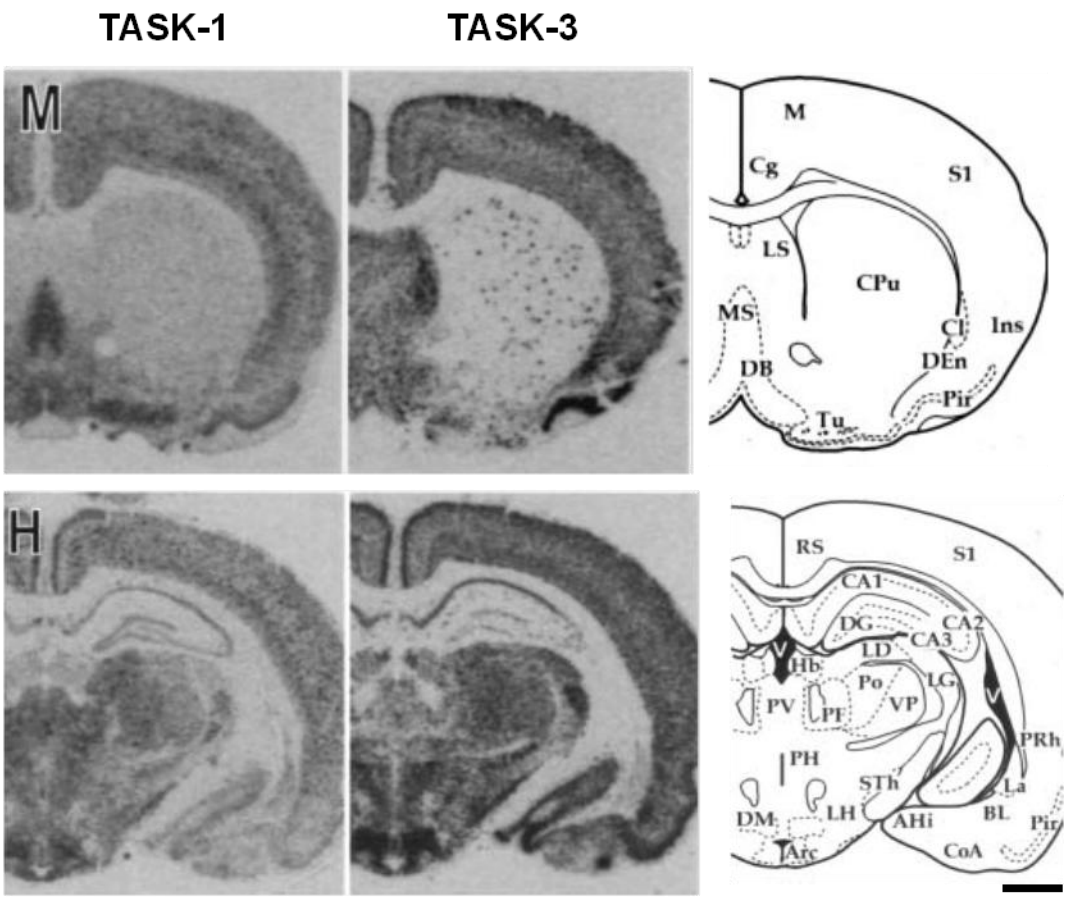

Figure 5.13 Heterogeneous distribution of TASK channels in the mouse brain. *TASK-1 channels are expressed strongly in the medial septum (MS), whereas TASK-3 channels are expressed in the lateral septum (LS) and cholinergic neurons in the caudate putamen (CPu). [Adapted from Talley et al. (2001); Scale bar = 1 mm]*

Further to this, a small-scale comparison between TASK-1 KO and wildtype mice revealed subtle differences in ECoG characteristics in response to halothane. The shape of the maximum halothane-induced type-2 theta peak is similar between the two genotypes ($p = 0.92$); however, the Q-factor is maximal in TASK-1 KO mice at a halothane concentration of 1.09 ± 0.04 %, which is significantly higher than that for wildtype mice of 0.80 ± 0.04 % halothane, as in figure 5.14A ($p < 0.05$, $n = 3$). And, in addition, the frequency of this maximum peak is significantly lower in TASK-1 KO mice, being 3.99 ± 0.13 Hz compared to 4.69 ± 0.15 Hz in wildtype mice ($p < 0.05$), as in figure 5.14B.

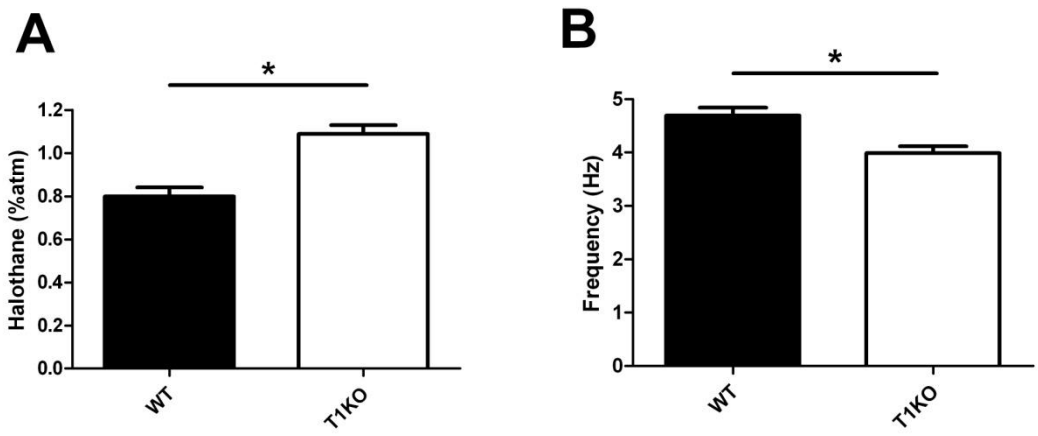

Figure 5.14 TASK-1 KO theta statistics.

*TASK-1 KO (T1KO) mice have a longer-lasting and lower-frequency type-2 theta oscillation in response to halothane. A – The maximum Q-factor occurs at a higher concentration of halothane in TASK-1 KO mice compared to wildtype (WT). B – The maximum Q-factor occurs at a lower resonant frequency in TASK-1 KO mice. (*p < 0.05)*

Although the expression of other 2PK channels is purported to be unchanged as a result of TASK-1 deletion (Linden *et al.*, 2006), functional upregulation of TASK-3 channels in the absence of TASK-1 – additional to that of $GABA_A$ receptors (Linden *et al.*, 2008) – could explain how this region might be able to support type-2 theta oscillations for longer and at lower resonant frequencies in the TASK-1 KO mice, consistent with the above results. Functional compensation by TASK-3 channels in this instance could also explain why halothane LORR is unchanged in TASK-1 KO mice (Linden *et al.*, 2006).

While other work in this report precludes the medial septum as having an involvement in halothane LORR, it would nevertheless be interesting to see how anaesthetic sensitivity changes in TASK-3 KO mice with restored TASK-3 expression in the medial septum. Future work would also seek to understand why hippocampal infection has been thus far unsuccessful. The AAV-1 serotype used in this study has been shown to efficiently infect neurons in the hippocampus (McClure *et al.*, 2011); however, strong heparin-affinity – a quality possessed by the second AAV-2 serotype used in the chimeric capsid – has been shown to reduce transduction efficiency in neurons (Arnett *et al.*, 2012). In fact, even single amino acid changes can affect the tissue tropism of AAV serotypes (Wu *et al.*, 2006), so while the eGFP-2A-TASK-3 rAAV could readily infect neurons in the medial septum, a small mutation in the capsid could explain why hippocampal cells were not infected.

Further work should clarify whether the large cell bodies infected in the medial septum are cholinergic or GABAergic using immunohistochemical techniques. Additionally, the electrophysiological characteristics – including the reversal potential and halothane sensitivity – of the GFP-positive cells need to be established to confirm membranous TASK-3 channel expression.

Another comparison to be made in future experiments would be to infect the medial septum with the Cre-2A-Flp rAAV. This will answer whether endogenous expression of the TASK-3 gene in the medial septum is enough to rescue type-2 theta, or if supra-normal levels are needed, as is a possible consequence of eGFP-2A-TASK-3 rAAV infection. Furthermore, the Cre-2A-Flp rAAV could also be used to infect the hippocampus.

That the type-2 theta rescue was only partial with medial septum infection indicates that TASK-3 channels are required in other brain regions for normal oscillatory dynamics. Once hippocampal expression of the virus is validated then the entire septohippocampal network can be investigated. It is possible though that the remaining type-2 theta impairment exists because of a TASK-3 deficit in extra-hippocampal regions. TASK-3 channels are expressed widely throughout all layers of the cortex, in the thalamus and in aminergic nuclei of the brainstem (Talley *et al.*, 2001). Moreover, as well as having a potential role in the type-2 theta oscillation (Maru *et al.*, 1979), these brainstem areas, which include the raphe nucleus and the locus coeruleus, could be probed using the rAAVs to investigate the sleep and anaesthetic phenotypes of TASK-3 KO mice.

CONCLUSION

6.1 Linking anaesthesia, type-2 theta oscillations, and TASK-3 channels

This study had several streams, interlinked by an overarching theme of anaesthesia. As explained in the introduction, the phenomenon of how anaesthetic drugs act to induce unconsciousness is not completely known. This in itself provides a reason to investigate the neurobiological mechanisms at play in the process and, additionally, investigations into unconsciousness might add to the understanding of what makes animals conscious.

The search for possible mechanisms of anaesthesia has included the analysis of synchronous brain activity by either electroencephalogram or more invasive recording techniques. Oscillations of this kind are representative of the ongoing activity of the brain and have long been known to correlate with different states of consciousness during, for example, the sleep-wake cycle, in epileptic seizures and in coma.

One of the most prominent of these oscillations is in the theta range of frequencies (4-12 Hz). Recorded from the hippocampus during waking activity and REM sleep, type-1 theta oscillations are sensitive to anaesthetics, whereas type-2 theta oscillations are present during immobility-related sensorimotor processing and during anaesthetics such as halothane, urethane and dexmedetomidine.

Two pieces of evidence warranted the further study of type-2 theta in relation to halothane anaesthesia: (i) type-2 theta has a sensorimotor role that might mediate resistance to anaesthesia; and (ii) mice lacking the two-pore potassium channel TASK-3 have no type-2 theta activity and a decreased sensitivity to halothane.

In this study, no specific correlation was found between the dynamics of the theta oscillation in C57Bl6 mice and loss of righting reflex, a correlate of human loss of consciousness. Additionally, ablating the theta oscillation with muscarinic antagonism by atropine sulfate, both systemically and centrally, had no effect on sensitivity to halothane anaesthesia. Thus, the type-2 theta oscillation appears to be an epiphenomenal event in terms of loss of consciousness in halothane anaesthesia. Therefore, other mechanisms are responsible for the decreased sensitivity to halothane of TASK-3 KO mice.

Further investigations into the role of the type-2 theta oscillation in other aspects of anaesthesia revealed a possible link between altered theta dynamics and emergence agitation. This fits with the function of theta as being a mechanism for sensory integration, and future research in this area would be interesting. For example,

would TASK-3 KO mice exhibit the hyper-locomotion associated with emergence agitation? These studies should also incorporate multiple recording electrodes in specific brain regions, such as the hippocampus and prefrontal cortex, to understand how different brain regions interact during anaesthesia and cognitive dysfunction.

The next part of the study investigated the behaviour of TASK-3 KO mice directly. The type-2 theta oscillation deficit of TASK-3 KO mice during halothane anaesthesia indicated impaired hippocampal function that could explain previously observed cognitive deficits in these mice.

This study shows that TASK-3 KO mice also have deficits in the type-2 theta oscillation during alert immobility, a state of behavioural arousal and sensorimotor processing. While TASK-3 KO mice showed normal object recognition and aversive context memory, they did show a mild working memory impairment in the T-maze. Future studies would aim to correlate this deficit to potential impairment in hippocampal-prefrontal theta synchrony, again using multiple brain region recordings.

The final section investigated the mechanism of the TASK-3-dependent type-2 theta oscillations. Using an Adeno-associated virus-approach, TASK-3 channels were selectively expressed only in the medial septum. This was enough to partially rescue the type-2 theta oscillation recorded from the cortex, indicating that, whether or not TASK-3 channels are expressed in this region normally, their ectopic expression there can restore anaesthetic-related oscillations. Since the medial septum has been ruled out of mediating LORR, future studies involving rAAVs should investigate how septohippocampal TASK-3 expression might affect other anaesthetic endpoints like delirium and emergence agitation, as well as theta-dependent memory processing.

Additionally, the two rAAVs created in this study provide a way of manipulating various other pathways involved in anaesthesia, cognition, and disease.

6.2 Main findings

1. The type-2 theta oscillation plays no active role in halothane LORR.
2. Emergence agitation correlates with altered theta oscillation dynamics.
3. TASK-3 KO mice have reduced type-2 theta power during immobility.
4. TASK-3 channel deletion causes mild impairments in working memory.
5. The type-2 theta oscillation can be partially rescued in TASK-3 KO mice by medial septum TASK-3 channel expression.

REFERENCES

Albieri G Development of behavioral assays to study the role of TASK-3 channel in hippocampal type II theta oscillations (Masters Thesis), University of Padua, 2009.

Alkire MT, Asher CD, Franciscus AM, Hahn EL (2009). Thalamic microinfusion of antibody to a voltage-gated potassium channel restores consciousness during anesthesia. *Anesthesiology* **110**(4)**:** 766-773.

Alkire MT, Hudetz AG, Tononi G (2008). Consciousness and anesthesia. *Science* **322**(5903)**:** 876-880.

Alkire MT, McReynolds JR, Hahn EL, Trivedi AN (2007). Thalamic microinjection of nicotine reverses sevoflurane-induced loss of righting reflex in the rat. *Anesthesiology* **107**(2)**:** 264-272.

Anagnostaras SG, Maren S, Sage JR, Goodrich S, Fanselow MS (1999). Scopolamine and Pavlovian fear conditioning in rats: dose-effect analysis. *Neuropsychopharmacology* **21**(6)**:** 731-744.

Aouad MT, Nasr VG (2005). Emergence agitation in children: an update. *Curr Opin Anaesthesiol* **18**(6)**:** 614-619.

Arnett AL, Beutler LR, Quintana A, Allen J, Finn E, Palmiter RD, *et al.* (2012). Heparin-binding correlates with increased efficiency of AAV1- and AAV6-mediated transduction of striated muscle, but negatively impacts CNS transduction. *Gene Ther***:** [Epub ahead of print].

Balleine BW, Curthoys IS (1991). Differential effects of escapable and inescapable footshock on hippocampal theta activity. *Behav Neurosci* **105**(1)**:** 202-209.

Bartel MA, Weinstein JR, Schaffer DV (2012). Directed evolution of novel adeno-associated viruses for therapeutic gene delivery. *Gene Ther* **19**(6)**:** 694-700.

Bayliss DA, Sirois JE, Talley EM (2003). The TASK family: two-pore domain background K+ channels. *Mol Interv* **3**(4)**:** 205-219.

Berg AP, Talley EM, Manger JP, Bayliss DA (2004). Motoneurons express heteromeric TWIK-related acid-sensitive K+ (TASK) channels containing TASK-1 (KCNK3) and TASK-3 (KCNK9) subunits. *J Neurosci* **24**(30)**:** 6693-6702.

Berry SD, Seager MA (2001). Hippocampal theta oscillations and classical conditioning. *Neurobiol Learn Mem* **76**(3)**:** 298-313.

Bevins RA, Besheer J (2006). Object recognition in rats and mice: a one-trial non-matching-to-sample learning task to study 'recognition memory'. *Nat Protoc* **1**(3)**:** 1306-1311.

Binder S, Baier PC, Molle M, Inostroza M, Born J, Marshall L (2012). Sleep enhances memory consolidation in the hippocampus-dependent object-place recognition task in rats. *Neurobiol Learn Mem* **97**(2)**:** 213-219.

Bland BH, Bland CE, Colom LV, Roth SH, DeClerk S, Dypvik A, *et al.* (2003). Effect of halothane on type 2 immobility-related hippocampal theta field activity and theta-on/theta-off cell discharges. *Hippocampus* **13**(1)**:** 38-47.

Bland BH, Declerck S, Jackson J, Glasgow S, Oddie S (2007a). Septohippocampal properties of N-methyl-D-aspartate-induced theta-band oscillation and synchrony. *Synapse* **61**(3)**:** 185-197.

Bland BH, Derie-Gillespie D, Mestek P, Jackson J, Crooks R, Cormican A (2007b). To move or not: previous experience in a runway avoidance task determines the appearance of hippocampal Type 2 sensory processing theta. *Behav Brain Res* **179**(2)**:** 299-304.

Bland BH, Oddie SD (2001). Theta band oscillation and synchrony in the hippocampal formation and associated structures: the case for its role in sensorimotor integration. *Behav Brain Res* **127**(1-2)**:** 119-136.

Bland BH, Sainsbury RS, Seto M, Sinclair BR, Whishaw IQ (1981). The use of sodium pentobarbital for the study of immobility-related (Type 2) hippocampal theta. *Physiol Behav* **27**(2)**:** 363-368.

Bland BH, Whishaw IQ (1976). Generators and topography of hippocampal theta (RSA) in the anaesthetized and freely moving rat. *Brain Res* **118**(2)**:** 259-280.

Boucetta S, Jones BE (2009). Activity profiles of cholinergic and intermingled GABAergic and putative glutamatergic neurons in the pontomesencephalic tegmentum of urethane-anesthetized rats. *J Neurosci* **29**(14)**:** 4664-4674.

Brickley SG, Aller MI, Sandu C, Veale EL, Alder FG, Sambi H, *et al.* (2007). TASK-3 two-pore domain potassium channels enable sustained high-frequency firing in cerebellar granule neurons. *J Neurosci* **27**(35)**:** 9329-9340.

Brohawn SG, del Marmol J, MacKinnon R (2012). Crystal structure of the human K2P TRAAK, a lipid- and mechano-sensitive K+ ion channel. *Science* **335**(6067)**:** 436-441.

Burdakov D, Jensen LT, Alexopoulos H, Williams RH, Fearon IM, O'Kelly I, *et al.* (2006). Tandem-pore K+ channels mediate inhibition of orexin neurons by glucose. *Neuron* **50**(5)**:** 711-722.

Buzsaki G (2002). Theta oscillations in the hippocampus. *Neuron* **33**(3)**:** 325-340.

Buzsaki G, Anastassiou CA, Koch C (2012). The origin of extracellular fields and currents--EEG, ECoG, LFP and spikes. *Nat Rev Neurosci* **13**(6)**:** 407-420.

Chaput AJ, Bryson GL (2012). Postoperative delirium: risk factors and management: continuing professional development. *Can J Anaesth* **59**(3)**:** 304-320.

Clement EA, Richard A, Thwaites M, Ailon J, Peters S, Dickson CT (2008). Cyclic and sleep-like spontaneous alternations of brain state under urethane anaesthesia. *PLoS ONE* **3**(4)**:** e2004.

Clody DE, Carlton PL (1969). Behavioral effects of lesions of the medial septum of rats. *J Comp Physiol Psychol* **67**(3)**:** 344-351.

Coburn CA, Luo Y, Cui M, Wang J, Soll R, Dong J, *et al.* (2012). Discovery of a pharmacologically active antagonist of the two-pore-domain potassium channel K2P9.1 (TASK-3). *ChemMedChem* **7**(1)**:** 123-133.

Cravero J, Surgenor S, Whalen K (2000). Emergence agitation in paediatric patients after sevoflurane anaesthesia and no surgery: a comparison with halothane. *Paediatr Anaesth* **10**(4)**:** 419-424.

Crick F, Koch C (1998). Consciousness and neuroscience. *Cereb Cortex* **8**(2)**:** 97-107.

Crick F, Koch C (2003). A framework for consciousness. *Nat Neurosci* **6**(2)**:** 119-126.

Daya S, Berns KI (2008). Gene therapy using adeno-associated virus vectors. *Clin Microbiol Rev* **21**(4)**:** 583-593.

Dickinson R, White I, Lieb WR, Franks NP (2000). Stereoselective loss of righting reflex in rats by isoflurane. *Anesthesiology* **93**(3)**:** 837-843.

Doesburg SM, Green JJ, McDonald JJ, Ward LM (2009). Rhythms of consciousness: binocular rivalry reveals large-scale oscillatory network dynamics mediating visual perception. *PLoS One* **4**(7)**:** e6142.

Donnelly ML, Gani D, Flint M, Monaghan S, Ryan MD (1997). The cleavage activities of aphthovirus and cardiovirus 2A proteins. *J Gen Virol* **78 (Pt 1):** 13-21.

Edelman GM, Gally JA, Baars BJ (2011). Biology of consciousness. *Front Psychol* **2:** 4.

Eger EI, 2nd, Raines DE, Shafer SL, Hemmings HC, Jr., Sonner JM (2008). Is a new paradigm needed to explain how inhaled anesthetics produce immobility? *Anesth Analg* **107**(3)**:** 832-848.

Eger EI, 2nd, Zhang Y, Laster M, Flood P, Kendig JJ, Sonner JM (2002). Acetylcholine receptors do not mediate the immobilization produced by inhaled anesthetics. *Anesth Analg* **94**(6)**:** 1500-1504.

Egger GJ, Livesey PJ, Dawson RG (1973). Ontogenetic aspects of central cholinergic involvement in spontaneous alternation behavior. *Dev Psychobiol* **6**(4)**:** 289-299.

Ehrengruber MU, Hennou S, Bueler H, Naim HY, Deglon N, Lundstrom K (2001). Gene transfer into neurons from hippocampal slices: comparison of recombinant Semliki Forest Virus, adenovirus, adeno-associated virus, lentivirus, and measles virus. *Mol Cell Neurosci* **17**(5)**:** 855-871.

Fassoulaki A, Sarantopoulos C, Derveniotis C (1997). Physostigmine increases the dose of propofol required to induce anaesthesia. *Can J Anaesth* **44**(11)**:** 1148-1151.

Fendt M, Endres T, Lowry CA, Apfelbach R, McGregor IS (2005). TMT-induced autonomic and behavioral changes and the neural basis of its processing. *Neurosci Biobehav Rev* **29**(8)**:** 1145-1156.

Field RH, Gossen A, Cunningham C (2012). Prior pathology in the basal forebrain cholinergic system predisposes to inflammation-induced working memory deficits: reconciling inflammatory and cholinergic hypotheses of delirium. *J Neurosci* **32**(18)**:** 6288-6294.

Fink M, Duprat F, Lesage F, Reyes R, Romey G, Heurteaux C, *et al.* (1996). Cloning, functional expression and brain localization of a novel unconventional outward rectifier K+ channel. *Embo J* **15**(24)**:** 6854-6862.

Fiset P, Paus T, Daloze T, Plourde G, Meuret P, Bonhomme V, *et al.* (1999). Brain mechanisms of propofol-induced loss of consciousness in humans: a positron emission tomographic study. *J Neurosci* **19**(13)**:** 5506-5513.

Flecknell PA (2009). *Laboratory animal anaesthesia*. 3rd ed. edn. Academic: Amsterdam ; London.

Flohr H, Glade U, Motzko D (1998). The role of the NMDA synapse in general anesthesia. *Toxicol Lett* **100-101:** 23-29.

Florian C, Vecsey CG, Halassa MM, Haydon PG, Abel T (2011). Astrocyte-derived adenosine and A1 receptor activity contribute to sleep loss-induced deficits in hippocampal synaptic plasticity and memory in mice. *J Neurosci* **31**(19)**:** 6956-6962.

Franks NP (2008). General anaesthesia: from molecular targets to neuronal pathways of sleep and arousal. *Nat Rev Neurosci* **9**(5)**:** 370-386.

Franks NP, Lieb WR (1978). Where do general anaesthetics act? *Nature* **274**(5669)**:** 339-342.

Franks NP, Lieb WR (1981). Is membrane expansion relevant to anaesthesia? *Nature* **292**(5820)**:** 248-251.

Franks NP, Lieb WR (1982). Molecular mechanisms of general anaesthesia. *Nature* **300**(5892)**:** 487-493.

Franks NP, Lieb WR (1984). Do general anaesthetics act by competitive binding to specific receptors? *Nature* **310**(5978)**:** 599-601.

Franks NP, Lieb WR (1988). Volatile general anaesthetics activate a novel neuronal K+ current. *Nature* **333**(6174)**:** 662-664.

Franks NP, Lieb WR (1990). Mechanisms of general anesthesia. *Environ Health Perspect* **87:** 199-205.

Franks NP, Lieb WR (1994). Molecular and cellular mechanisms of general anaesthesia. *Nature* **367**(6464)**:** 607-614.

Freund TF, Antal M (1988). GABA-containing neurons in the septum control inhibitory interneurons in the hippocampus. *Nature* **336**(6195)**:** 170-173.

Gadecki W, Majewski J (1969). New observations on atropine coma treatment in psychoses. *Pol Med J* **8**(6)**:** 1515-1517.

Gale GD, Anagnostaras SG, Fanselow MS (2001). Cholinergic modulation of pavlovian fear conditioning: effects of intrahippocampal scopolamine infusion. *Hippocampus* **11**(4)**:** 371-376.

Gavrilov VV, Wiener SI, Berthoz A (1995). Enhanced hippocampal theta EEG during whole body rotations in awake restrained rats. *Neurosci Lett* **197**(3)**:** 239-241.

Gerlai R (1998). Contextual learning and cue association in fear conditioning in mice: a strain comparison and a lesion study. *Behav Brain Res* **95**(2)**:** 191-203.

Gerlai R (2001). Behavioral tests of hippocampal function: simple paradigms complex problems. *Behav Brain Res* **125**(1-2)**:** 269-277.

Gerstein H, O'Riordan K, Osting S, Schwarz M, Burger C (2012). Rescue of synaptic plasticity and spatial learning deficits in the hippocampus of Homer1 knockout mice by recombinant Adeno-associated viral gene delivery of Homer1c. *Neurobiol Learn Mem* **97**(1)**:** 17-29.

Ghiani CA, Dazzi L, Maciocco E, Flore G, Maira G, Biggio G (1998). Antagonism by abecarnil of enhanced acetylcholine release in the rat brain during anticipation but not consumption of food. *Pharmacol Biochem Behav* **59**(3)**:** 657-662.

Givens B, Olton DS (1995). Bidirectional modulation of scopolamine-induced working memory impairments by muscarinic activation of the medial septal area. *Neurobiol Learn Mem* **63**(3)**:** 269-276.

Givens BS, Olton DS (1990). Cholinergic and GABAergic modulation of medial septal area: effect on working memory. *Behav Neurosci* **104**(6)**:** 849-855.

Goldstein SA, Price LA, Rosenthal DN, Pausch MH (1996). ORK1, a potassium-selective leak channel with two pore domains cloned from Drosophila melanogaster by expression in Saccharomyces cerevisiae. *Proc Natl Acad Sci U S A* **93**(23)**:** 13256-13261.

Gompf H, Chen J, Sun Y, Yanagisawa M, Aston-Jones G, Kelz MB (2009). Halothane-induced hypnosis is not accompanied by inactivation of orexinergic output in rodents. *Anesthesiology* **111**(5)**:** 1001-1009.

Gotter AL, Santarelli VP, Doran SM, Tannenbaum PL, Kraus RL, Rosahl TW, *et al.* (2011). TASK-3 as a potential antidepressant target. *Brain Res* **1416:** 69-79.

Guillem K, Bloem B, Poorthuis RB, Loos M, Smit AB, Maskos U, *et al.* (2011). Nicotinic acetylcholine receptor beta2 subunits in the medial prefrontal cortex control attention. *Science* **333**(6044)**:** 888-891.

Hameroff SR (2006). The entwined mysteries of anesthesia and consciousness: is there a common underlying mechanism? *Anesthesiology* **105**(2)**:** 400-412.

Han S, Tai C, Westenbroek RE, Yu FH, Cheah CS, Potter GB, *et al.* (2012). Autistic-like behaviour in Scn1a+/- mice and rescue by enhanced GABA-mediated neurotransmission. *Nature* **489**(7416)**:** 385-390.

Hangya B, Borhegyi Z, Szilagyi N, Freund TF, Varga V (2009). GABAergic neurons of the medial septum lead the hippocampal network during theta activity. *J Neurosci* **29**(25)**:** 8094-8102.

Hasselmo ME (2005). What is the function of hippocampal theta rhythm?--Linking behavioral data to phasic properties of field potential and unit recording data. *Hippocampus* **15**(7)**:** 936-949.

Hasselmo ME, Barkai E (1995). Cholinergic modulation of activity-dependent synaptic plasticity in the piriform cortex and associative memory function in a network biophysical simulation. *J Neurosci* **15**(10)**:** 6592-6604.

Hasselmo ME, Fehlau BP (2001). Differences in time course of ACh and GABA modulation of excitatory synaptic potentials in slices of rat hippocampus. *J Neurophysiol* **86**(4)**:** 1792-1802.

Hentschke H, Schwarz C, Antkowiak B (2005). Neocortex is the major target of sedative concentrations of volatile anaesthetics: strong depression of firing rates and increase of GABAA receptor-mediated inhibition. *Eur J Neurosci* **21**(1)**:** 93-102.

Hille B (1973). Potassium channels in myelinated nerve. Selective permeability to small cations. *J Gen Physiol* **61**(6)**:** 669-686.

Hodgkin AL, Huxley AF (1952). A quantitative description of membrane current and its application to conduction and excitation in nerve. *J Physiol* **117**(4)**:** 500-544.

Hofle N, Paus T, Reutens D, Fiset P, Gotman J, Evans AC, *et al.* (1997). Regional cerebral blood flow changes as a function of delta and spindle activity during slow wave sleep in humans. *J Neurosci* **17**(12)**:** 4800-4808.

Huang LY, Barker JL (1980). Pentobarbital: stereospecific actions of (+) and (-) isomers revealed on cultured mammalian neurons. *Science* **207**(4427)**:** 195-197.

Hudetz AG (2002). Effect of volatile anesthetics on interhemispheric EEG cross-approximate entropy in the rat. *Brain Res* **954**(1)**:** 123-131.

Hudetz AG, Wood JD, Kampine JP (2003). Cholinergic reversal of isoflurane anesthesia in rats as measured by cross-approximate entropy of the electroencephalogram. *Anesthesiology* **99**(5)**:** 1125-1131.

Hwang E, Kim S, Shin HS, Choi JH (2010). The forced walking test: a novel test for pinpointing the anesthetic-induced transition in consciousness in mouse. *J Neurosci Methods* **188**(1)**:** 14-23.

Hyman JM, Zilli EA, Paley AM, Hasselmo ME (2005). Medial prefrontal cortex cells show dynamic modulation with the hippocampal theta rhythm dependent on behavior. *Hippocampus* **15**(6)**:** 739-749.

Hyman JM, Zilli EA, Paley AM, Hasselmo ME (2010). Working Memory Performance Correlates with Prefrontal-Hippocampal Theta Interactions but not with Prefrontal Neuron Firing Rates. *Front Integr Neurosci* **4:** 2.

Ishizawa Y (2000). Selective blockade of muscarinic receptor subtypes in the brain stem reticular formation in rats: effects on anesthetic requirements. *Brain Res* **873**(1)**:** 124-126.

James W (1890). *The Principles of Psychology*. edn. H. Holt & Co.: New York.

John ER, Prichep LS (2005). The anesthetic cascade: a theory of how anesthesia suppresses consciousness. *Anesthesiology* **102**(2)**:** 447-471.

Johnson CT, Olton DS, Gage FH, 3rd, Jenko PG (1977). Damage to hippocampus and hippocampal connections: effects on DRL and spontaneous alternation. *J Comp Physiol Psychol* **91**(3)**:** 508-522.

Johr M (1999). Excitation following sevoflurane: a problem in pediatric anesthesia? *Anaesthesist* **48**(12)**:** 917-918.

Jones MW, Wilson MA (2005). Phase precession of medial prefrontal cortical activity relative to the hippocampal theta rhythm. *Hippocampus* **15**(7)**:** 867-873.

Kandel ER, Schwartz JH, Jessell TM (2000). *Principles of neural science*. 4th ed. edn. McGraw-Hill, Health Professions Division: New York ; London.

Kang D, Han J, Talley EM, Bayliss DA, Kim D (2004). Functional expression of TASK-1/TASK-3 heteromers in cerebellar granule cells. *J Physiol* **554**(Pt 1)**:** 64-77.

Kapp BS, Frysinger RC, Gallagher M, Haselton JR (1979). Amygdala central nucleus lesions: effect on heart rate conditioning in the rabbit. *Physiol Behav* **23**(6)**:** 1109-1117.

Keifer JC, Baghdoyan HA, Becker L, Lydic R (1994). Halothane decreases pontine acetylcholine release and increases EEG spindles. *Neuroreport* **5**(5)**:** 577-580.

Keifer JC, Baghdoyan HA, Lydic R (1996). Pontine cholinergic mechanisms modulate the cortical electroencephalographic spindles of halothane anesthesia. *Anesthesiology* **84**(4)**:** 945-954.

Kelz MB, Sun Y, Chen J, Cheng Meng Q, Moore JT, Veasey SC, *et al.* (2008). An essential role for orexins in emergence from general anesthesia. *Proc Natl Acad Sci U S A* **105**(4)**:** 1309-1314.

Ketchum KA, Joiner WJ, Sellers AJ, Kaczmarek LK, Goldstein SA (1995). A new family of outwardly rectifying potassium channel proteins with two pore domains in tandem. *Nature* **376**(6542)**:** 690-695.

Kitamura A, Marszalec W, Yeh JZ, Narahashi T (2003). Effects of halothane and propofol on excitatory and inhibitory synaptic transmission in rat cortical neurons. *J Pharmacol Exp Ther* **304**(1)**:** 162-171.

Klausberger T, Somogyi P (2008). Neuronal diversity and temporal dynamics: the unity of hippocampal circuit operations. *Science* **321**(5885)**:** 53-57.

Kramis R, Vanderwolf CH, Bland BH (1975). Two types of hippocampal rhythmical slow activity in both the rabbit and the rat: relations to behavior and effects of atropine, diethyl ether, urethane, and pentobarbital. *Exp Neurol* **49**(1 Pt 1)**:** 58-85.

Laalou FZ, de Vasconcelos AP, Oberling P, Jeltsch H, Cassel JC, Pain L (2008). Involvement of the basal cholinergic forebrain in the mediation of general (propofol) anesthesia. *Anesthesiology* **108**(5)**:** 888-896.

Lackner JR, DiZio P (2000a). Human orientation and movement control in weightless and artificial gravity environments. *Exp Brain Res* **130**(1)**:** 2-26.

Lackner JR, DiZio PA (2000b). Aspects of body self-calibration. *Trends Cogn Sci* **4**(7)**:** 279-288.

Laitio RM, Kaisti KK, Laangsjo JW, Aalto S, Salmi E, Maksimow A, *et al.* (2007). Effects of xenon anesthesia on cerebral blood flow in humans: a positron emission tomography study. *Anesthesiology* **106**(6)**:** 1128-1133.

Lawson VH, Bland BH (1993). The role of the septohippocampal pathway in the regulation of hippocampal field activity and behavior: analysis by the intraseptal microinfusion of carbachol, atropine, and procaine. *Exp Neurol* **120**(1)**:** 132-144.

Lazarenko RM, Willcox SC, Shu S, Berg AP, Jevtovic-Todorovic V, Talley EM, *et al.* (2010). Motoneuronal TASK channels contribute to immobilizing effects of inhalational general anesthetics. *J Neurosci* **30**(22)**:** 7691-7704.

Lesage F, Guillemare E, Fink M, Duprat F, Lazdunski M, Romey G, *et al.* (1996). TWIK-1, a ubiquitous human weakly inward rectifying K+ channel with a novel structure. *Embo J* **15**(5)**:** 1004-1011.

Leung LS, Petropoulos S, Shen B, Luo T, Herrick I, Rajakumar N, *et al.* (2011). Lesion of cholinergic neurons in nucleus basalis enhances response to general anesthetics. *Exp Neurol* **228**(2)**:** 259-269.

Lin L, Faraco J, Li R, Kadotani H, Rogers W, Lin X, *et al.* (1999). The sleep disorder canine narcolepsy is caused by a mutation in the hypocretin (orexin) receptor 2 gene. *Cell* **98**(3)**:** 365-376.

Linden AM, Aller MI, Leppa E, Rosenberg PH, Wisden W, Korpi ER (2008). K+ channel TASK-1 knockout mice show enhanced sensitivities to ataxic and hypnotic effects of GABA(A) receptor ligands. *J Pharmacol Exp Ther* **327**(1)**:** 277-286.

Linden AM, Aller MI, Leppa E, Vekovischeva O, Aitta-Aho T, Veale EL, *et al.* (2006). The in vivo contributions of TASK-1-containing channels to the actions of inhalation anesthetics, the alpha(2) adrenergic sedative dexmedetomidine, and cannabinoid agonists. *J Pharmacol Exp Ther* **317**(2)**:** 615-626.

Linden AM, Sandu C, Aller MI, Vekovischeva OY, Rosenberg PH, Wisden W, *et al.* (2007). TASK-3 knockout mice exhibit exaggerated nocturnal activity, impairments in cognitive functions, and reduced sensitivity to inhalation anesthetics. *J Pharmacol Exp Ther* **323**(3)**:** 924-934.

Lisman J (2005). The theta/gamma discrete phase code occuring during the hippocampal phase precession may be a more general brain coding scheme. *Hippocampus* **15**(7)**:** 913-922.

Lu J, Sherman D, Devor M, Saper CB (2006). A putative flip-flop switch for control of REM sleep. *Nature* **441**(7093)**:** 589-594.

Lydic R, Baghdoyan HA (1993). Pedunculopontine stimulation alters respiration and increases ACh release in the pontine reticular formation. *Am J Physiol* **264**(3 Pt 2)**:** R544-554.

Lydic R, Baghdoyan HA (2005). Sleep, anesthesiology, and the neurobiology of arousal state control. *Anesthesiology* **103**(6)**:** 1268-1295.

Ma J, Leung LS (2006). Limbic system participates in mediating the effects of general anesthetics. *Neuropsychopharmacology* **31**(6)**:** 1177-1192.

Ma J, Shen B, Stewart LS, Herrick IA, Leung LS (2002). The septohippocampal system participates in general anesthesia. *J Neurosci* **22**(2)**:** RC200.

Maren S, Quirk GJ (2004). Neuronal signalling of fear memory. *Nat Rev Neurosci* **5**(11)**:** 844-852.

Maru E, Takahashi LK, Iwahara S (1979). Effects of median raphe nucleus lesions on hippocampal EEG in the freely moving rat. *Brain Res* **163**(2)**:** 223-234.

Mathie A (2007). Neuronal two-pore-domain potassium channels and their regulation by G protein-coupled receptors. *J Physiol* **578**(Pt 2)**:** 377-385.

McClure C, Cole KL, Wulff P, Klugmann M, Murray AJ (2011). Production and titering of recombinant adeno-associated viral vectors. *J Vis Exp*(57)**:** e3348.

Meuth SG, Aller MI, Munsch T, Schuhmacher T, Seidenbecher T, Meuth P, *et al.* (2006). The contribution of TWIK-related acid-sensitive K+-containing channels to the function of dorsal lateral geniculate thalamocortical relay neurons. *Mol Pharmacol* **69**(4)**:** 1468-1476.

Meuth SG, Budde T, Kanyshkova T, Broicher T, Munsch T, Pape HC (2003). Contribution of TWIK-related acid-sensitive K+ channel 1 (TASK1) and TASK3 channels to the control of activity modes in thalamocortical neurons. *J Neurosci* **23**(16)**:** 6460-6469.

Meyer HH (1899). Welche eigenschaft der anasthetica bedingt inre Narkotische wirkung? *Arch. Exp. Pathol. Pharmakol.* **42**((2–4))**:** 109–118.

Miller AN, Long SB (2012). Crystal structure of the human two-pore domain potassium channel K2P1. *Science* **335**(6067)**:** 432-436.

Mimura M, Namiki A, Kishi R, Ikeda T, Miyake H (1990). Antagonistic effect of physostigmine on ketamine-induced anesthesia. *Psychopharmacology (Berl)* **102**(3)**:** 399-403.

Murray AJ, Sauer JF, Riedel G, McClure C, Ansel L, Cheyne L, *et al.* (2011). Parvalbumin-positive CA1 interneurons are required for spatial working but not for reference memory. *Nat Neurosci* **14**(3)**:** 297-299.

Murray CL, Fibiger HC (1986). Pilocarpine and physostigmine attenuate spatial memory impairments produced by lesions of the nucleus basalis magnocellularis. *Behav Neurosci* **100**(1)**:** 23-32.

Myhrer T, de Groot DM (1988). Immobility-related hippocampal theta activity in rats during reaction to novelty. *Scand J Psychol* **29**(3-4)**:** 214-222.

Narayanan RT, Seidenbecher T, Kluge C, Bergado J, Stork O, Pape HC (2007). Dissociated theta phase synchronization in amygdalo- hippocampal circuits during various stages of fear memory. *Eur J Neurosci* **25**(6)**:** 1823-1831.

Nicoll RA, Madison DV (1982). General anesthetics hyperpolarize neurons in the vertebrate central nervous system. *Science* **217**(4564)**:** 1055-1057.

O'Keefe J, Conway DH (1978). Hippocampal place units in the freely moving rat: why they fire where they fire. *Exp Brain Res* **31**(4)**:** 573-590.

Oddie SD, Bland BH (1998). Hippocampal formation theta activity and movement selection. *Neurosci Biobehav Rev* **22**(2)**:** 221-231.

Oddie SD, Kirk IJ, Whishaw IQ, Bland BH (1997). Hippocampal formation is involved in movement selection: evidence from medial septal cholinergic modulation and concurrent slow-wave (theta rhythm) recording. *Behav Brain Res* **88**(2)**:** 169-180.

Okada K, Okaichi H (2010). Functional cooperation between the hippocampal subregions and the medial septum in unreinforced and reinforced spatial memory tasks. *Behav Brain Res* **209**(2)**:** 295-304.

Osten P, Grinevich V, Cetin A (2007). Viral vectors: a wide range of choices and high levels of service. *Handb Exp Pharmacol*(178)**:** 177-202.

Overton CE (1901). *Studien über die Narkose zugleich ein Beitrag zur allgemeinen Pharmakologie*. edn: Jena, Switzerland.

Palchykova S, Winsky-Sommerer R, Meerlo P, Durr R, Tobler I (2006). Sleep deprivation impairs object recognition in mice. *Neurobiol Learn Mem* **85**(3)**:** 263-271.

Pang D The Role of TASK Two-Pore-Domain Potassium Channels in General Anaesthesia (PhD Thesis), Imperial College London, 2010.

Pang DS, Robledo CJ, Carr DR, Gent TC, Vyssotski AL, Caley A, *et al.* (2009). An unexpected role for TASK-3 potassium channels in network oscillations with implications for sleep mechanisms and anesthetic action. *Proc Natl Acad Sci U S A* **106**(41)**:** 17546-17551.

Pape HC, Narayanan RT, Smid J, Stork O, Seidenbecher T (2005). Theta activity in neurons and networks of the amygdala related to long-term fear memory. *Hippocampus* **15**(7)**:** 874-880.

Patel AJ, Honore E, Lesage F, Fink M, Romey G, Lazdunski M (1999). Inhalational anesthetics activate two-pore-domain background K+ channels. *Nat Neurosci* **2**(5)**:** 422-426.

Perouansky M, Rau V, Ford T, Oh SI, Perkins M, Eger EI, 2nd, *et al.* (2010). Slowing of the hippocampal theta rhythm correlates with anesthetic-induced amnesia. *Anesthesiology* **113**(6)**:** 1299-1309.

Petsche H, Stumpf C, Gogolak G (1962). [The significance of the rabbit's septum as a relay station between the midbrain and the hippocampus. I. The control of hippocampus arousal activity by the septum cells]. *Electroencephalogr Clin Neurophysiol* **14:** 202-211.

Quirk GJ, Repa C, LeDoux JE (1995). Fear conditioning enhances short-latency auditory responses of lateral amygdala neurons: parallel recordings in the freely behaving rat. *Neuron* **15**(5)**:** 1029-1039.

Robinson MJ, Edwards SE, Iyengar S, Bymaster F, Clark M, Katon W (2009). Depression and pain. *Front Biosci* **14:** 5031-5051.

Robledo-Zapico CJ The role of two-pore domain potassium channels in anaesthesia and sleep (PhD Thesis), Imperial College London, 2008.

Rogers JL, Kesner RP (2004). Cholinergic modulation of the hippocampus during encoding and retrieval of tone/shock-induced fear conditioning. *Learn Mem* **11**(1)**:** 102-107.

Rose JA, Maizel JV, Jr., Inman JK, Shatkin AJ (1971). Structural proteins of adenovirus-associated viruses. *J Virol* **8**(5)**:** 766-770.

Roy RC, Stullken EH (1981). Electroencephalographic evidence of arousal in dogs from halothane after doxapram, physostigmine, or naloxone. *Anesthesiology* **55**(4)**:** 392-397.

Royo NC, Vandenberghe LH, Ma JY, Hauspurg A, Yu L, Maronski M, *et al.* (2008). Specific AAV serotypes stably transduce primary hippocampal and cortical cultures with high efficiency and low toxicity. *Brain Res* **1190:** 15-22.

Rudolph U, Antkowiak B (2004). Molecular and neuronal substrates for general anaesthetics. *Nat Rev Neurosci* **5**(9)**:** 709-720.

Sainsbury RS (1998). Hippocampal theta: a sensory-inhibition theory of function. *Neurosci Biobehav Rev* **22**(2)**:** 237-241.

Sainsbury RS, Heynen A, Montoya CP (1987). Behavioral correlates of hippocampal type 2 theta in the rat. *Physiol Behav* **39**(4)**:** 513-519.

Sainsbury RS, Montoya CP (1984). The relationship between type 2 theta and behavior. *Physiol Behav* **33**(4)**:** 621-626.

Sandu CG The generation and the characterization of the TASK-3 knockout mice. PhD, Ruperto-Carola University of Heidelberg, 2006.

Saper CB, Fuller PM, Pedersen NP, Lu J, Scammell TE (2010). Sleep state switching. *Neuron* **68**(6)**:** 1023-1042.

Save E, Buhot MC, Foreman N, Thinus-Blanc C (1992). Exploratory activity and response to a spatial change in rats with hippocampal or posterior parietal cortical lesions. *Behav Brain Res* **47**(2)**:** 113-127.

Schiffelholz T, Aldenhoff JB (2002). Novel object presentation affects sleep-wake behavior in rats. *Neurosci Lett* **328**(1)**:** 41-44.

Seidenbecher T, Laxmi TR, Stork O, Pape HC (2003). Amygdalar and hippocampal theta rhythm synchronization during fear memory retrieval. *Science* **301**(5634)**:** 846-850.

Shin J (2010). Passive rotation-induced theta rhythm and orientation homeostasis response. *Synapse* **64**(5)**:** 409-415.

Shin J, Gireesh G, Kim SW, Kim DS, Lee S, Kim YS, *et al.* (2009). Phospholipase C beta 4 in the medial septum controls cholinergic theta oscillations and anxiety behaviors. *J Neurosci* **29**(49)**:** 15375-15385.

Shin J, Kim D, Bianchi R, Wong RK, Shin HS (2005). Genetic dissection of theta rhythm heterogeneity in mice. *Proc Natl Acad Sci U S A* **102**(50)**:** 18165-18170.

Sirois JE, Lei Q, Talley EM, Lynch C, 3rd, Bayliss DA (2000). The TASK-1 two-pore domain K+ channel is a molecular substrate for neuronal effects of inhalation anesthetics. *J Neurosci* **20**(17)**:** 6347-6354.

Sloan TB (1998). Anesthetic effects on electrophysiologic recordings. *J Clin Neurophysiol* **15**(3)**:** 217-226.

Smythe JW, Cristie BR, Colom LV, Lawson VH, Bland BH (1991). Hippocampal theta field activity and theta-on/theta-off cell discharges are controlled by an ascending hypothalamo-septal pathway. *J Neurosci* **11**(7)**:** 2241-2248.

Sommer JM, Smith PH, Parthasarathy S, Isaacs J, Vijay S, Kieran J, *et al.* (2003). Quantification of adeno-associated virus particles and empty capsids by optical density measurement. *Mol Ther* **7**(1)**:** 122-128.

Steriade M (1993). Cholinergic blockage of network- and intrinsically generated slow oscillations promotes waking and REM sleep activity patterns in thalamic and cortical neurons. *Prog Brain Res* **98:** 345-355.

Steriade M (2003). The corticothalamic system in sleep. *Front Biosci* **8:** d878-899.

Steriade M, McCormick DA, Sejnowski TJ (1993). Thalamocortical oscillations in the sleeping and aroused brain. *Science* **262**(5134)**:** 679-685.

Stoppini L, Buchs PA, Muller D (1991). A simple method for organotypic cultures of nervous tissue. *J Neurosci Methods* **37**(2)**:** 173-182.

Tai SK, Ma J, Ossenkopp KP, Leung LS (2012). Activation of immobility-related hippocampal theta by cholinergic septohippocampal neurons during vestibular stimulation. *Hippocampus* **22**(4)**:** 914-925.

Talley EM, Solorzano G, Lei Q, Kim D, Bayliss DA (2001). Cns distribution of members of the two-pore-domain (KCNK) potassium channel family. *J Neurosci* **21**(19)**:** 7491-7505.

Torborg CL, Berg AP, Jeffries BW, Bayliss DA, McBain CJ (2006). TASK-like conductances are present within hippocampal CA1 stratum oriens interneuron subpopulations. *J Neurosci* **26**(28)**:** 7362-7367.

Trichas G, Begbie J, Srinivas S (2008). Use of the viral 2A peptide for bicistronic expression in transgenic mice. *BMC Biol* **6:** 40.

Usui S, Iwahara S (1977). Effects of atropine upon the hippocampal electrical activity in rats with special reference to paradoxical sleep. *Electroencephalogr Clin Neurophysiol* **42**(4)**:** 510-517.

Vanderwolf CH (1988). Cerebral activity and behavior: control by central cholinergic and serotonergic systems. *Int Rev Neurobiol* **30:** 225-340.

Vazdarjanova A, McGaugh JL (1998). Basolateral amygdala is not critical for cognitive memory of contextual fear conditioning. *Proc Natl Acad Sci U S A* **95**(25)**:** 15003-15007.

Velly LJ, Rey MF, Bruder NJ, Gouvitsos FA, Witjas T, Regis JM, *et al.* (2007). Differential dynamic of action on cortical and subcortical structures of anesthetic agents during induction of anesthesia. *Anesthesiology* **107**(2)**:** 202-212.

Washburn CP, Sirois JE, Talley EM, Guyenet PG, Bayliss DA (2002). Serotonergic raphe neurons express TASK channel transcripts and a TASK-like pH- and halothane-sensitive K+ conductance. *J Neurosci* **22**(4)**:** 1256-1265.

Waud DR (1972). On biological assays involving quantal responses. *J Pharmacol Exp Ther* **183**(3)**:** 577-607.

Westphalen RI, Krivitski M, Amarosa A, Guy N, Hemmings HC, Jr. (2007). Reduced inhibition of cortical glutamate and GABA release by halothane in mice lacking the K+ channel, TREK-1. *Br J Pharmacol* **152**(6)**:** 939-945.

Whishaw IQ (1976). Neuromuscular blockade: the effects on two hippocampal RSA (theta) systems and neocortical desynchronization. *Brain Res Bull* **1**(6)**:** 573-581.

Wisden W (2010). Cre-ating Ways to Serotonin. *Front Neurosci* **4:** 167.

Wu M, Shanabrough M, Leranth C, Alreja M (2000). Cholinergic excitation of septohippocampal GABA but not cholinergic neurons: implications for learning and memory. *J Neurosci* **20**(10)**:** 3900-3908.

Wu Z, Asokan A, Grieger JC, Govindasamy L, Agbandje-McKenna M, Samulski RJ (2006). Single amino acid changes can influence titer, heparin binding, and tissue tropism in different adeno-associated virus serotypes. *J Virol* **80**(22)**:** 11393-11397.

Wulff P, Ponomarenko AA, Bartos M, Korotkova TM, Fuchs EC, Bahner F, *et al.* (2009). Hippocampal theta rhythm and its coupling with gamma oscillations require fast inhibition onto parvalbumin-positive interneurons. *Proc Natl Acad Sci U S A* **106**(9)**:** 3561-3566.

Xie K, Yan Y, Fang X, Gao S, Hong B (2012). Characteristics and classification of hippocampal theta rhythm induced by passive translational displacement. *Neurosci Lett* **515**(1)**:** 18-22.

Yang M, Augustsson H, Markham CM, Hubbard DT, Webster D, Wall PM, *et al.* (2004). The rat exposure test: a model of mouse defensive behaviors. *Physiol Behav* **81**(3)**:** 465-473.

Yoder RM, Pang KC (2005). Involvement of GABAergic and cholinergic medial septal neurons in hippocampal theta rhythm. *Hippocampus* **15**(3)**:** 381-392.

Zhang Y, Laster MJ, Eger EI, 2nd, Sharma M, Sonner JM (2007). Blockade of acetylcholine receptors does not change the dose of etomidate required to produce immobility in rats. *Anesth Analg* **104**(4)**:** 850-852.

Zucker J (1991). Central cholinergic depression reduces MAC for isoflurane in rats. *Anesth Analg* **72**(6)**:** 790-795.